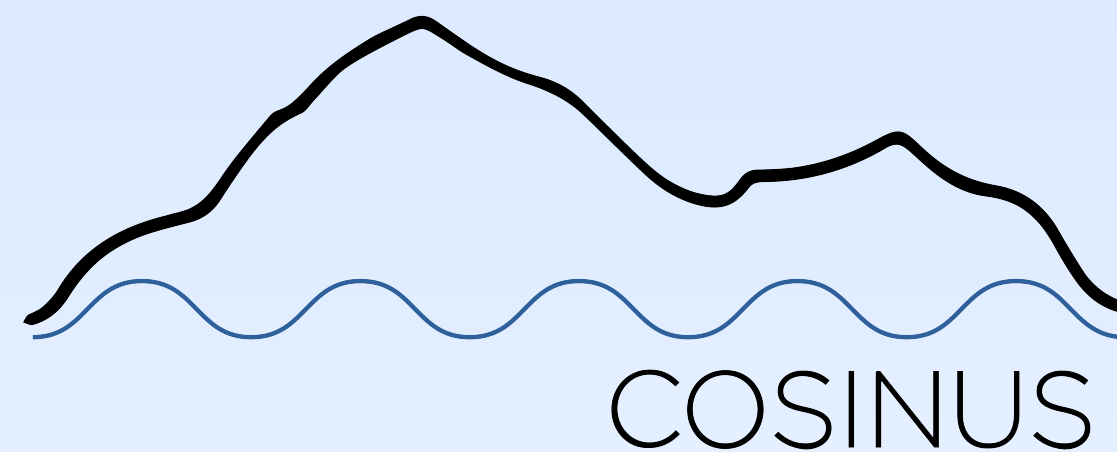




Illuminating the Invisible: deep underground dark matter search with COSINUS

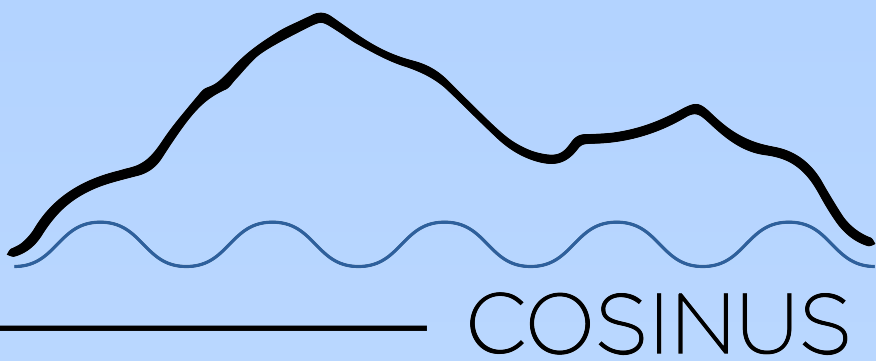
**TeV Particle Astrophysics
Napoli, 2023**

Mukund Bharadwaj | On behalf of the COSINUS collaboration
13.09.2023

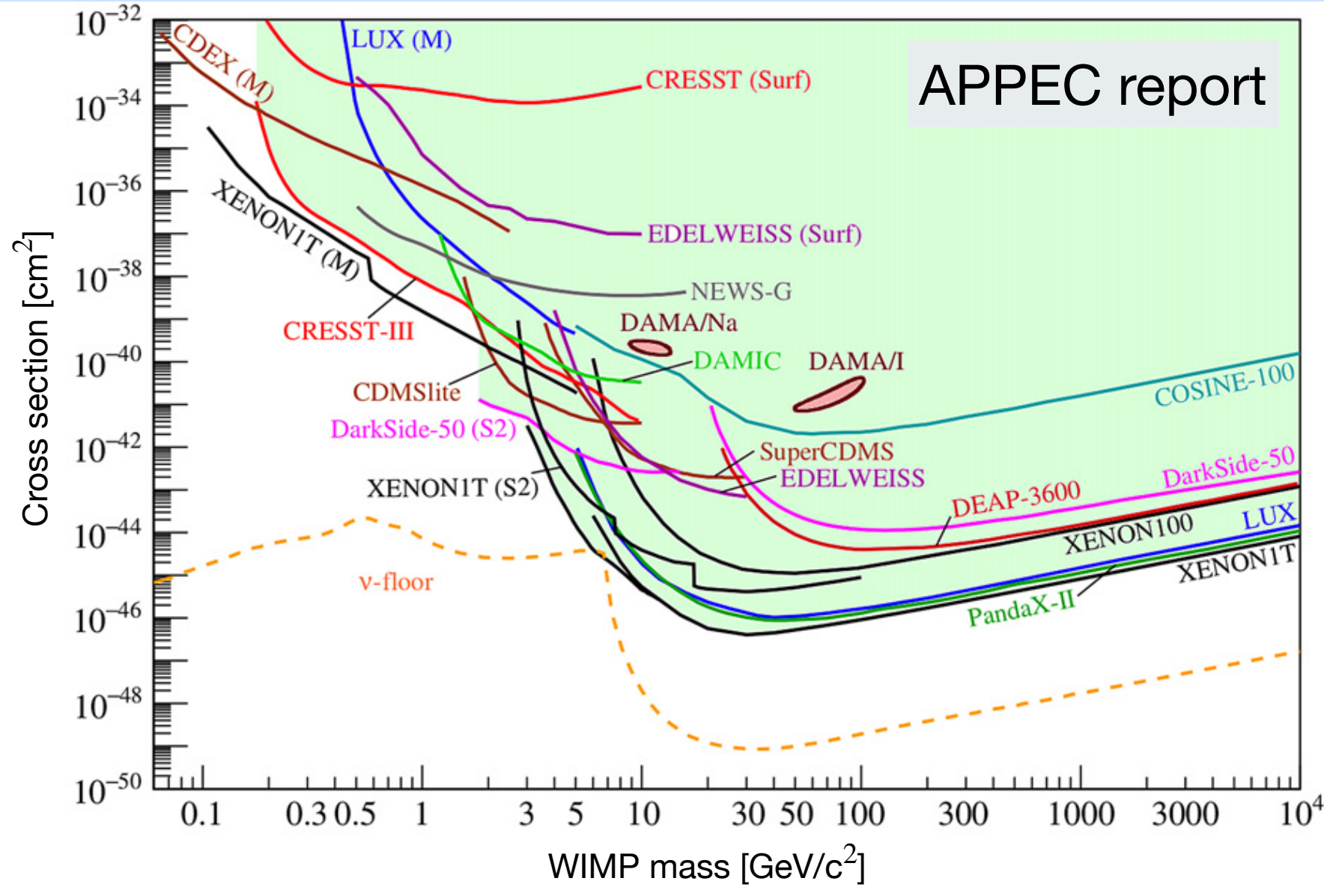


Direct DM searches

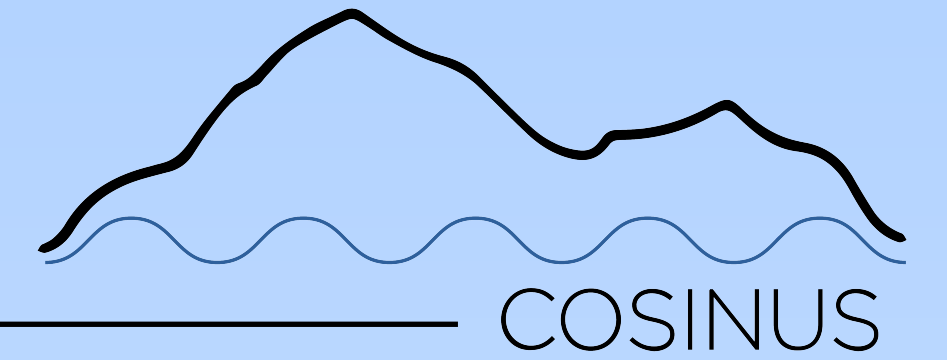
Primer



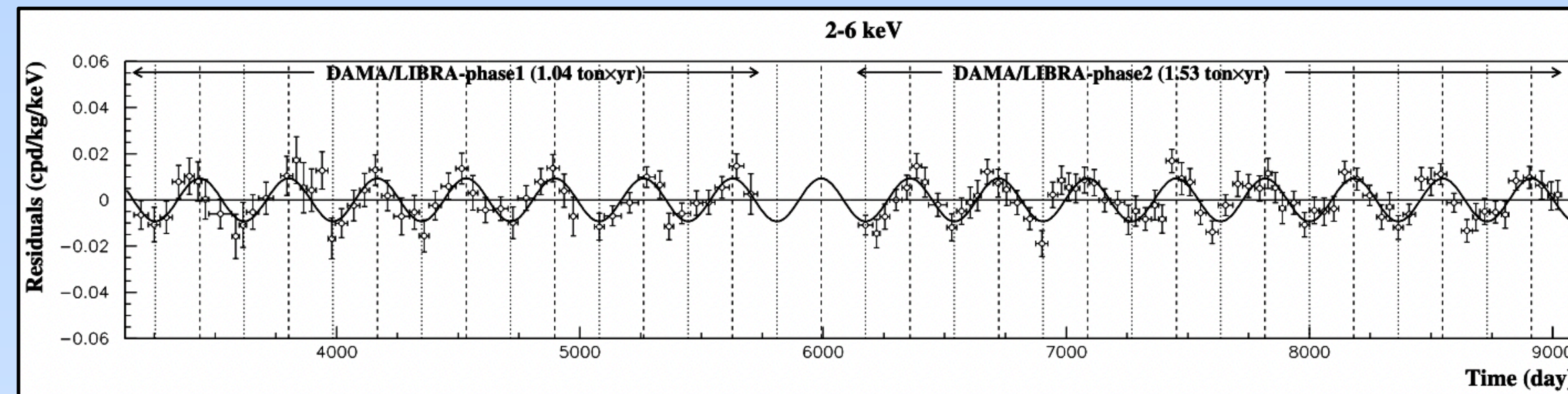
Julien Billard et al 2022 Rep. Prog. Phys. 85 056201



Direct DM searches



Primer

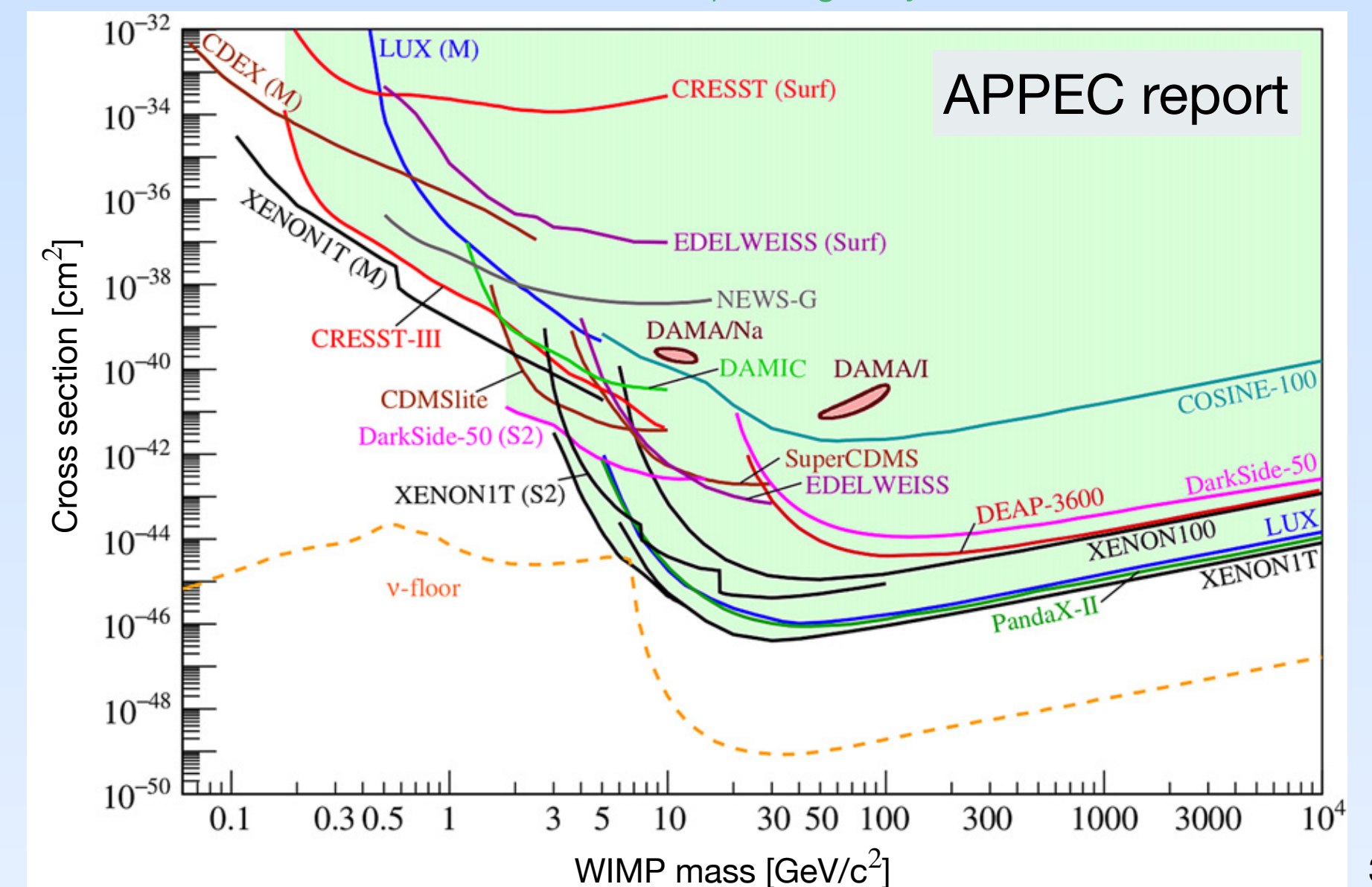


R. Bernabei et al., Nucl. Phys. At. Energy, 22(4):329–342, 2022.

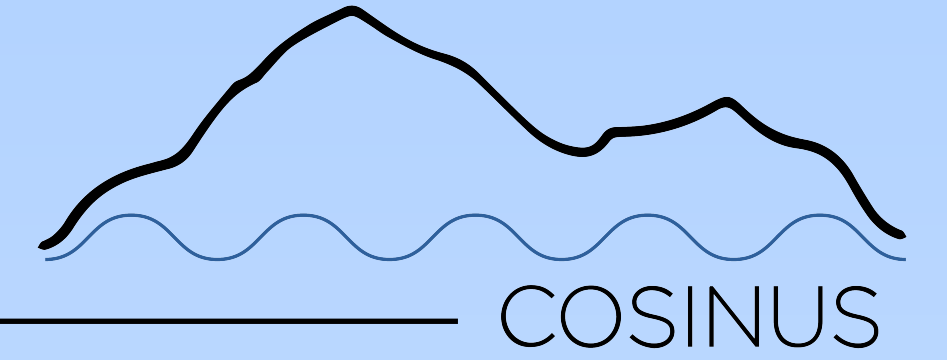


Julien Billard et al 2022 Rep. Prog. Phys. 85 056201

- Target material: NaI
- Total exposure: 2.86 tonne years
- Energy threshold: 0.75 keV_{ee}
- C.L: 13.7σ in $(2-6 \text{ keV}_{ee})$
 11.6σ in $(1-6 \text{ keV}_{ee})$



Direct DM searches



Motivation

Why a model-independent check is necessary?

from M.J Zurewsky, DSU 2022, Sydney

$$\frac{dR}{dE_R} = N_T \frac{\rho}{m_\chi} \frac{\sigma_0 m_T}{2\mu_N^2} \sum_{i,j} \sum_{a,b=0,1} \hat{c}_i^{(a)} \hat{c}_j^{(b)} \left(F_{ij}^{(ab),1}(q) \int \frac{f_{lab}(\vec{v})}{v} d^3v + F_{ij}^{(ab),2}(q) \int v f_{lab}(\vec{v}) d^3v \right).$$

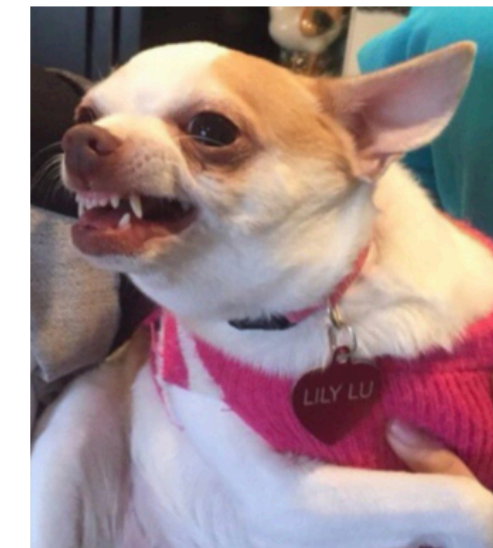
$$\frac{dR}{dE'} = \epsilon(E') \frac{1}{(2\pi)^{1/2}} \int_0^\infty \frac{dR}{dE_R} \frac{dE_R}{dE_{ee}} \frac{1}{\Delta E_{ee}} \exp \left[\frac{-(E' - E_{ee})^2}{2(\Delta E_{ee})^2} \right] dE_{ee}$$

Efficiency/threshold

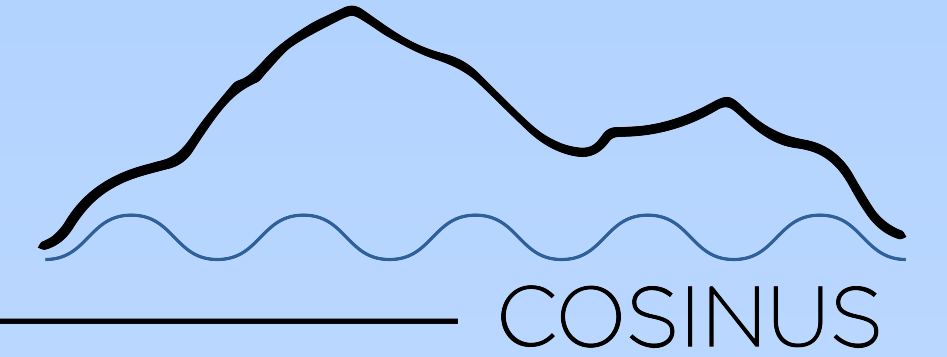
Number of nuclear recoils

Quenching factor

Resolution



Direct DM searches

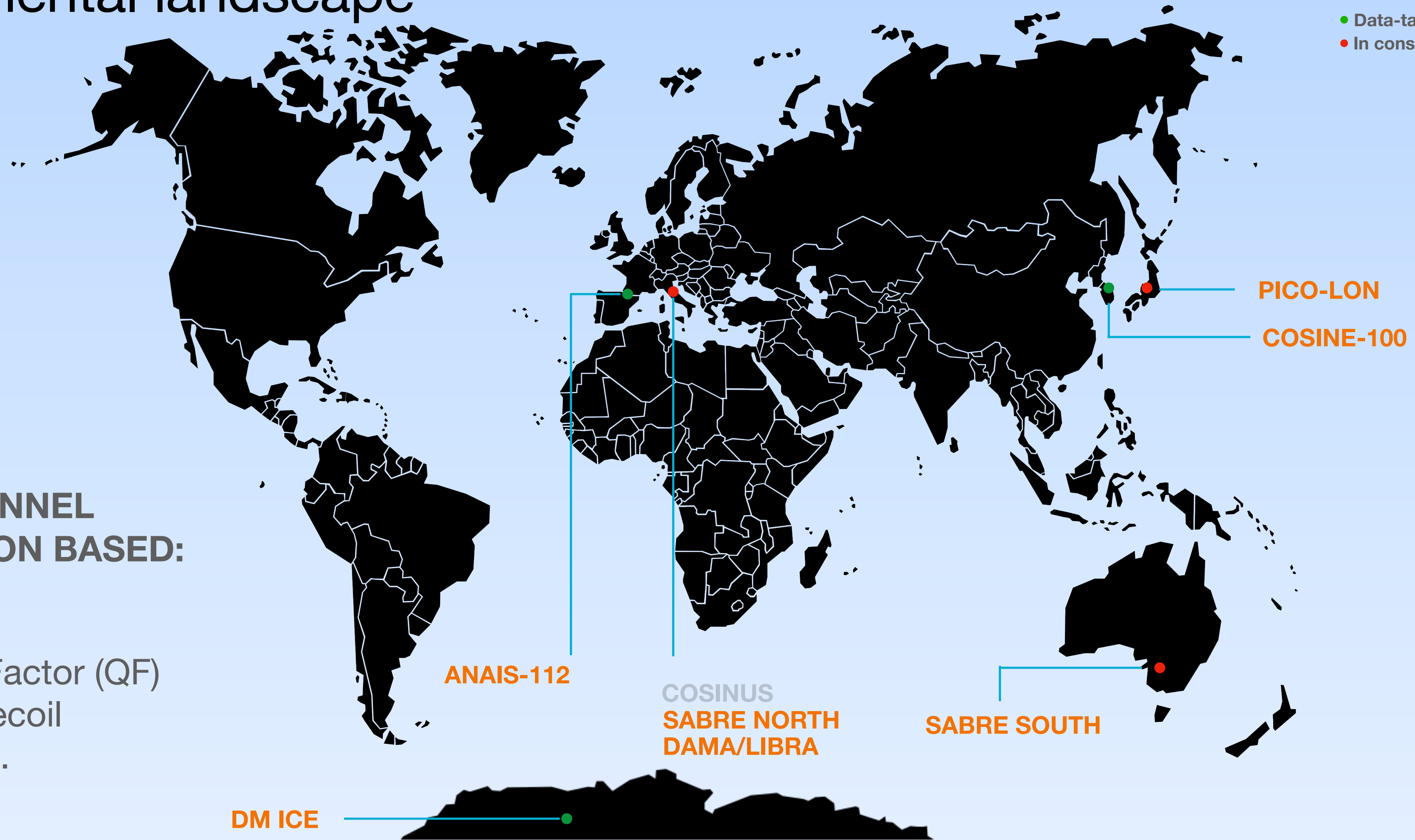


Nal experimental landscape

● Data-taking
● In construction

SINGLE-CHANNEL SCINTILLATION BASED:

- Influence of Quenching Factor (QF) on nuclear recoil energy scale.



DM ICE

ANAIS-112

COSINUS
SABRE NORTH
DAMA/LIBRA

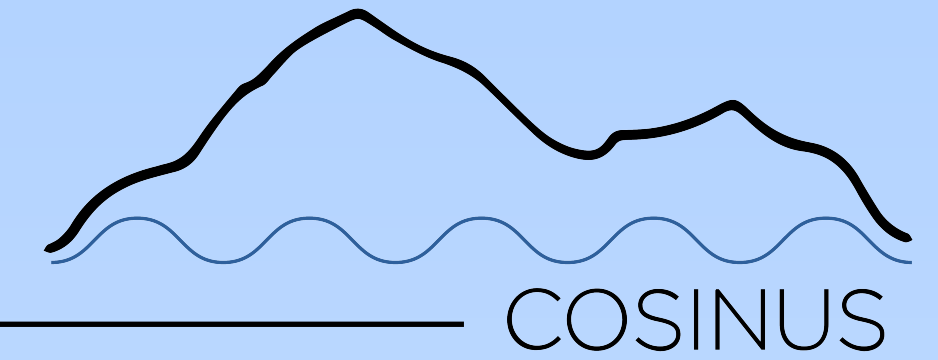
SABRE SOUTH

PICO-LON

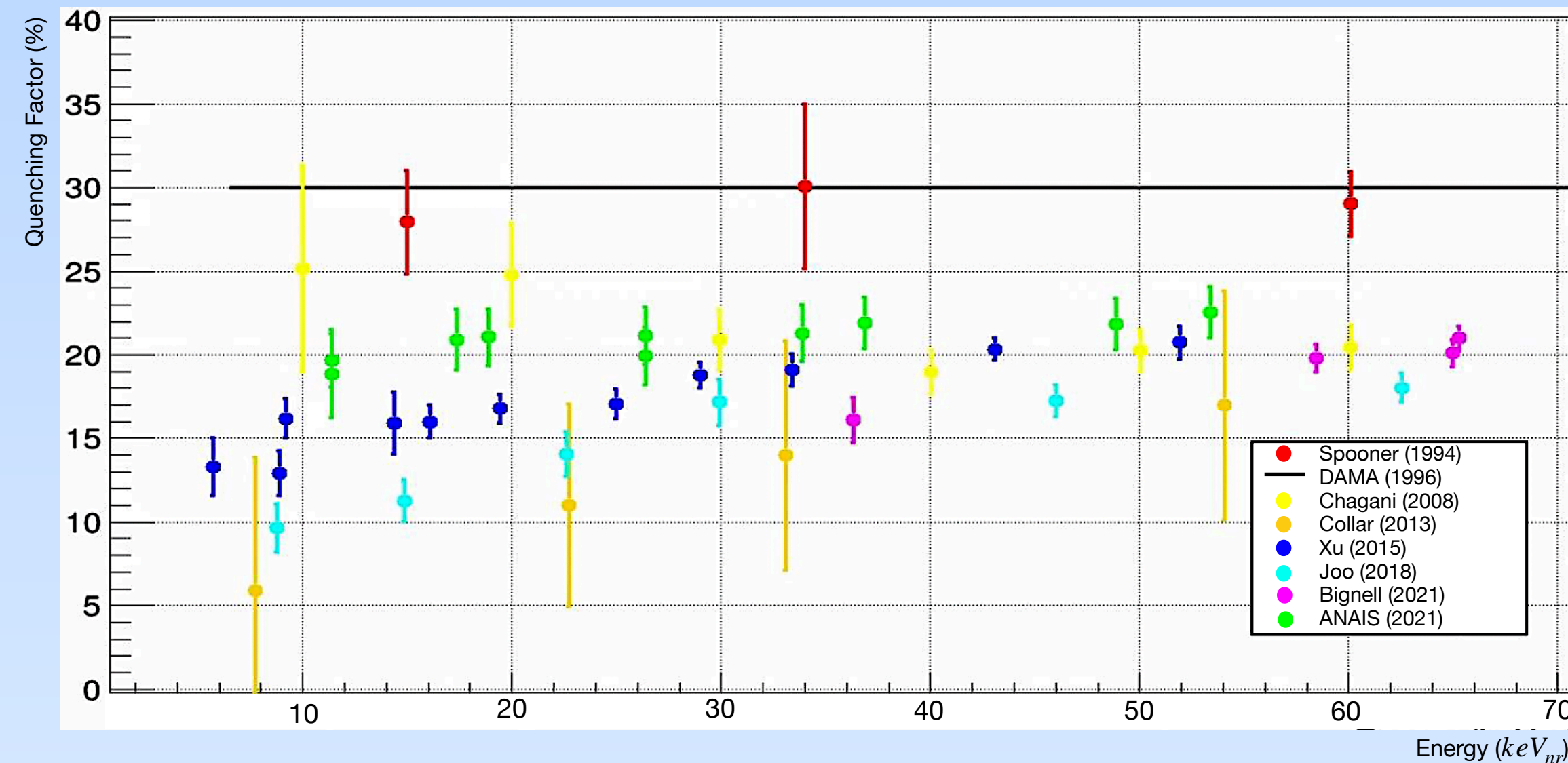
COSINE-100



Direct DM searches

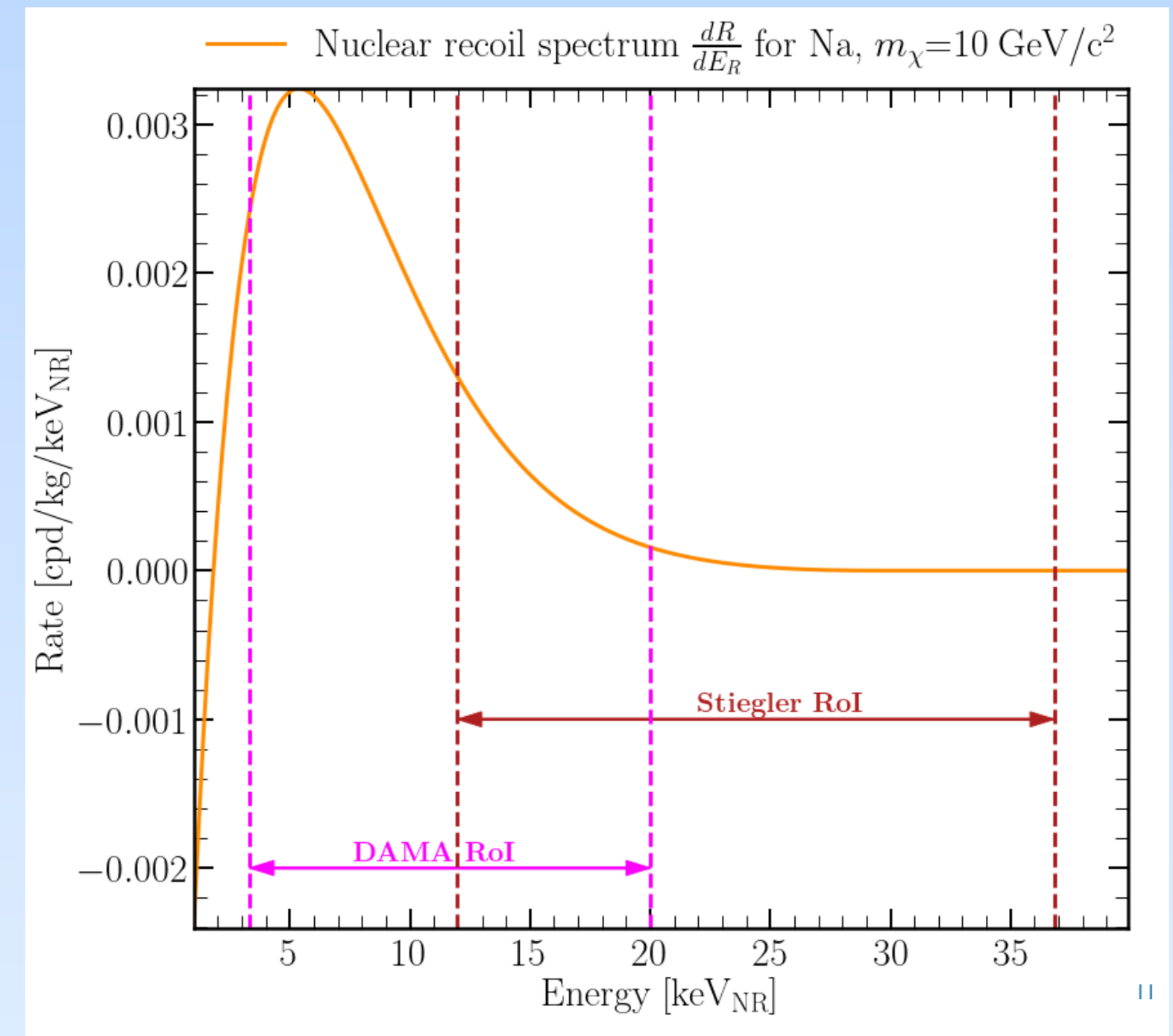


QF uncertainties in NaI

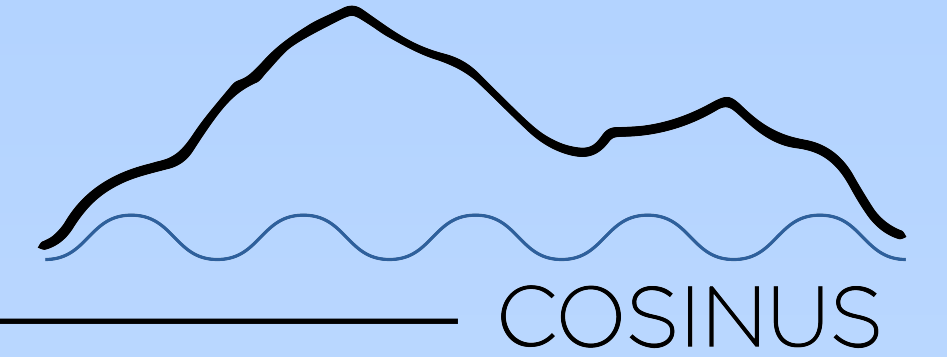


D. Cintas et al 2021 J. Phys.: Conf. Ser. 2156 012065

- Measurements of quenching factor (QF) at room temperature disagree.
- Potential dependence on TI dopant %
- Change of QF has a strong impact on observable rate.



Direct DM searches



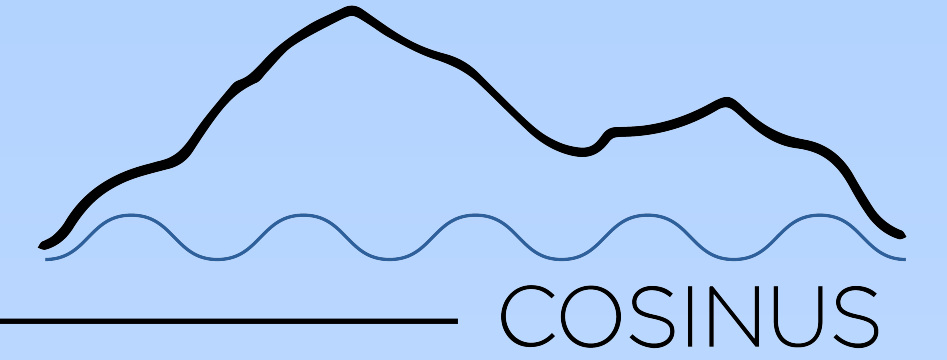
Nal experimental landscape

DUAL-CHANNEL BASED:

- True nuclear recoil energy scale.
- Particle discrimination.



COSINUS



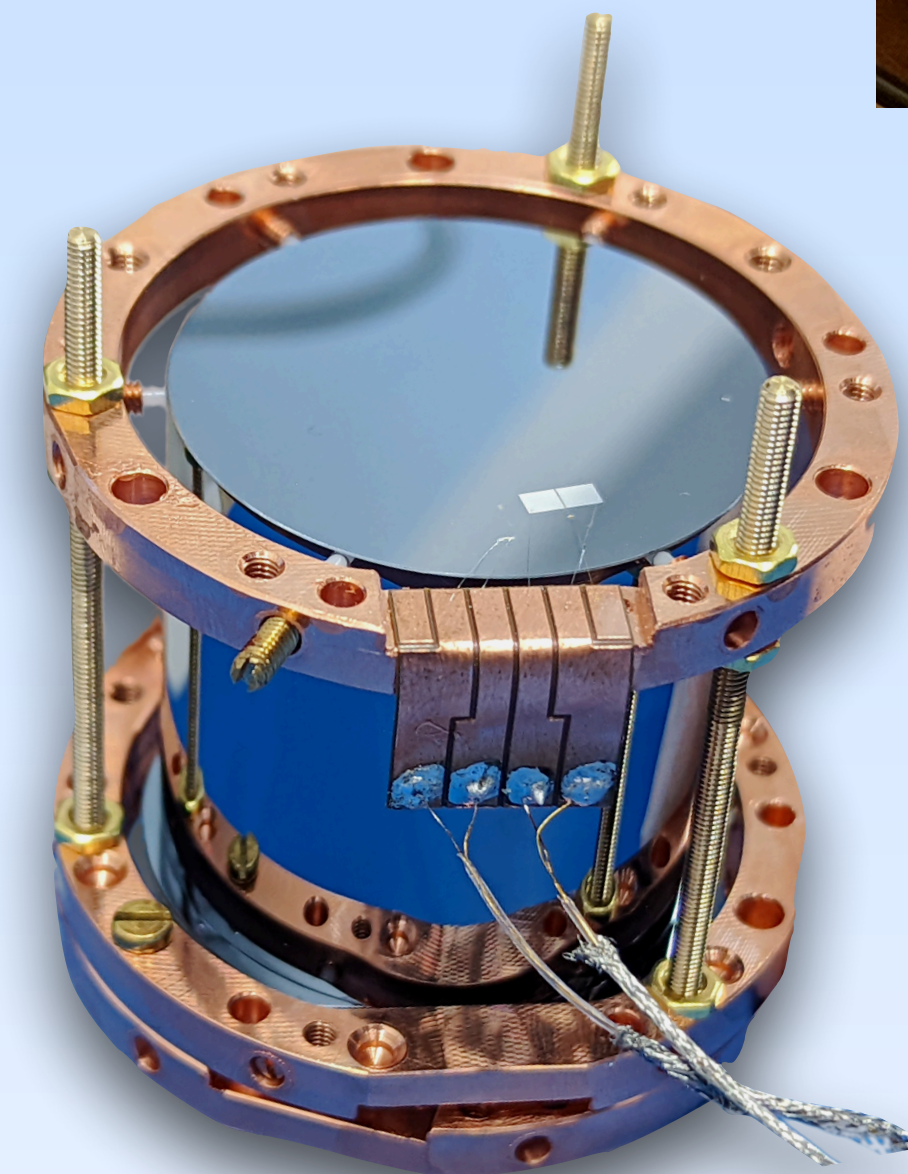
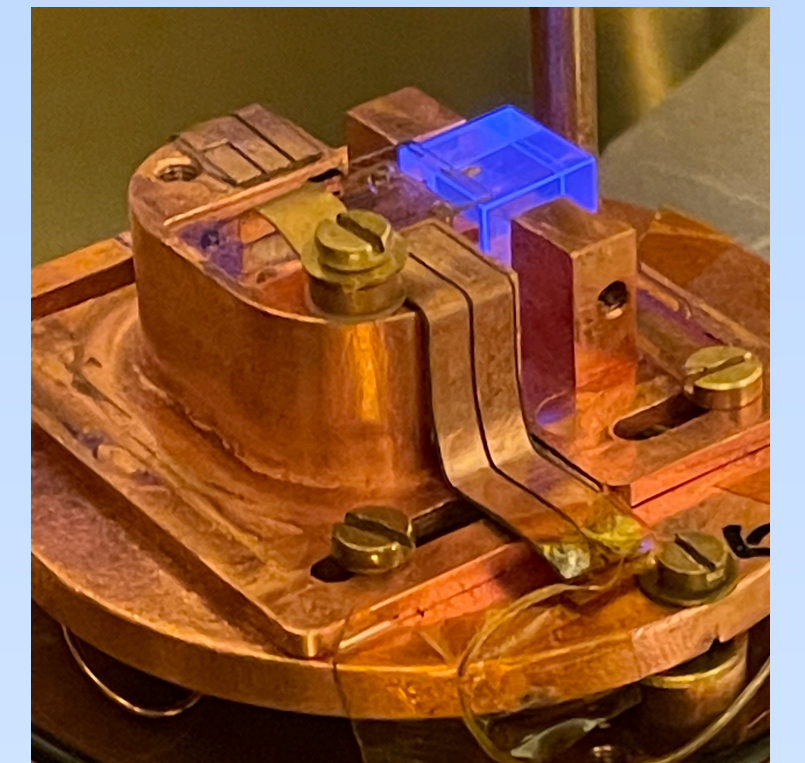
Cryogenic Observatory for Signatures seen in Next generation Underground Searches

Design aspects:

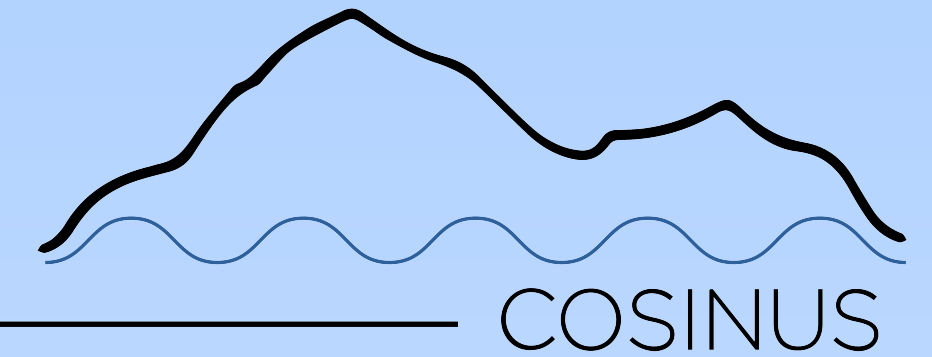
Provide a model-independent cross-check of DAMA/LIBRA

Target detector material: NaI

Novel operation of radio-pure NaI at cryogenic temperatures. $\mathcal{O}(mK)$

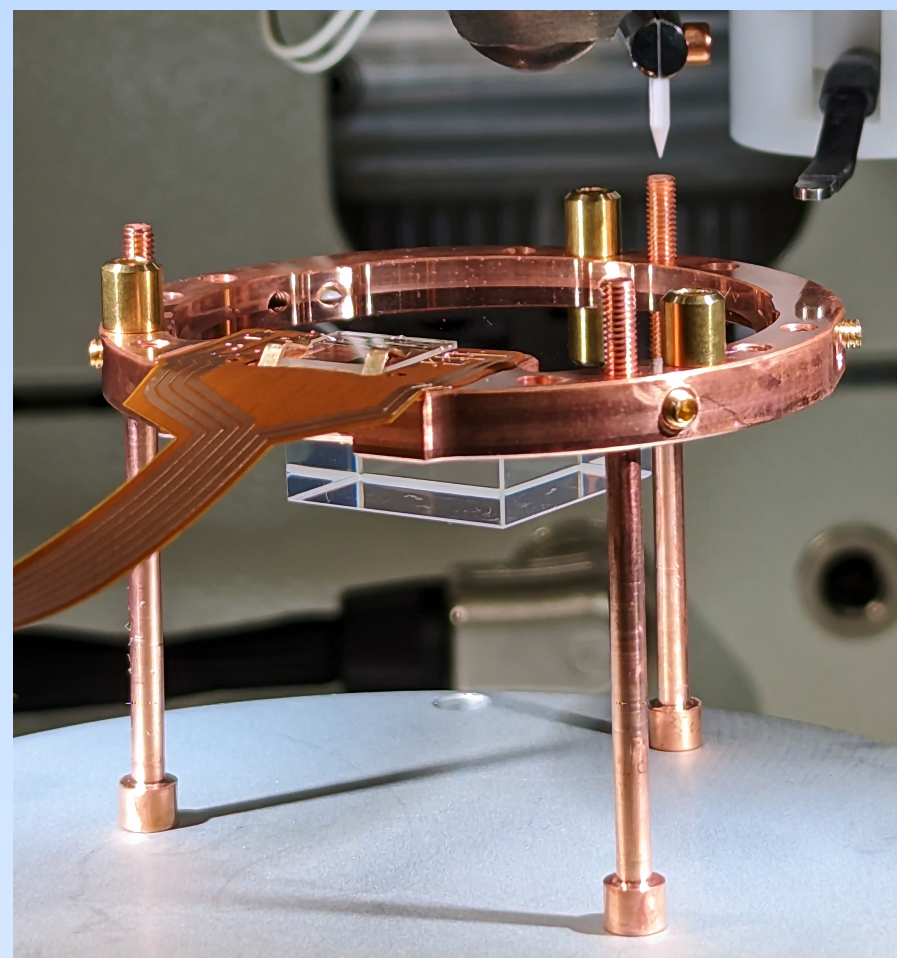


COSINUS



2 channel readout

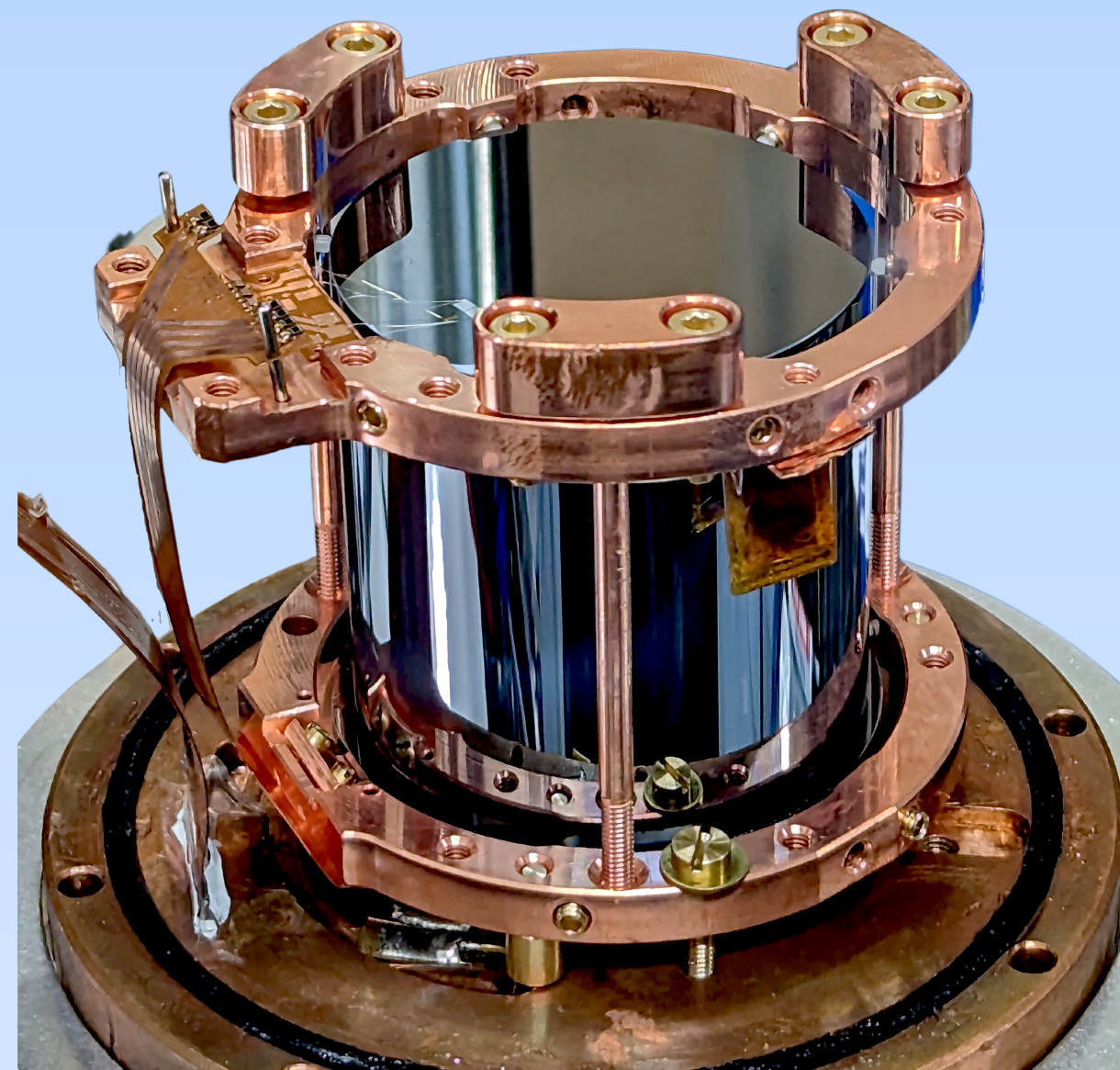
CHANNEL - 1: PHONON DETECTOR



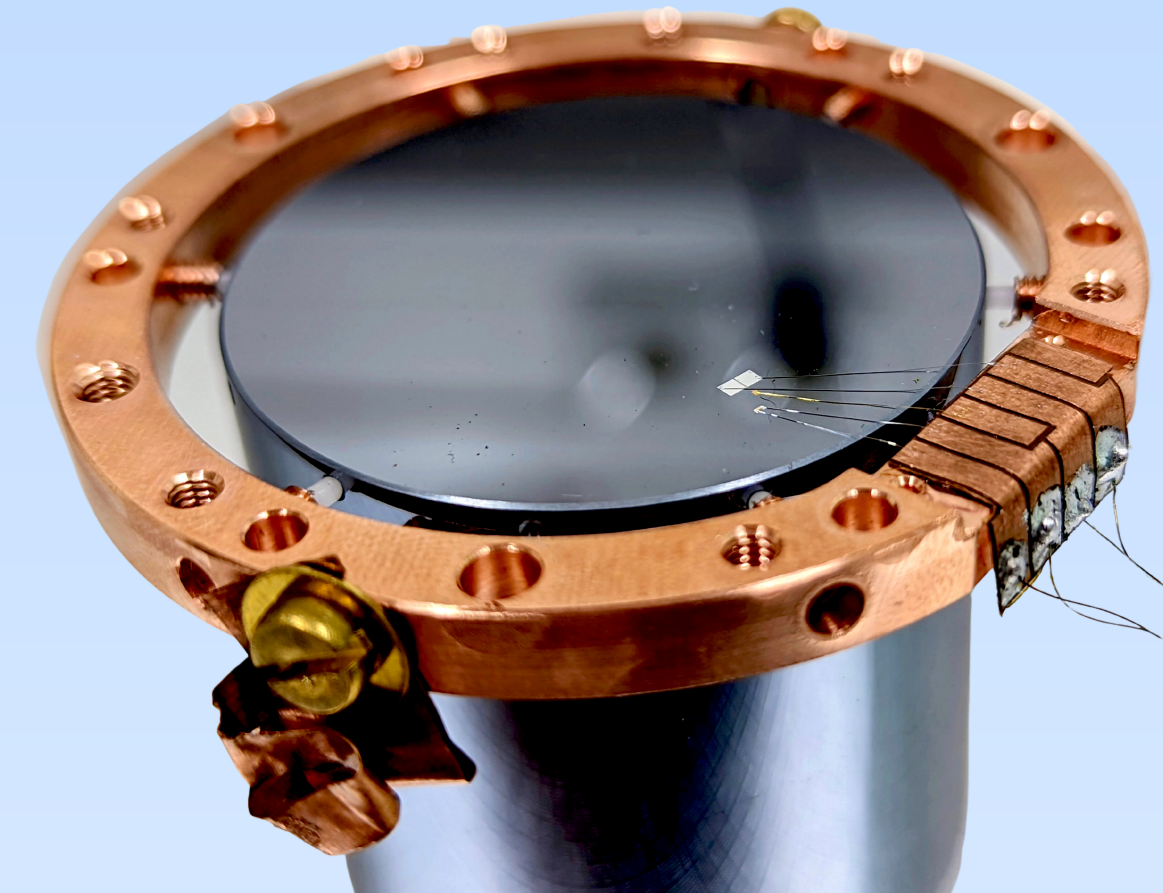
Phonon Signal

- (almost) independent of particle type

Nal + remoTES



CHANNEL - 2: LIGHT DETECTOR

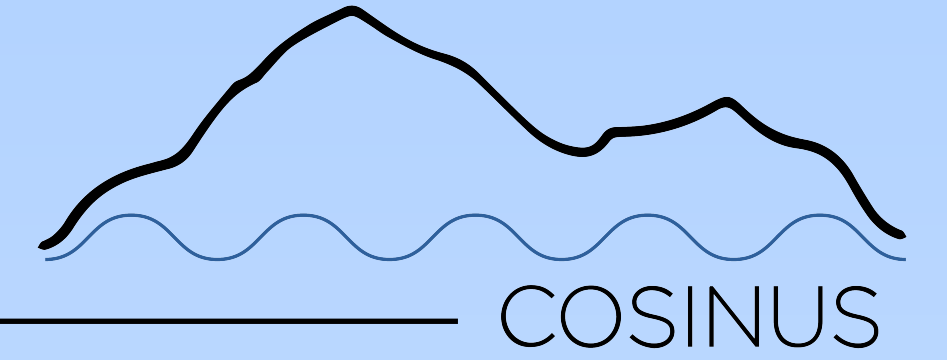


Light Signal

- Scintillation light strongly dependent on type of particle interaction

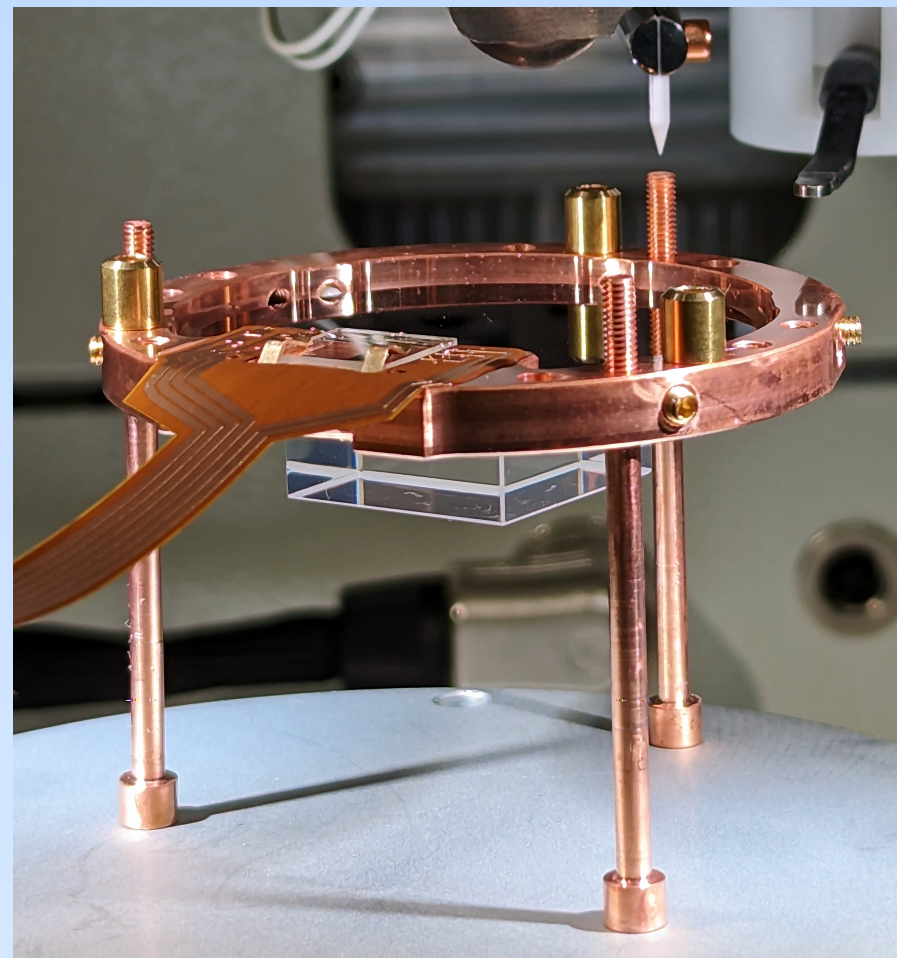
Si + TES

COSINUS



Advantages

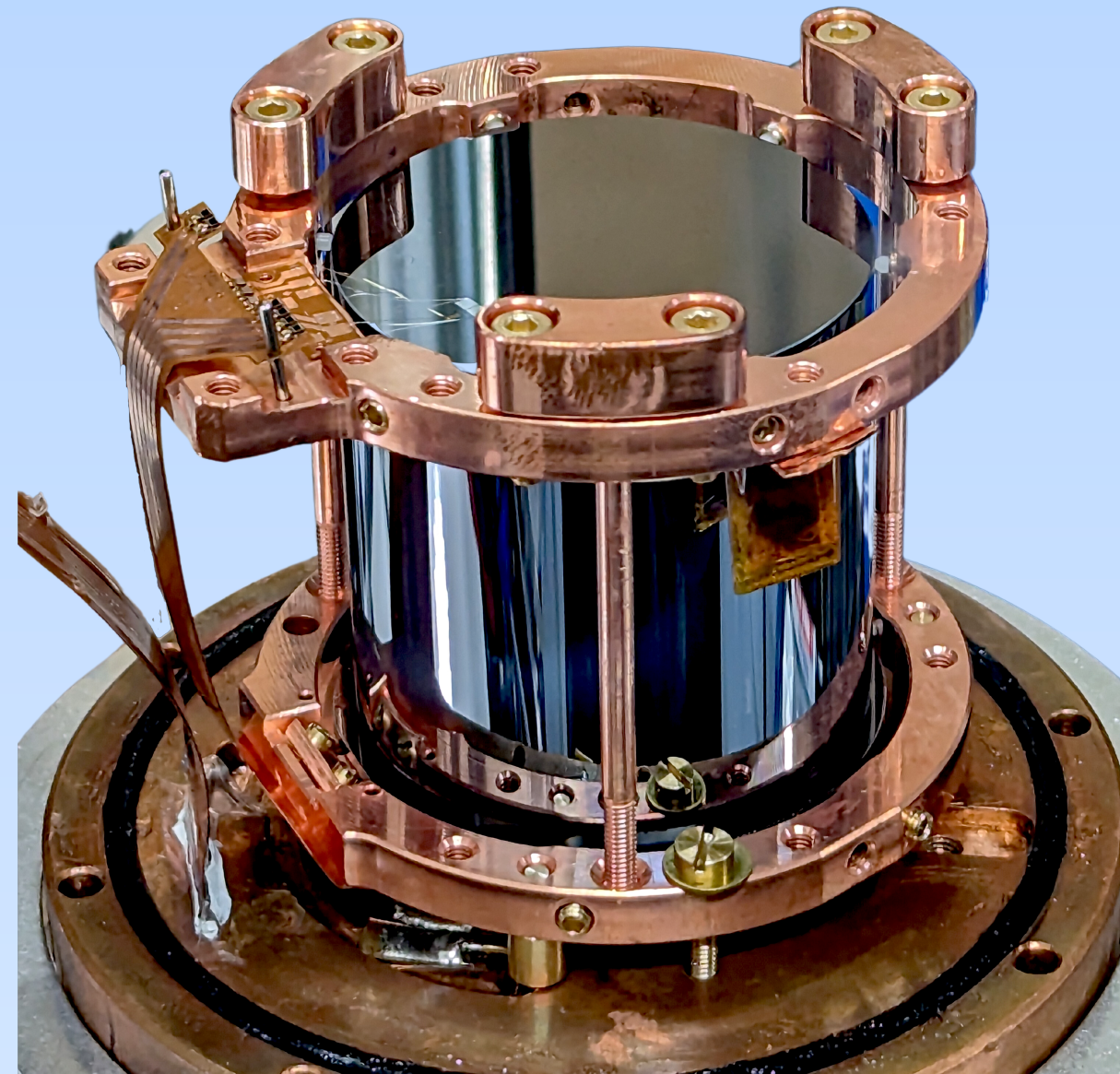
CHANNEL - 1: PHONON DETECTOR



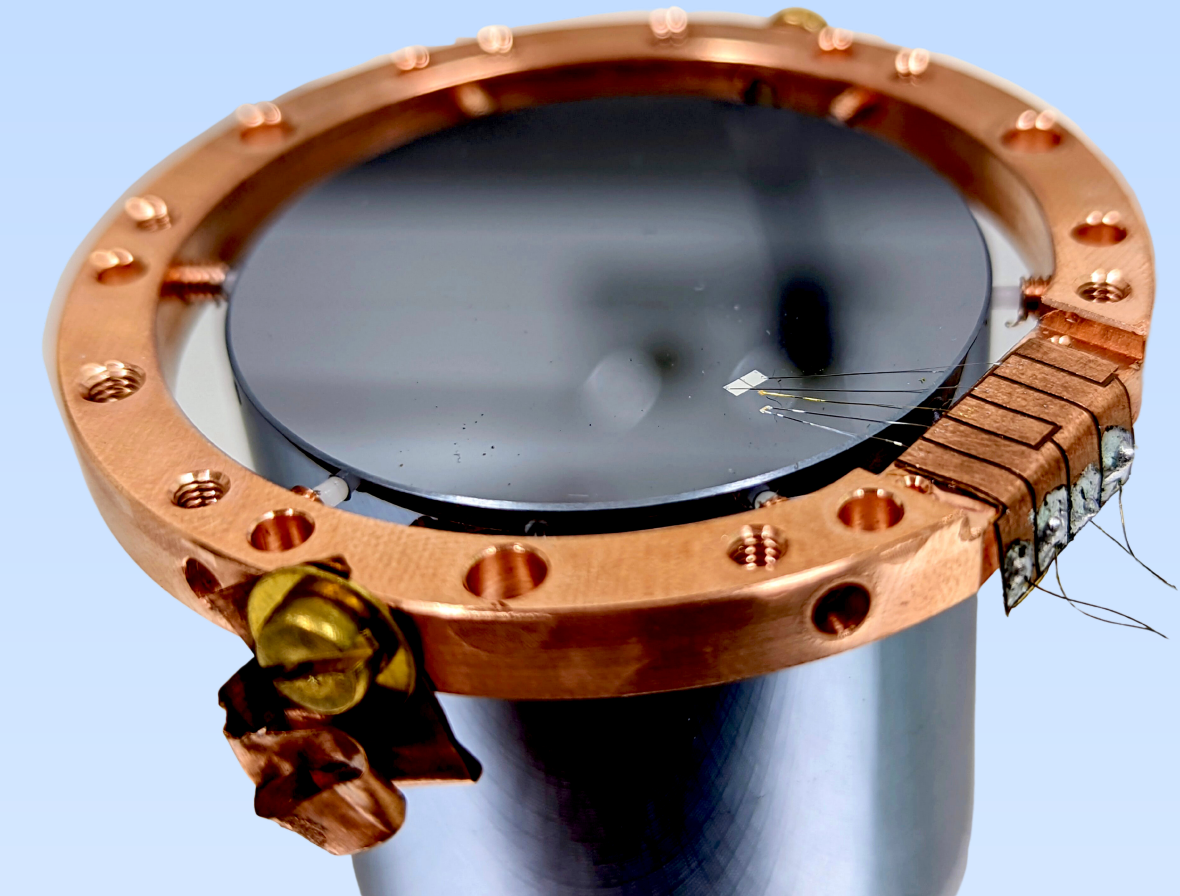
Phonon Signal

- (almost) independent of particle type

NaI + remoTES



CHANNEL - 2: LIGHT DETECTOR



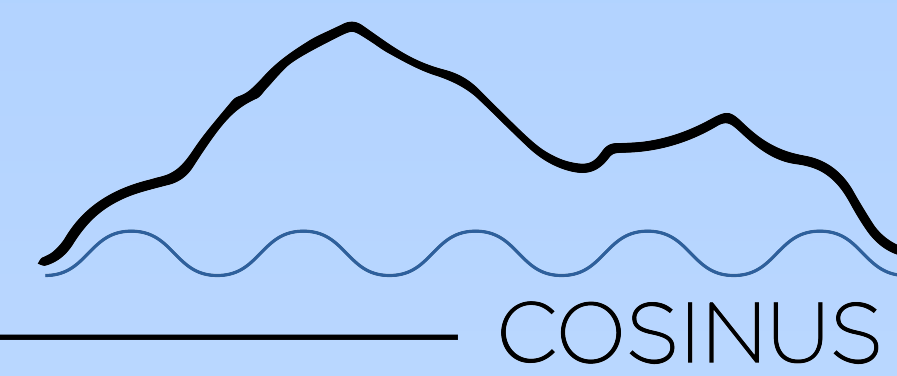
Light Signal

- Scintillation light strongly dependent on type of particle interaction

Si + TES

- Particle discrimination on per-event basis!
- Low threshold for nuclear recoils (TES based readout)
- In-situ measurement of QF

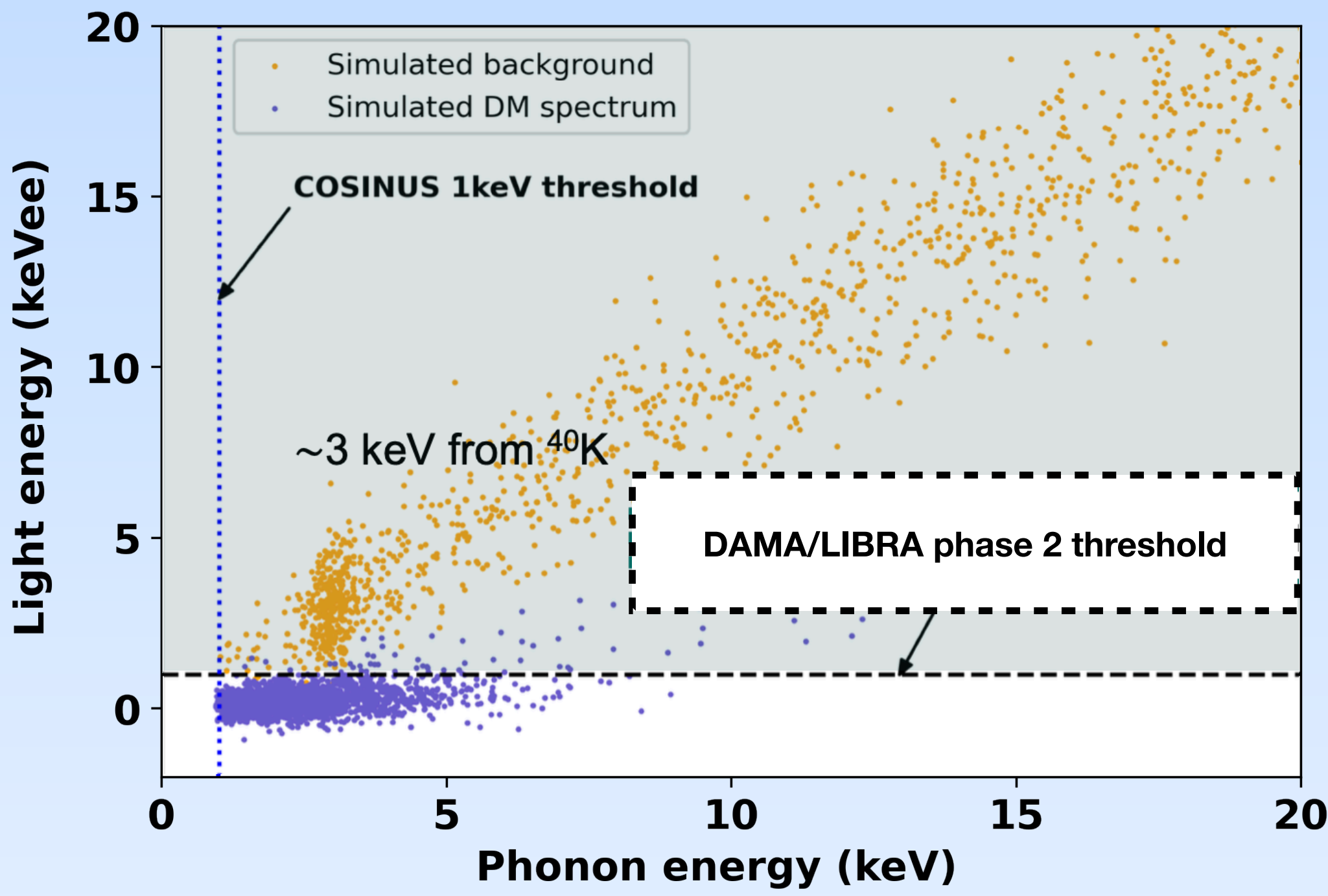
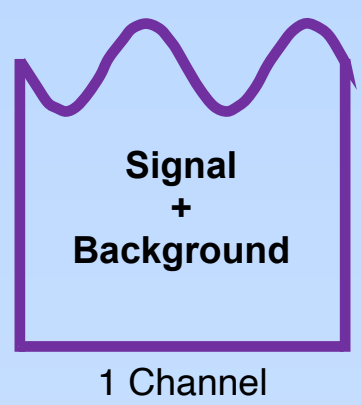
COSINUS



Advantages

What DAMA/LIBRA observes:

Simulated data for 100 kgd gross exposure

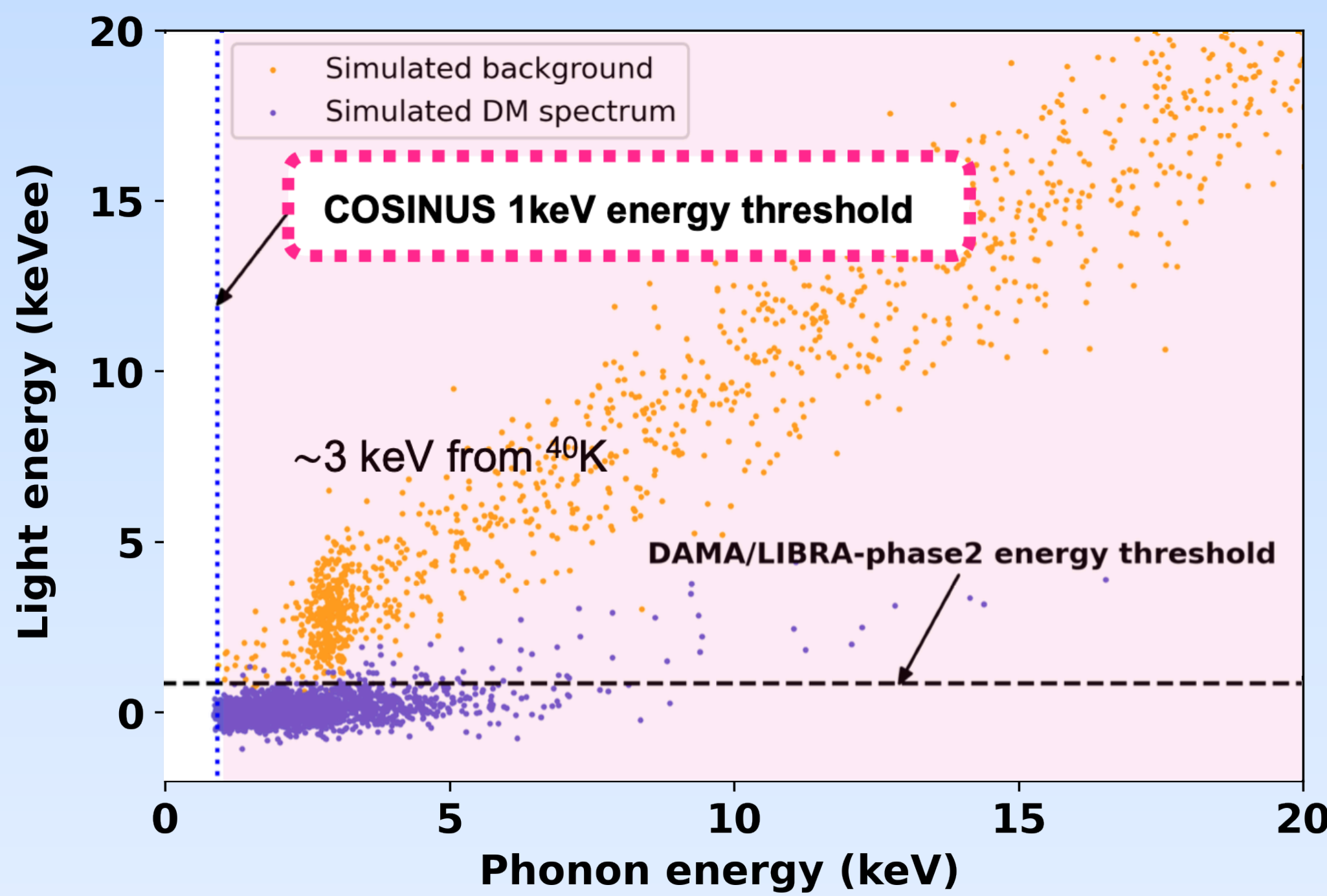
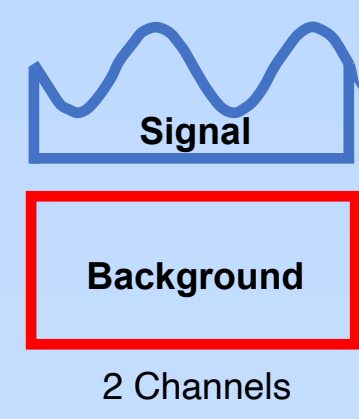


background: 20ppb ^{40}K + flat bkg (1/ keV kg d)

σ_{SI} : 2×10^{-4} pb, M_{DM} : 10 GeV/c²

What COSINUS observes:

Simulated data for 100 kgd gross exposure

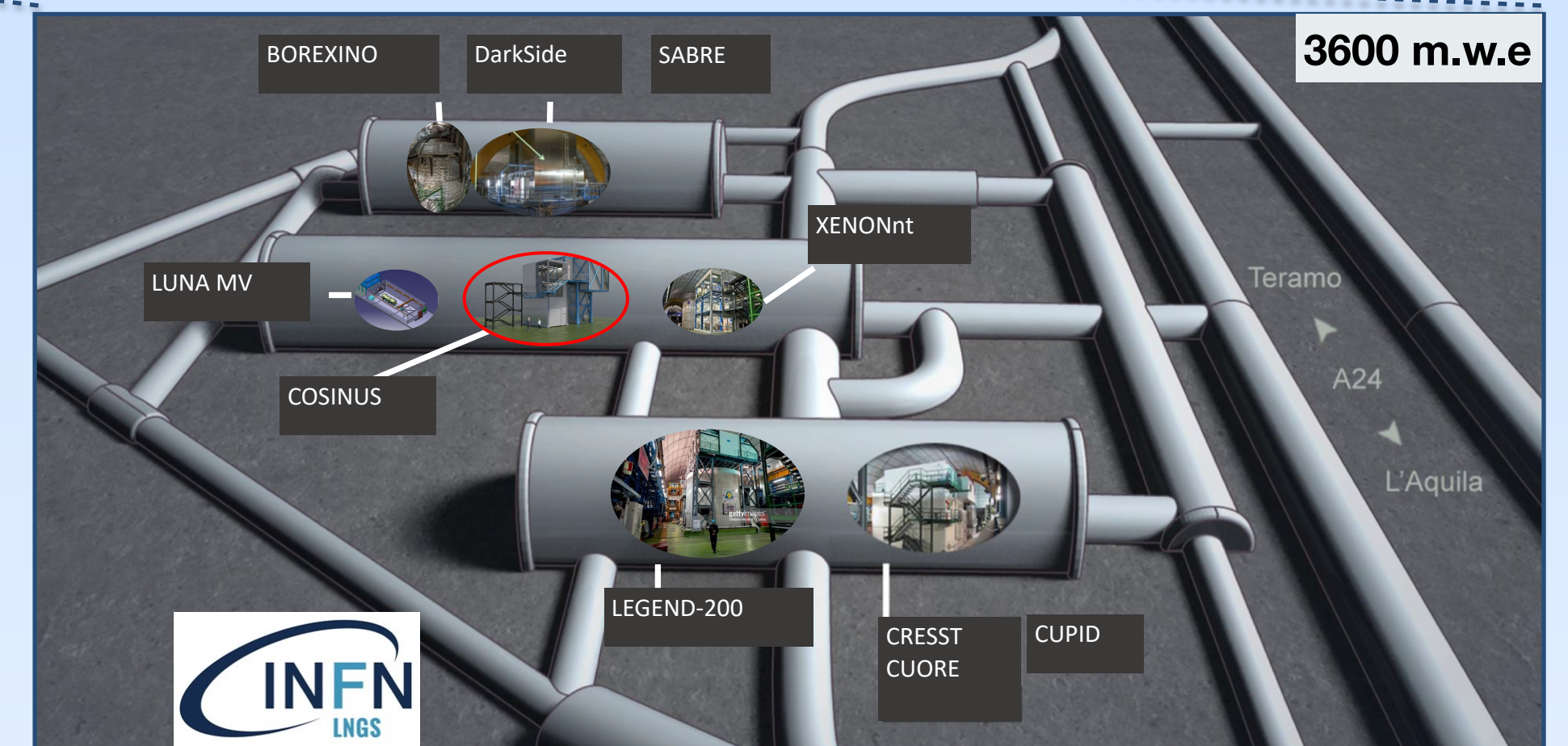
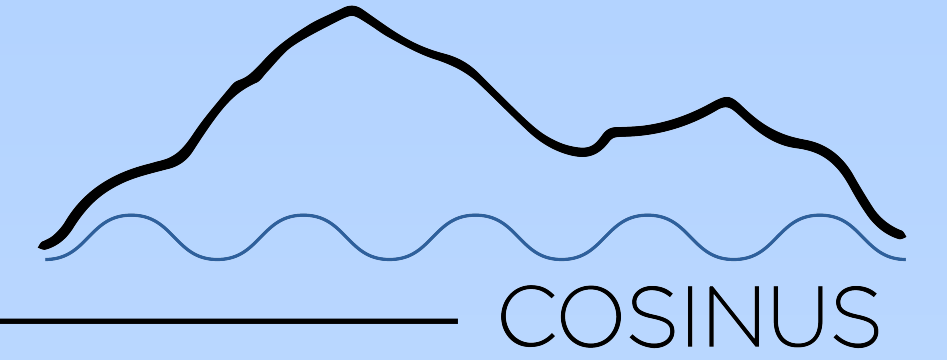


Efficiency between 20-50% at 1-2 keV, 50% above 2 keV



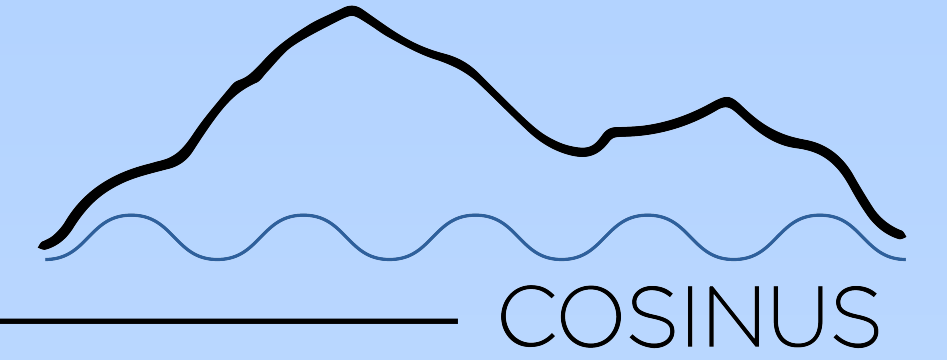
COSINUS

Low-background facility

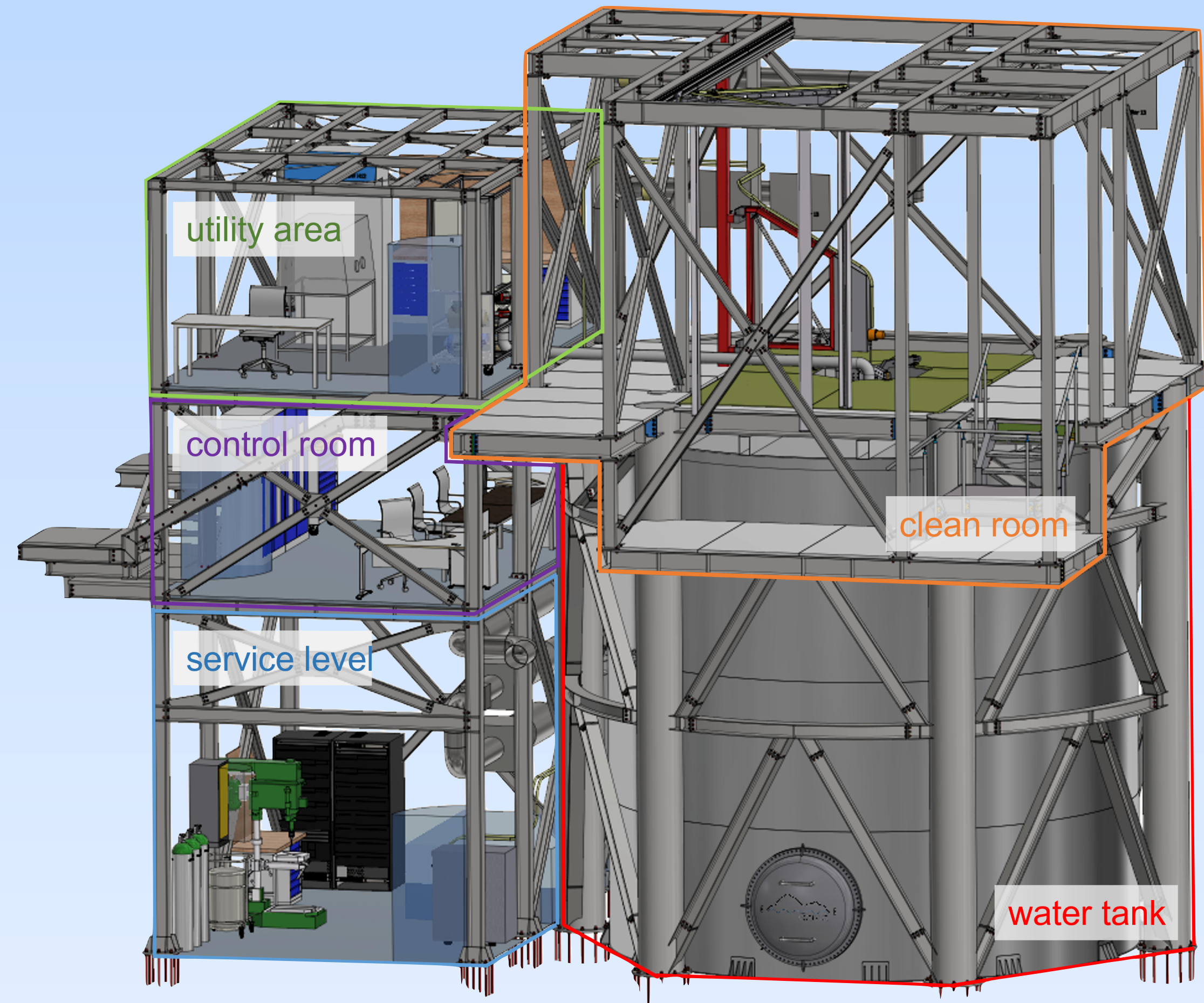


COSINUS

Low-background facility

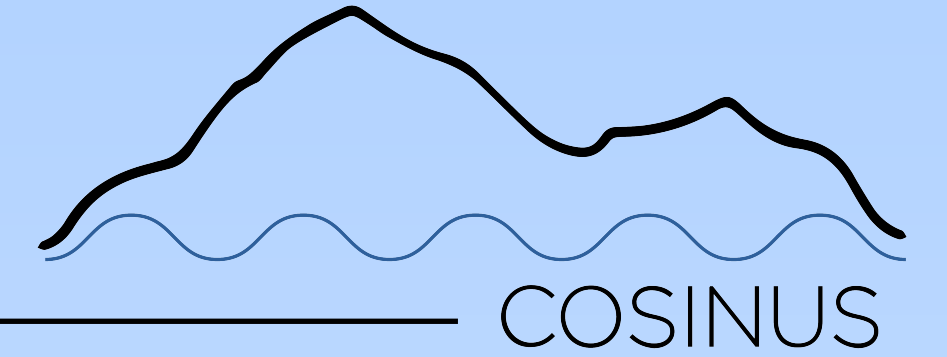


Eur. Phys. J. C (2022) 82: 248
Following work to be published

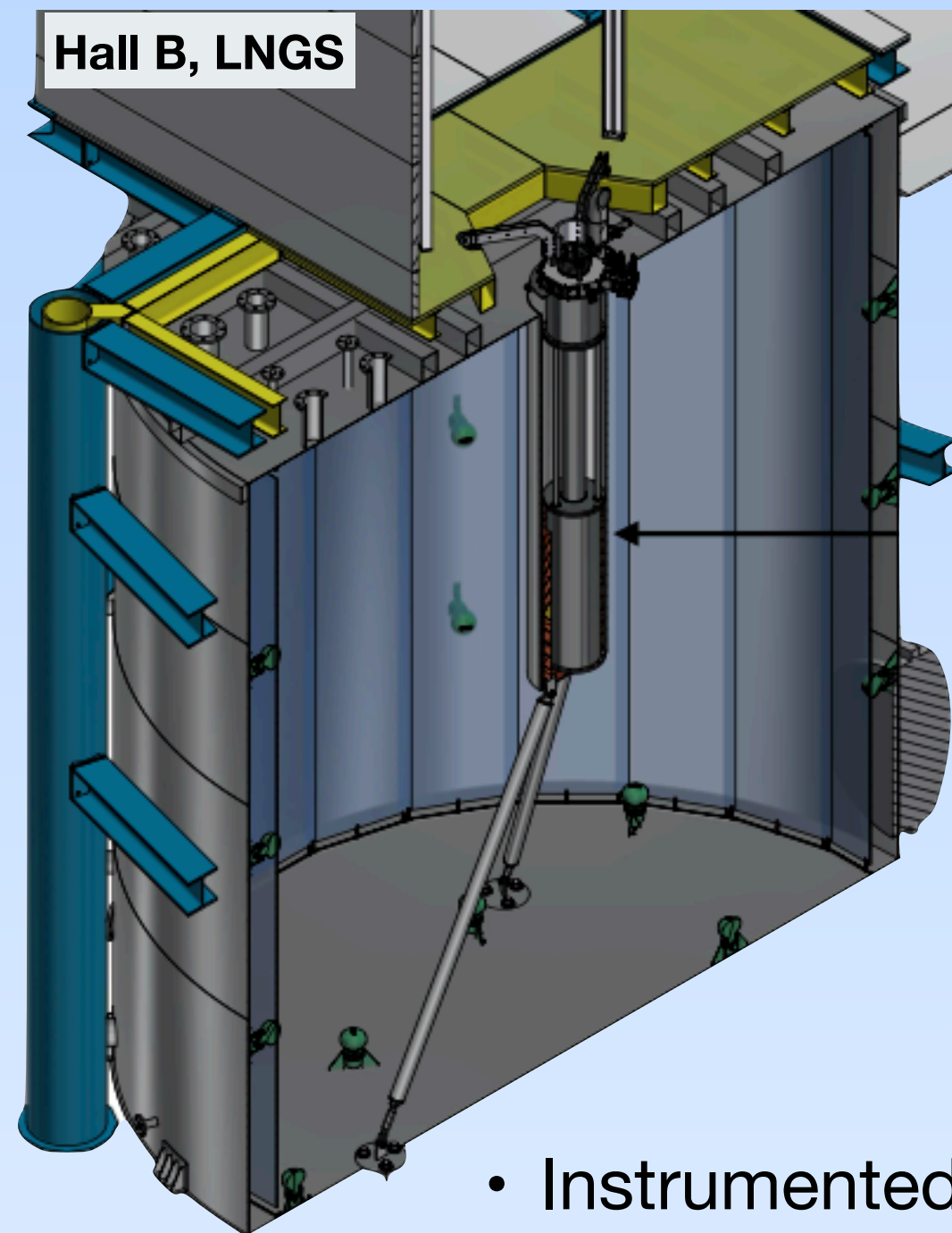


COSINUS

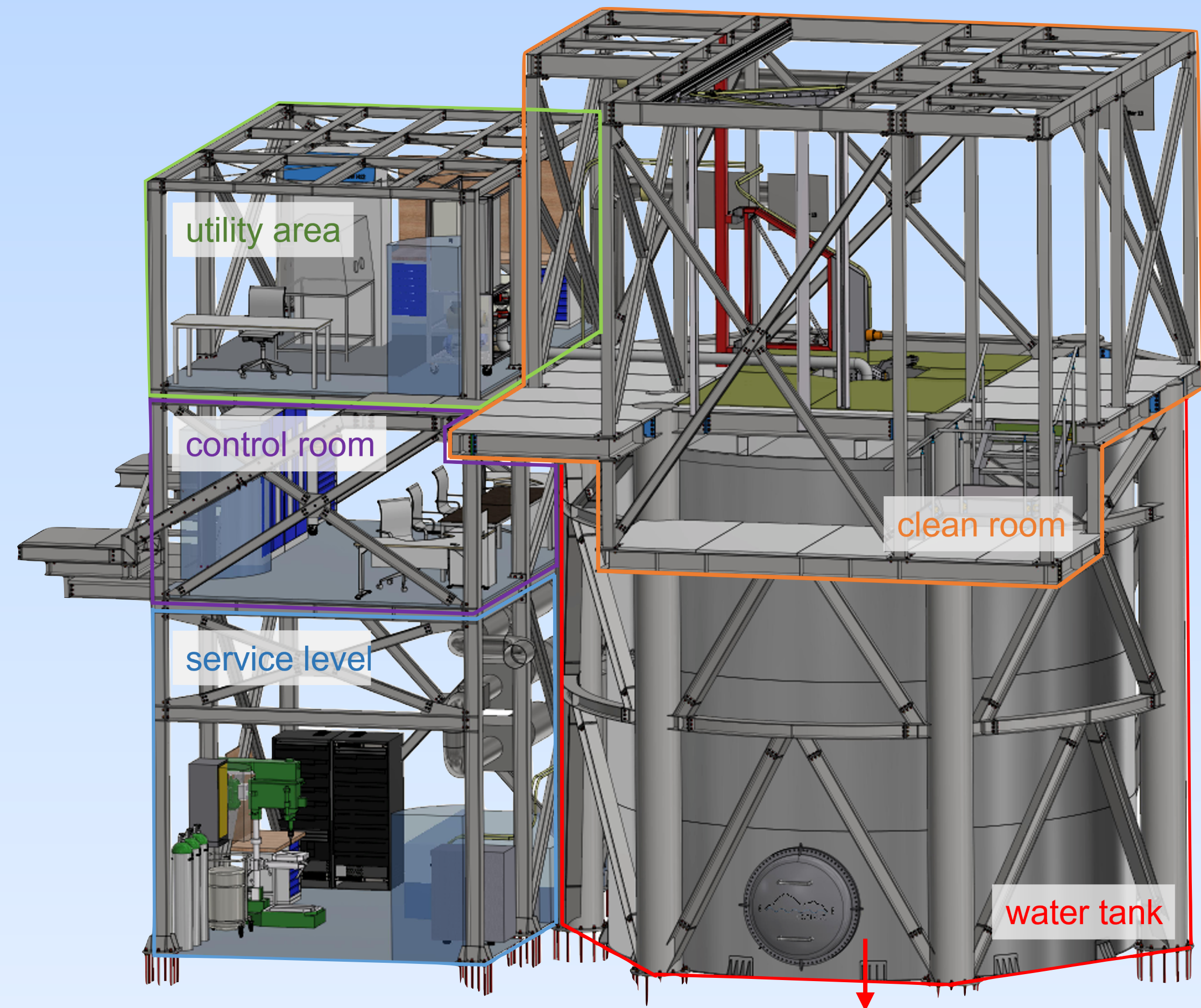
Low-background facility



Eur. Phys. J. C (2022) 82: 248
Follow-up work to be published



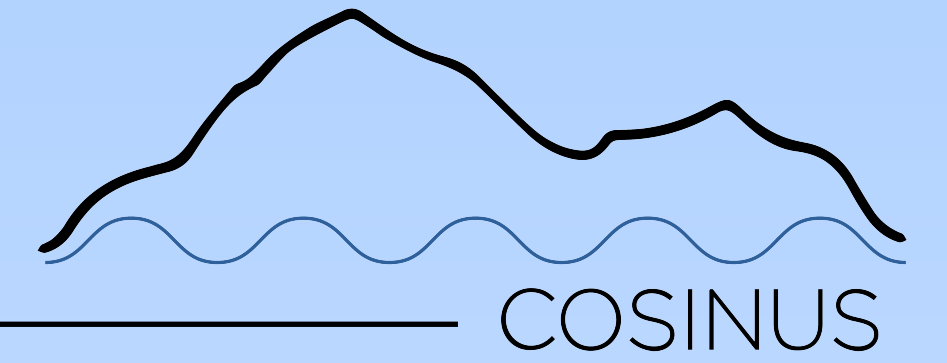
- Instrumented with 28 PMTs to reduce the cosmogenic neutron bkg.
- We simulate 99% muon event veto
45% shower event veto
97% of veto in total
- **no veto:** neutron rate (3.5 ± 0.7) cts $\text{kg}^{-1} \text{yr}^{-1}$
- **veto:** neutron rate (0.11 ± 0.08) cts $\text{kg}^{-1} \text{yr}^{-1}$



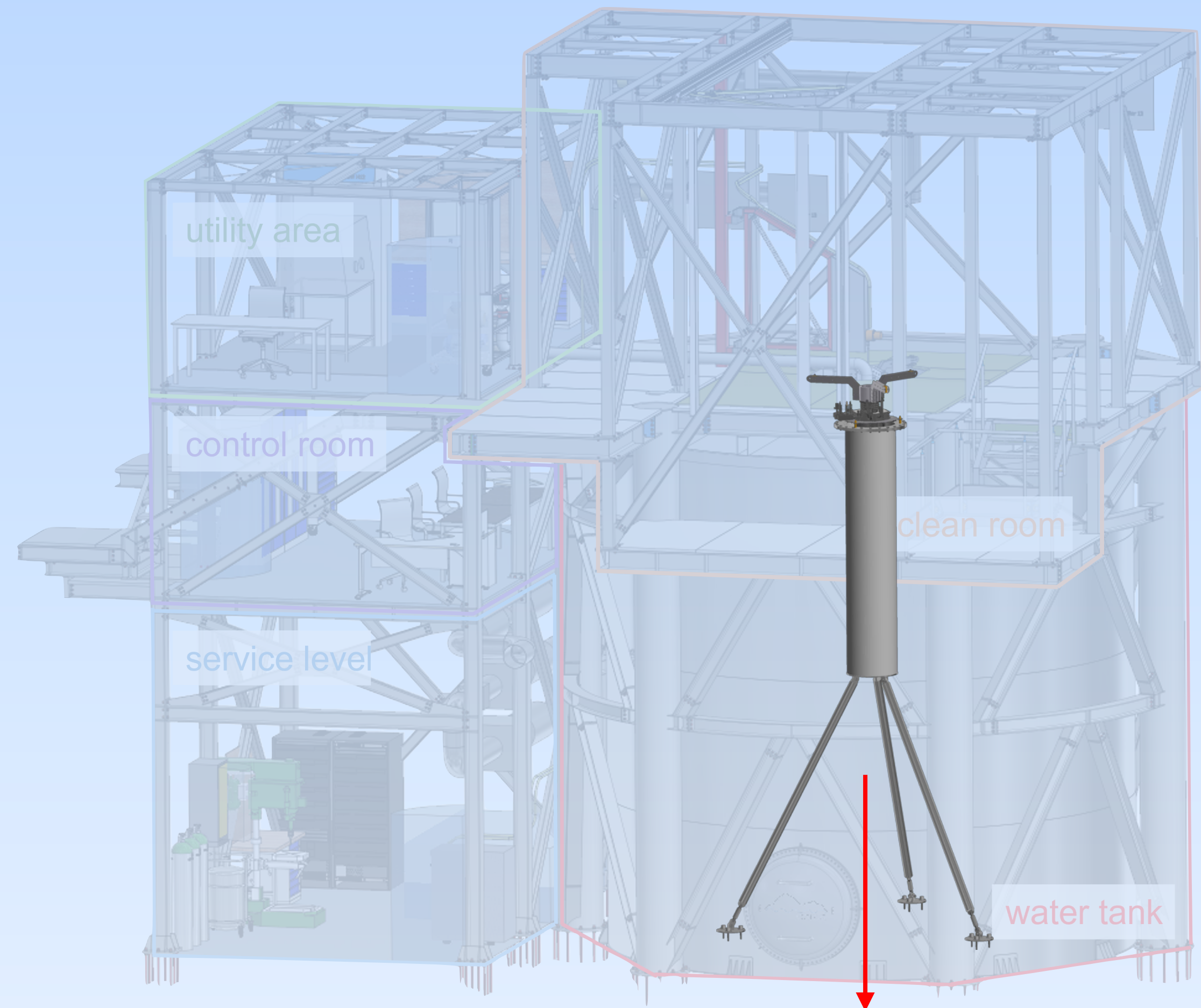
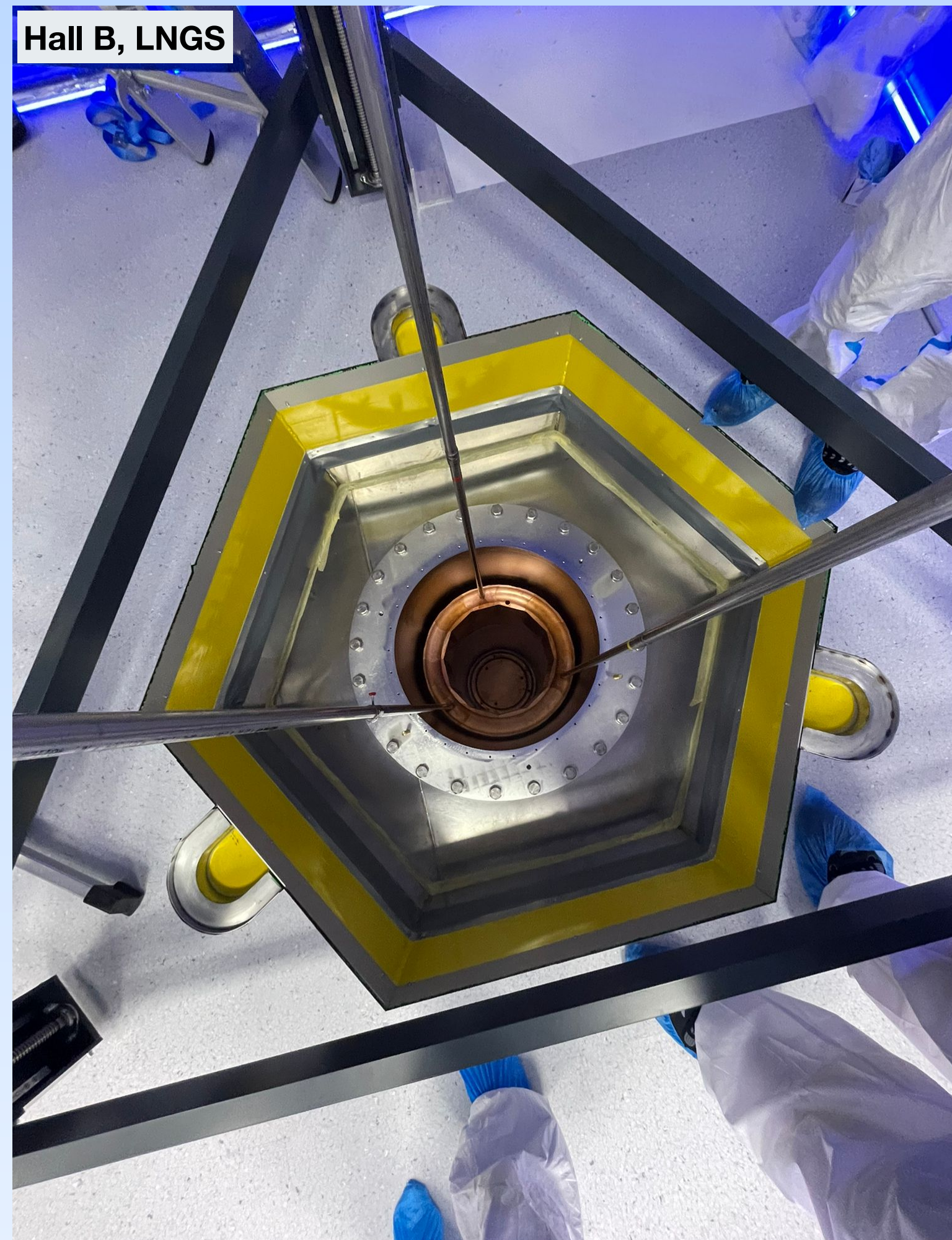
Water Cherenkov Muon Veto



COSINUS

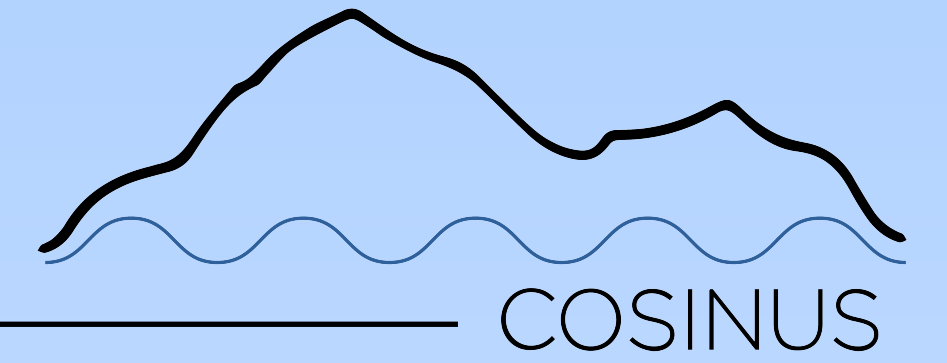


Low-background facility

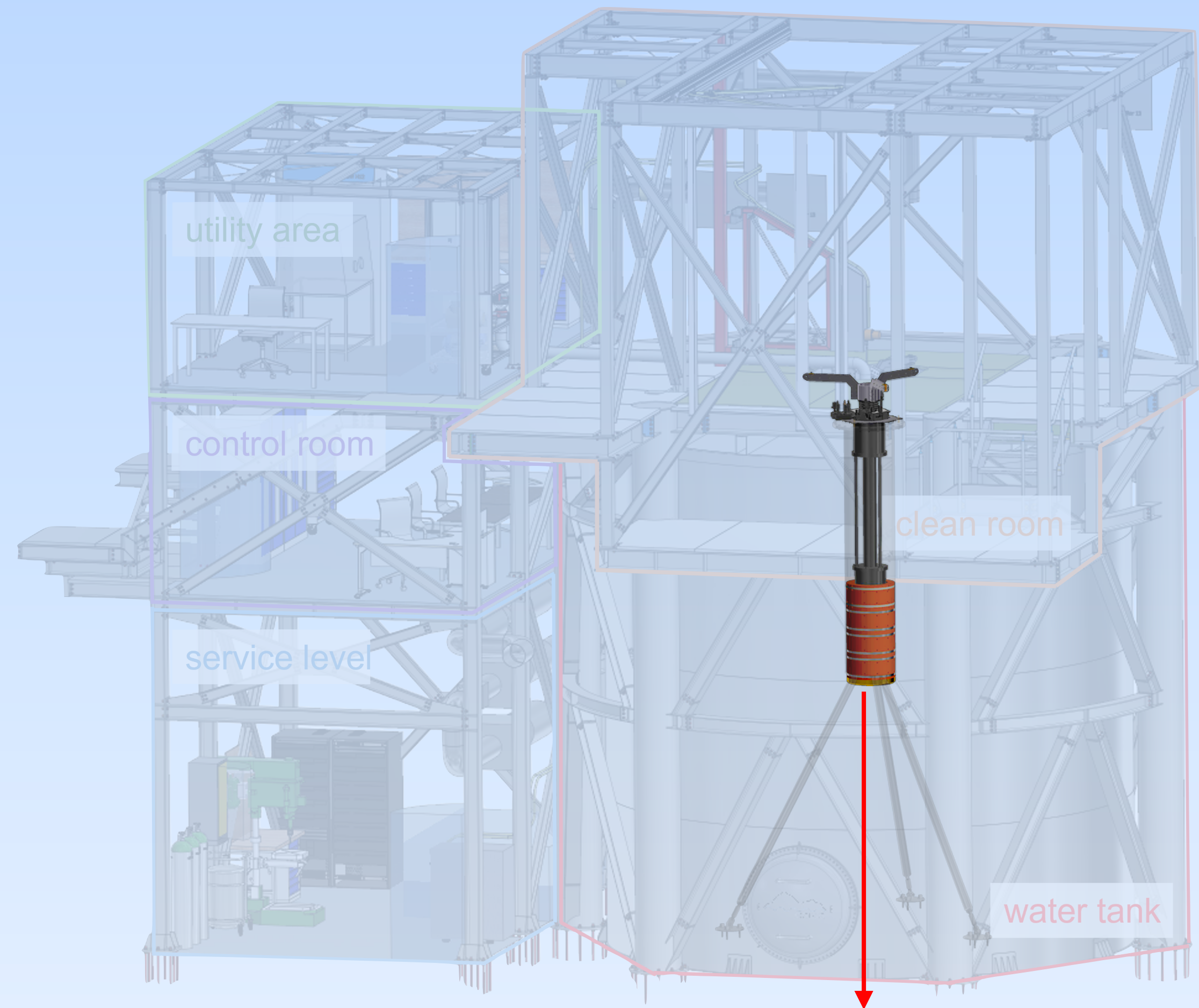
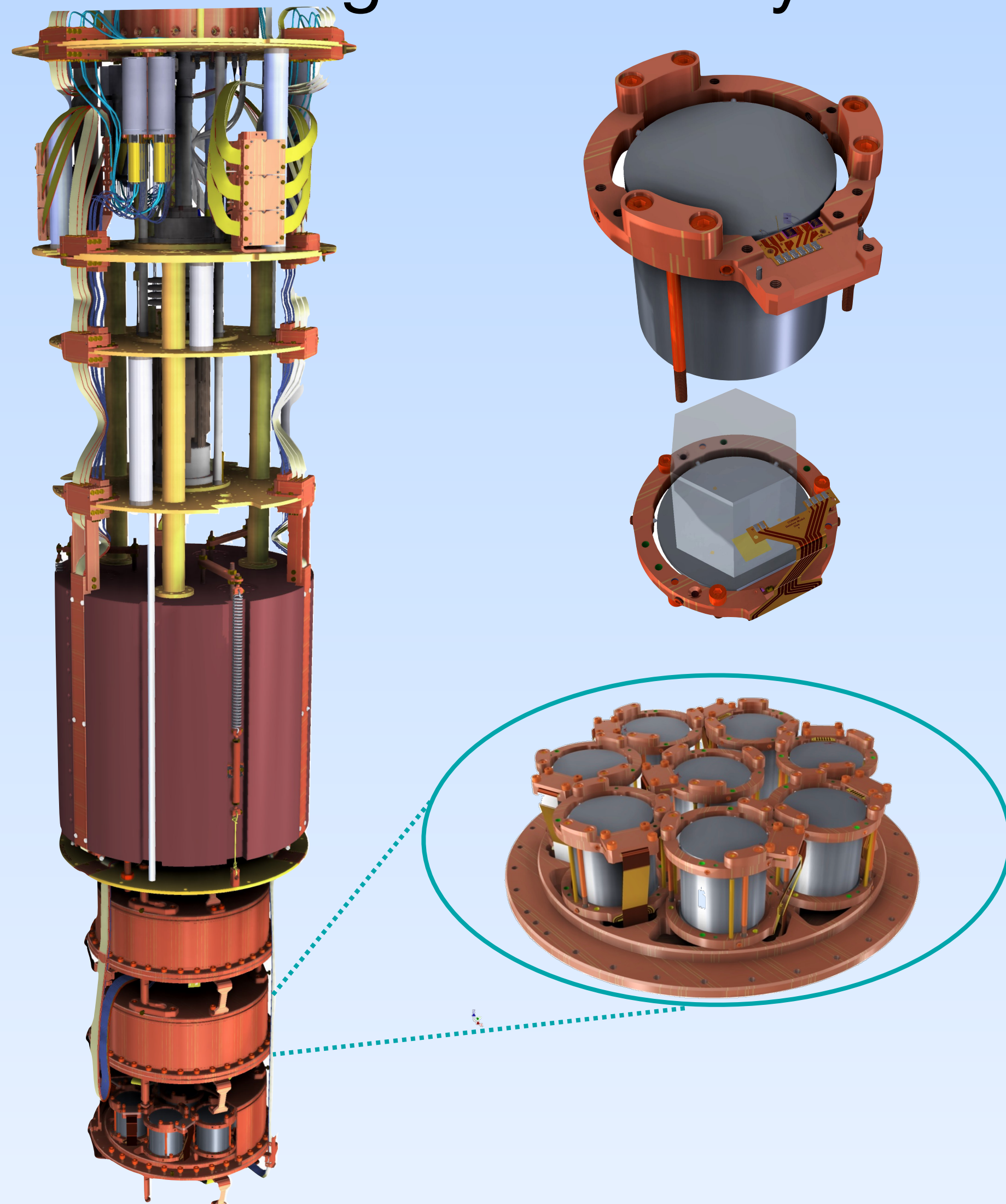


Dry well

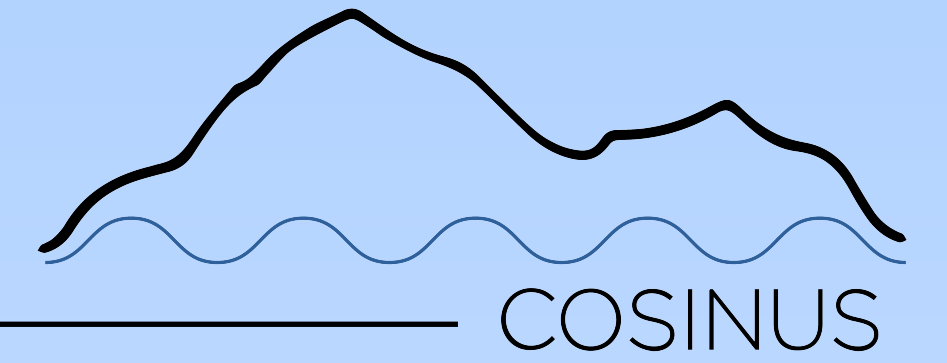
COSINUS



Low-background facility



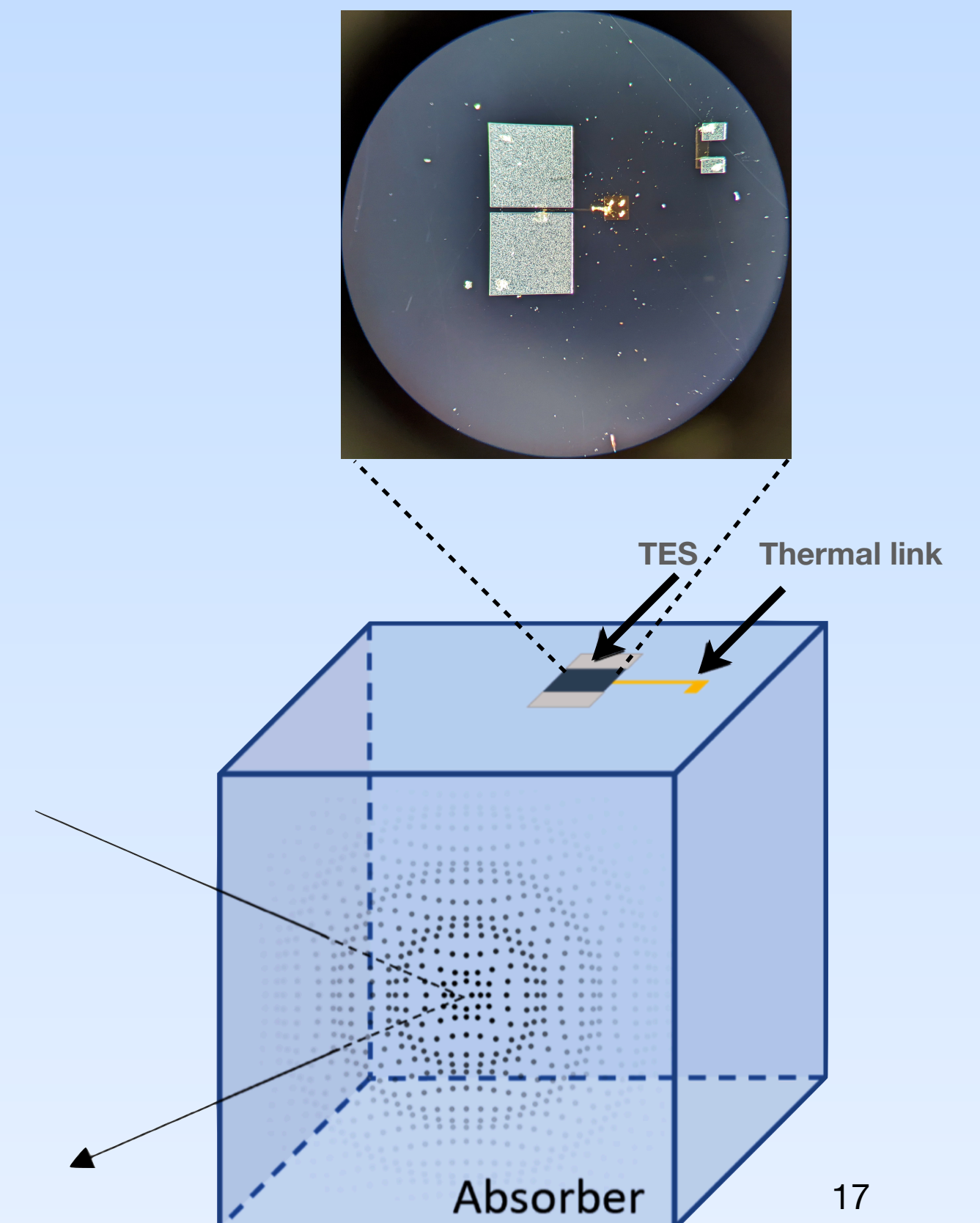
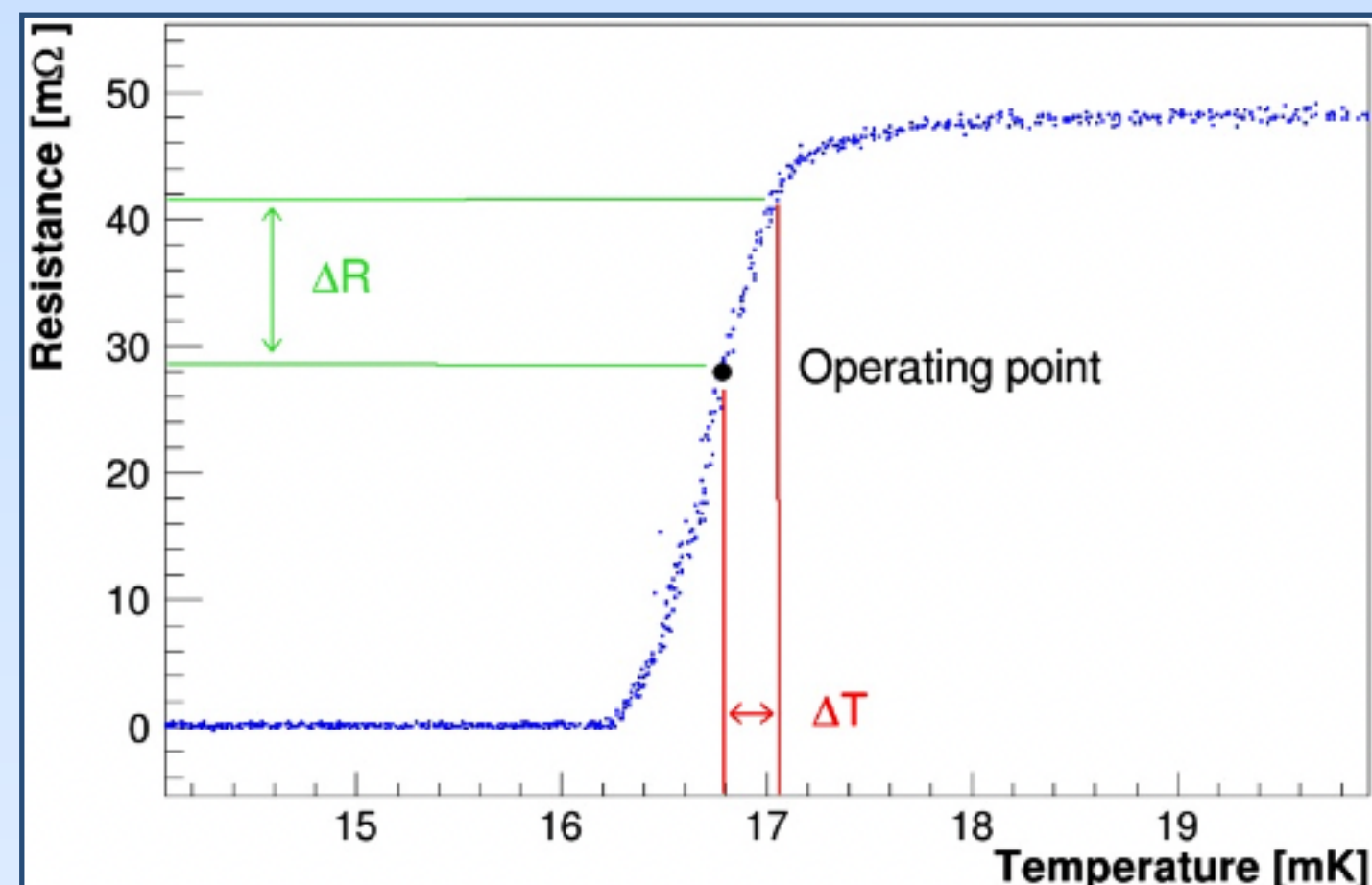
Detector design



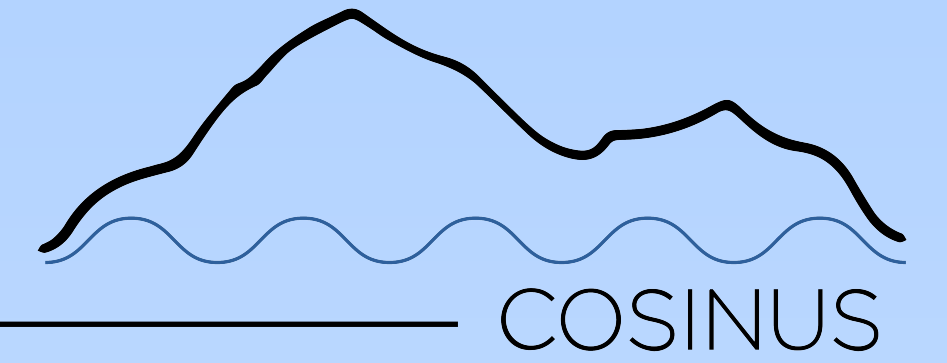
Working principle

- Transition Edge Sensors (TES): extremely sensitive phonon-mediated energy detectors.

Energy Deposition (keV) \rightarrow Temperature Change (μK) \rightarrow Resistance Change ($\text{m}\Omega$)



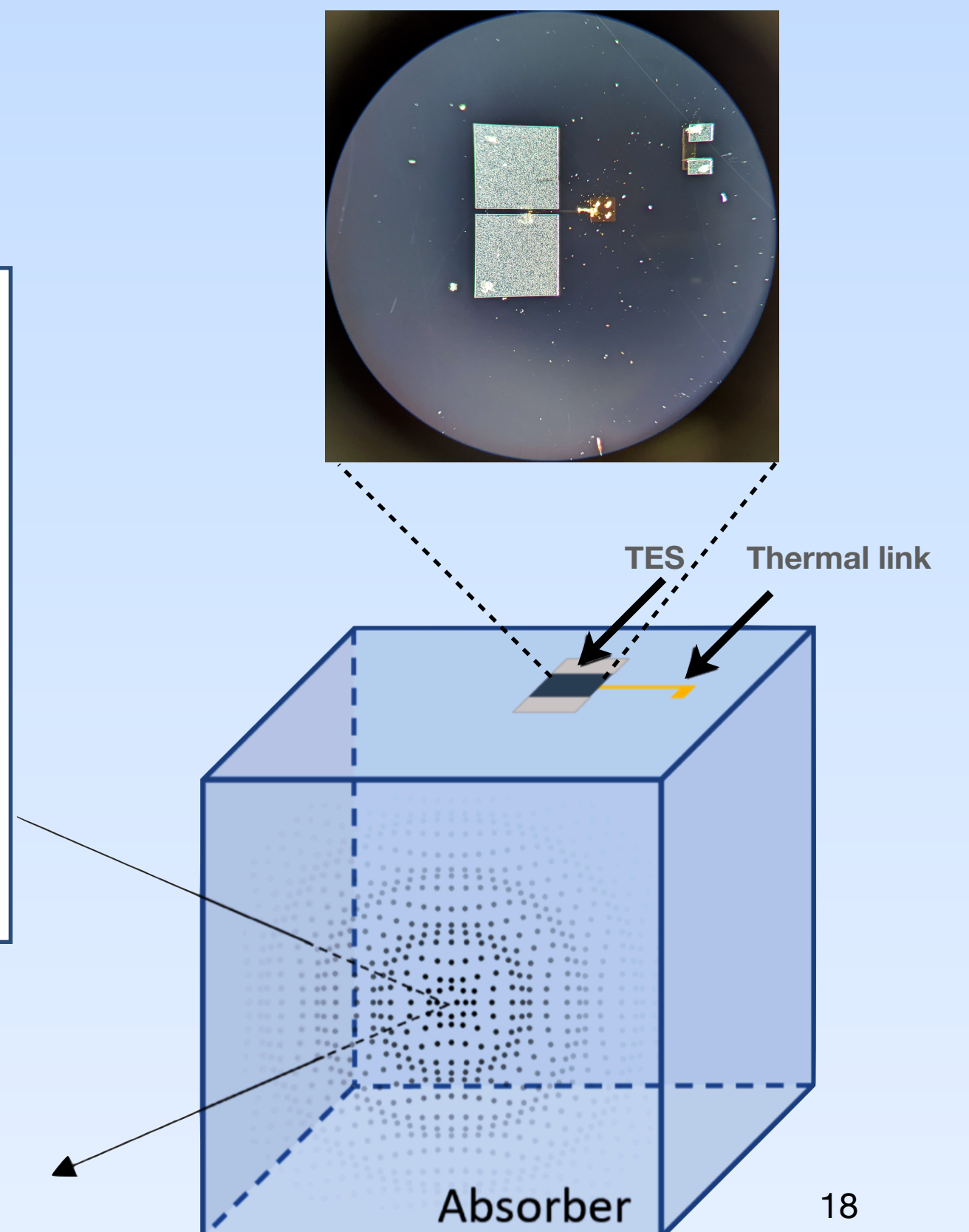
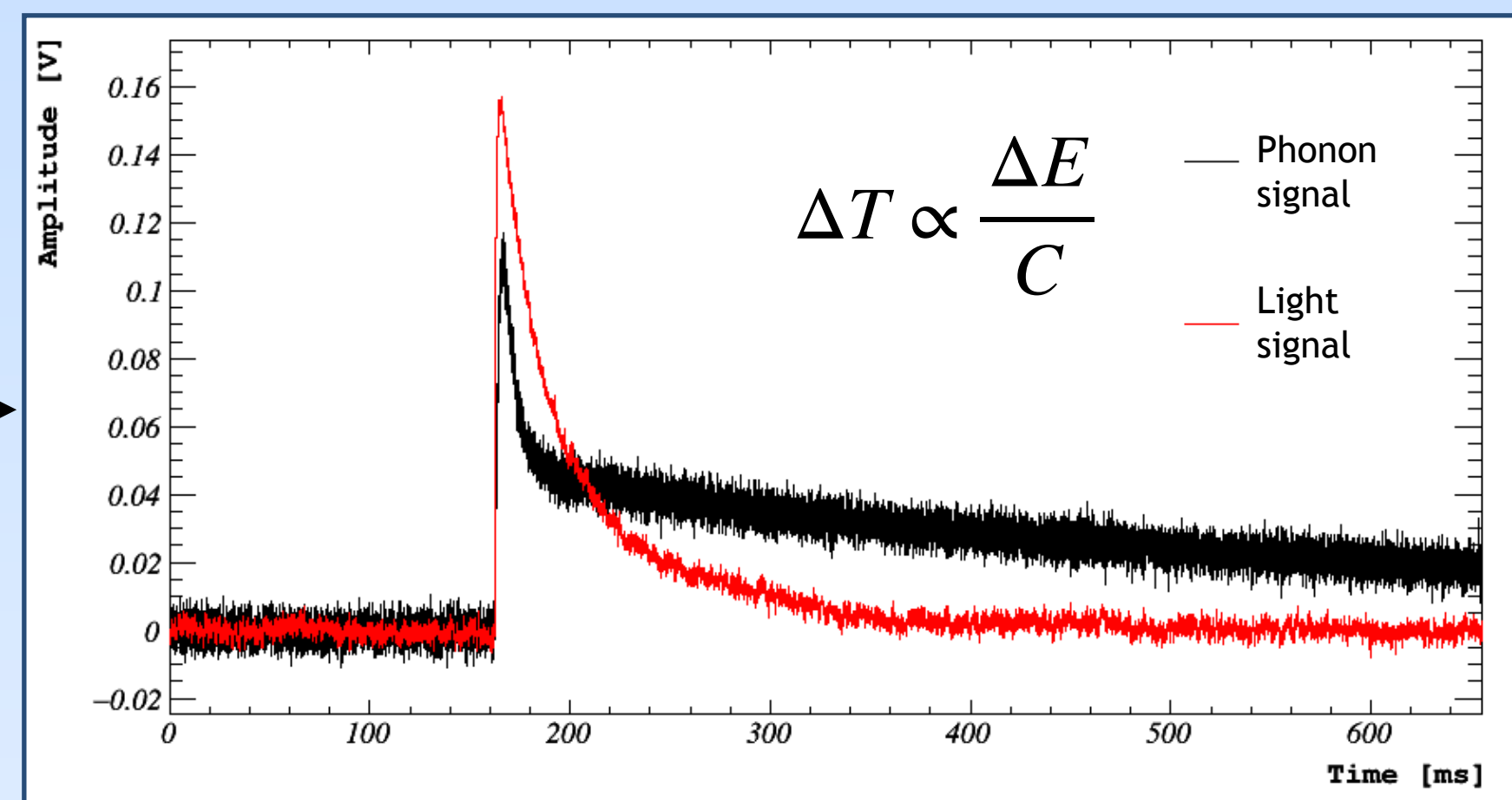
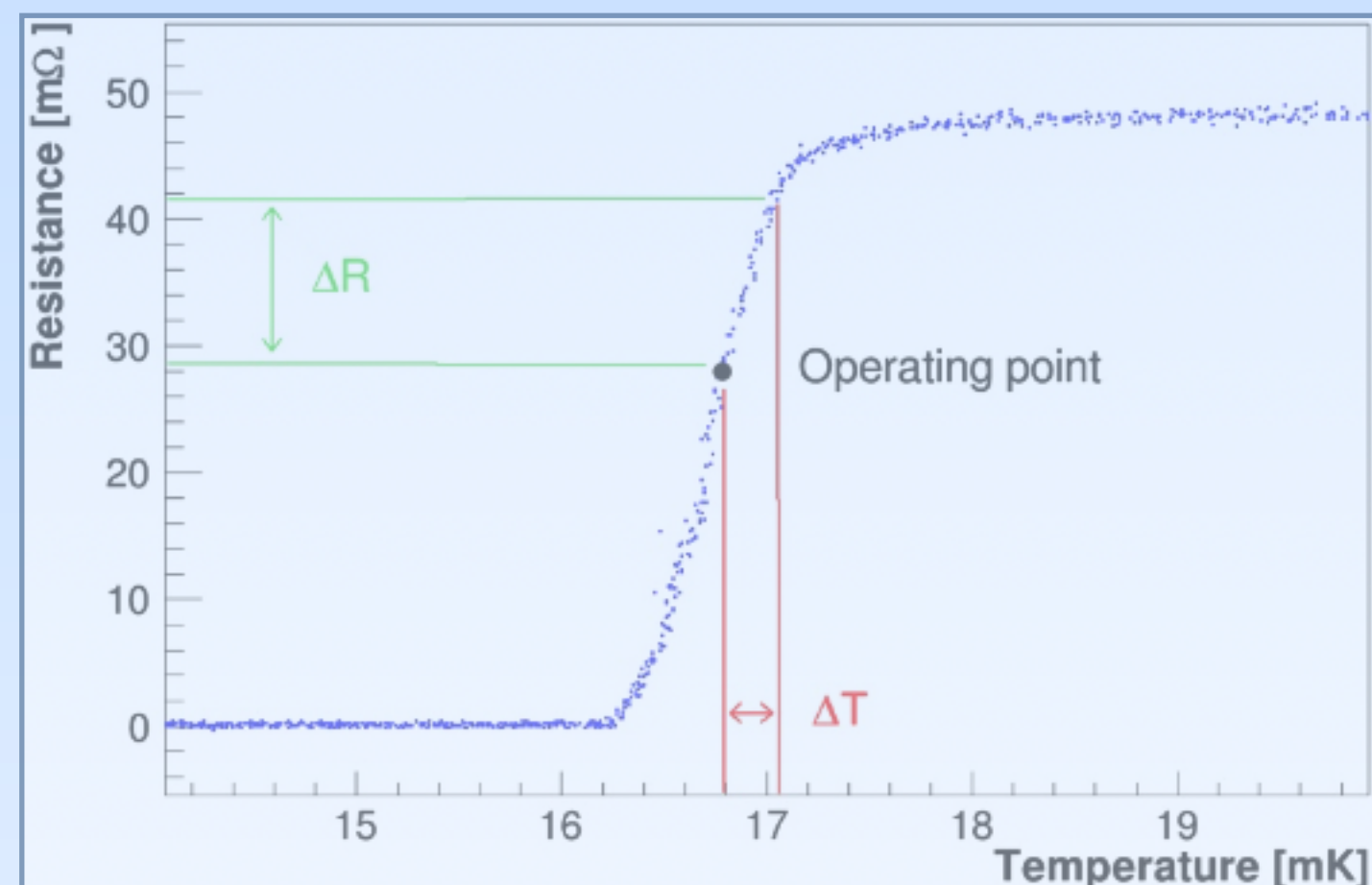
Detector design



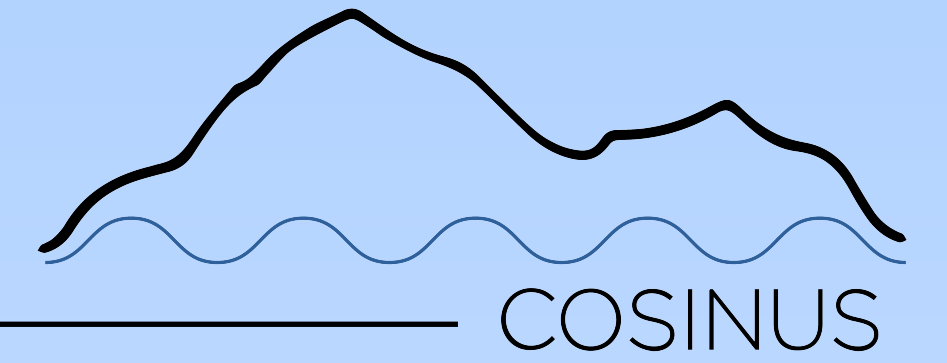
Working principle

- Transition Edge Sensors (TES): extremely sensitive phonon-mediated energy detectors.

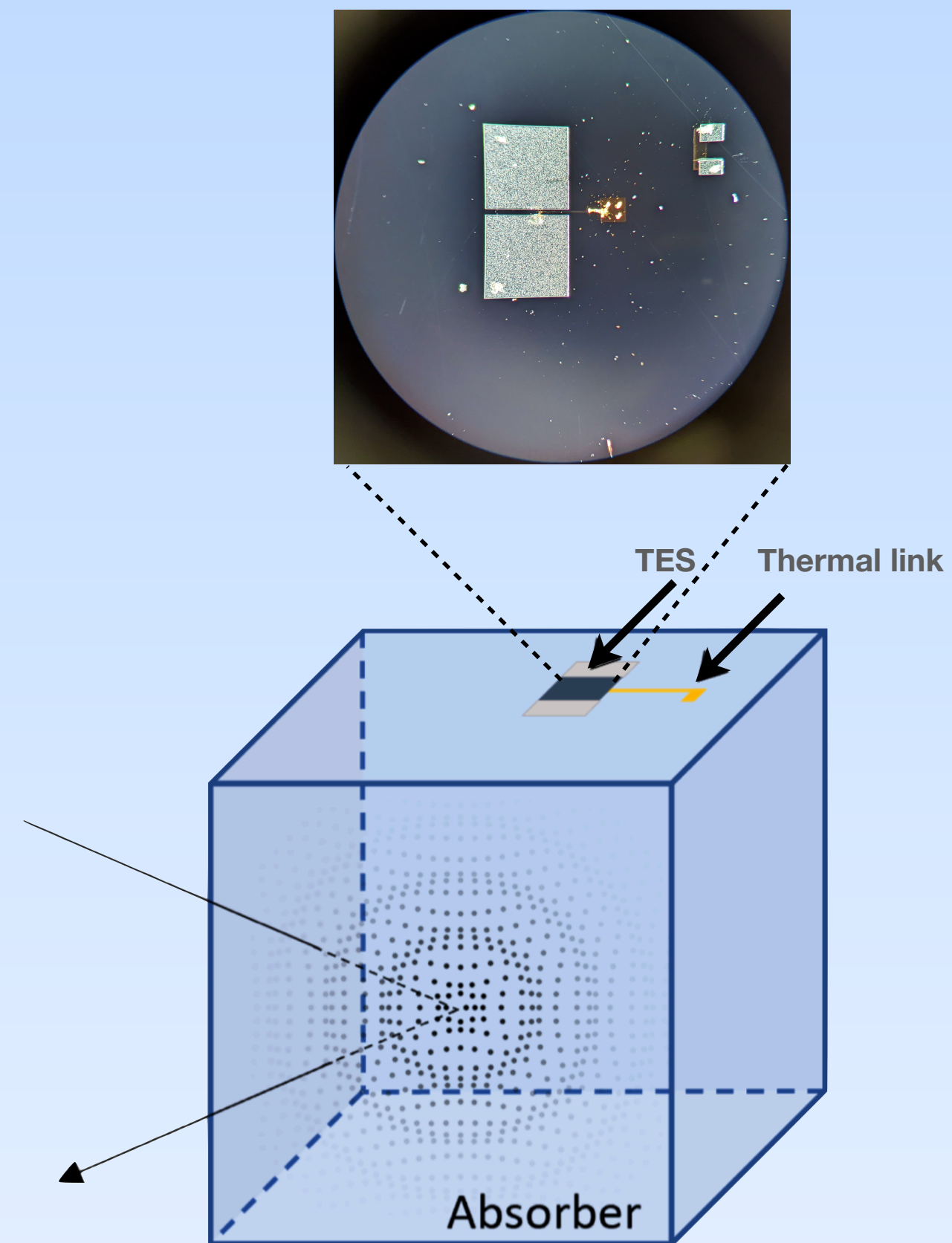
Energy Deposition (keV) \rightarrow Temperature Change (μK) \rightarrow Resistance Change ($\text{m}\Omega$)



Detector design

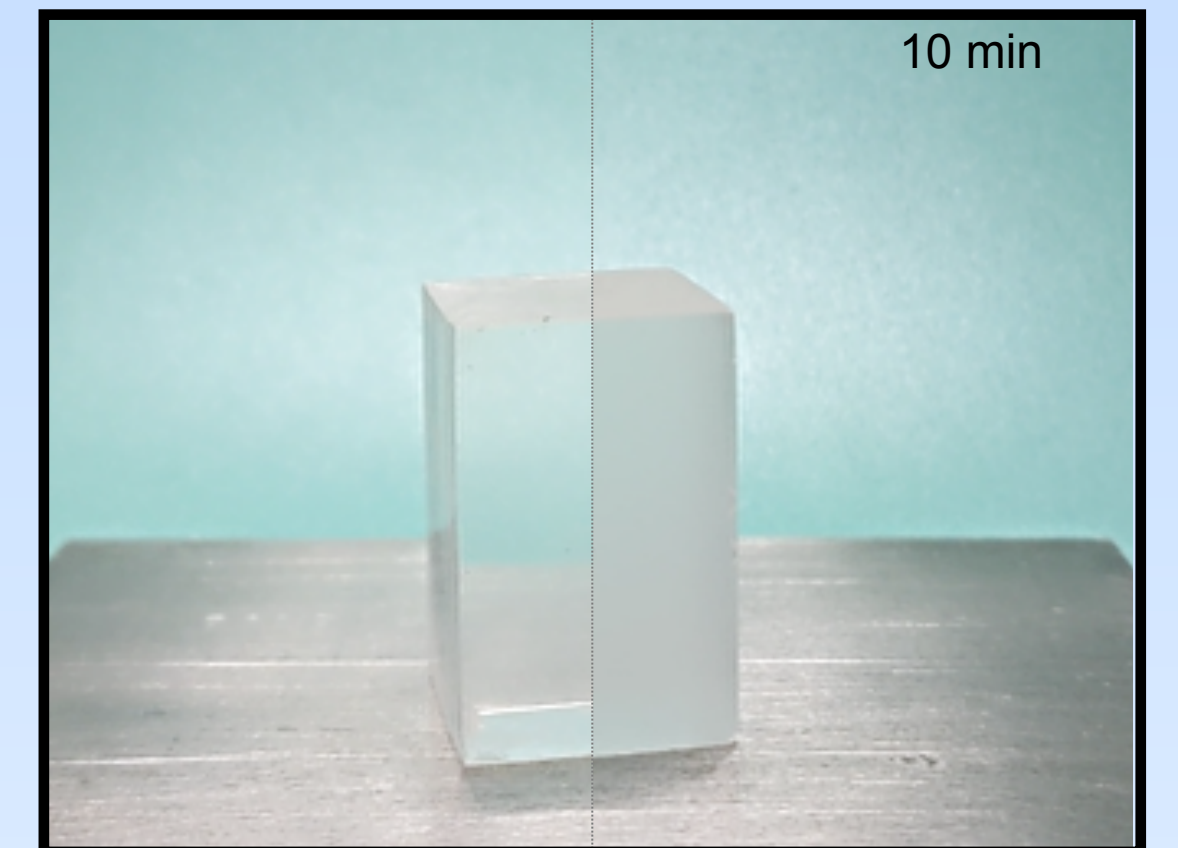


Why *remoTES*?



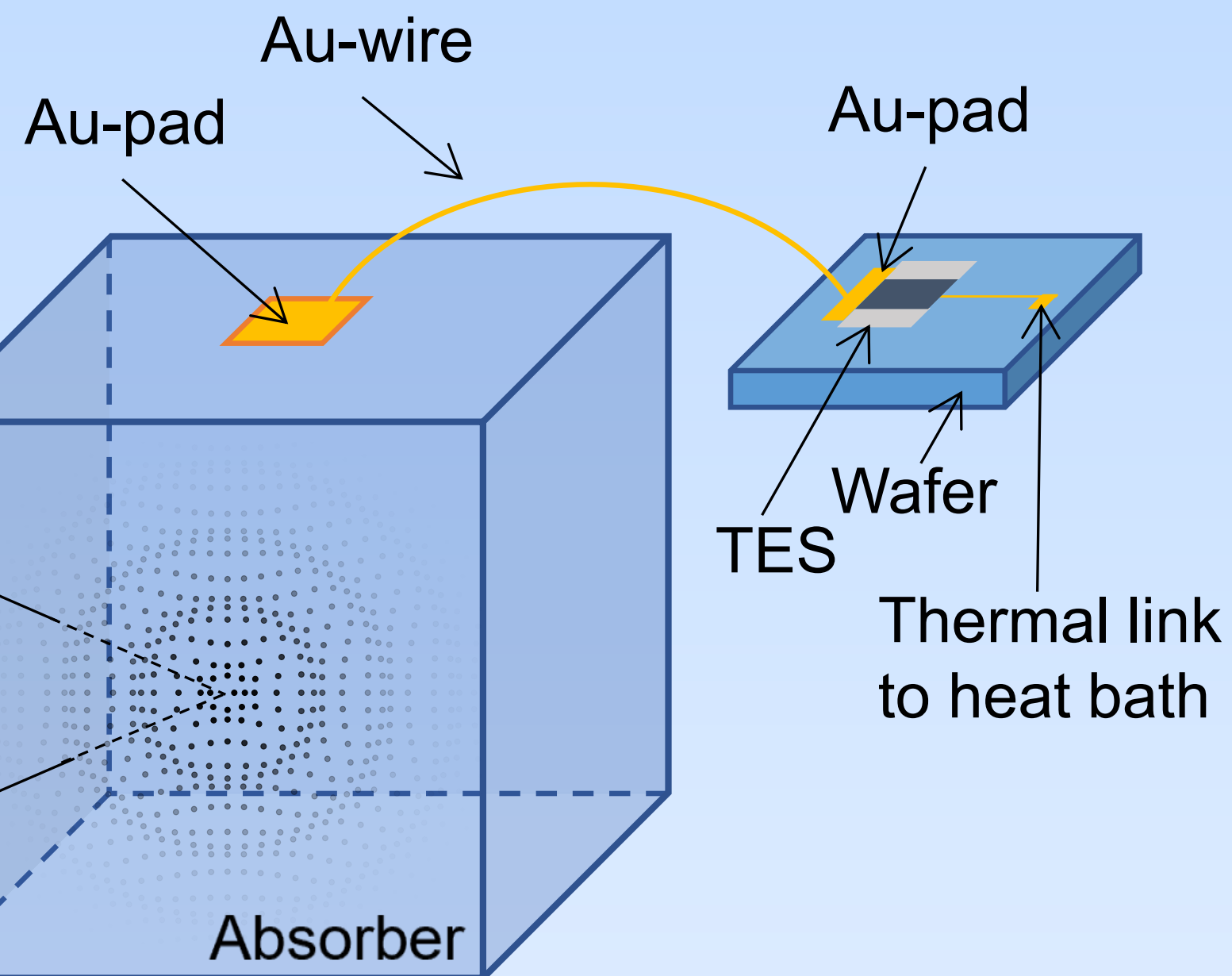
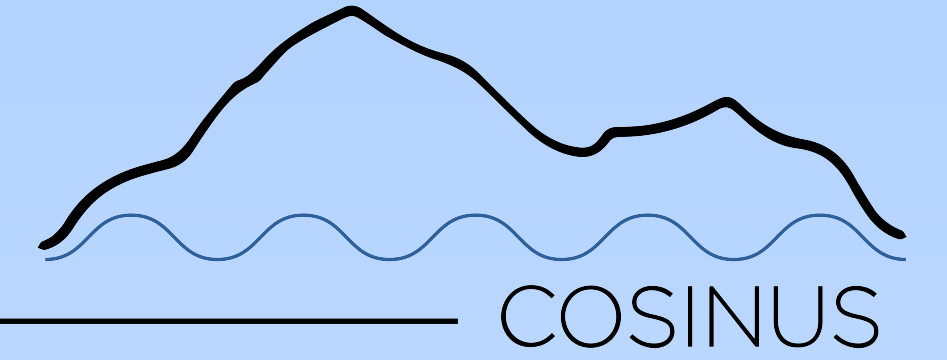
Problem: Traditional TES deposition not possible on NaI

- Hygroscopic
- Soft
- Low melting point



Detector design

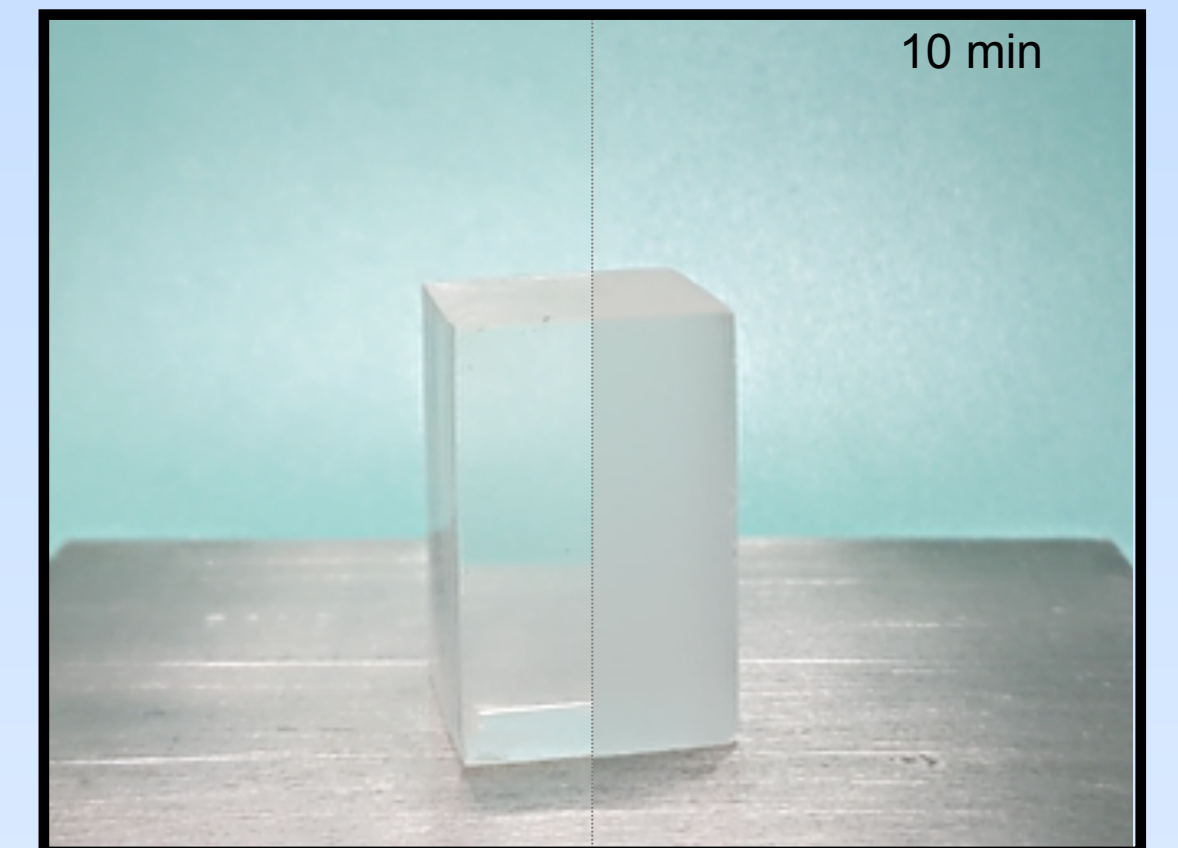
Why *remoTES*?



Problem: Traditional TES deposition not possible on NaI

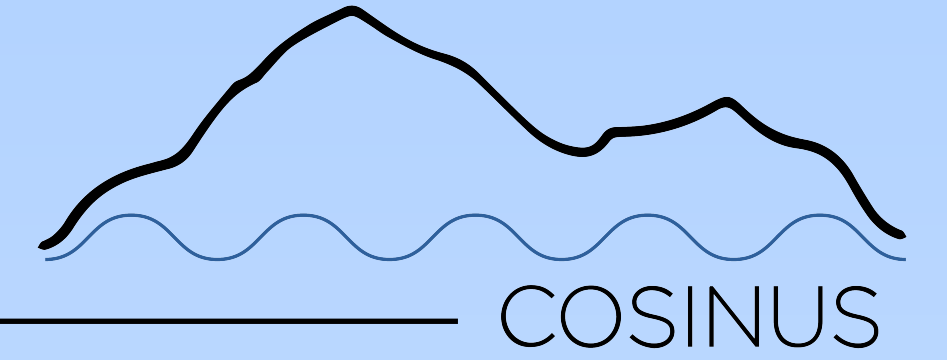
- Hygroscopic
- Soft
- Low melting point

● **Solution:** The remoTES design



First proposed in Matt Pyle *et al*, [arxiv:1503.01200](https://arxiv.org/abs/1503.01200)

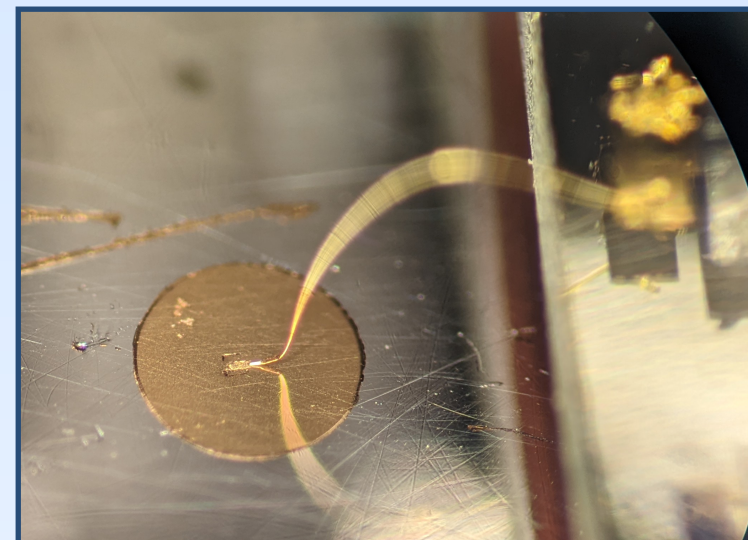
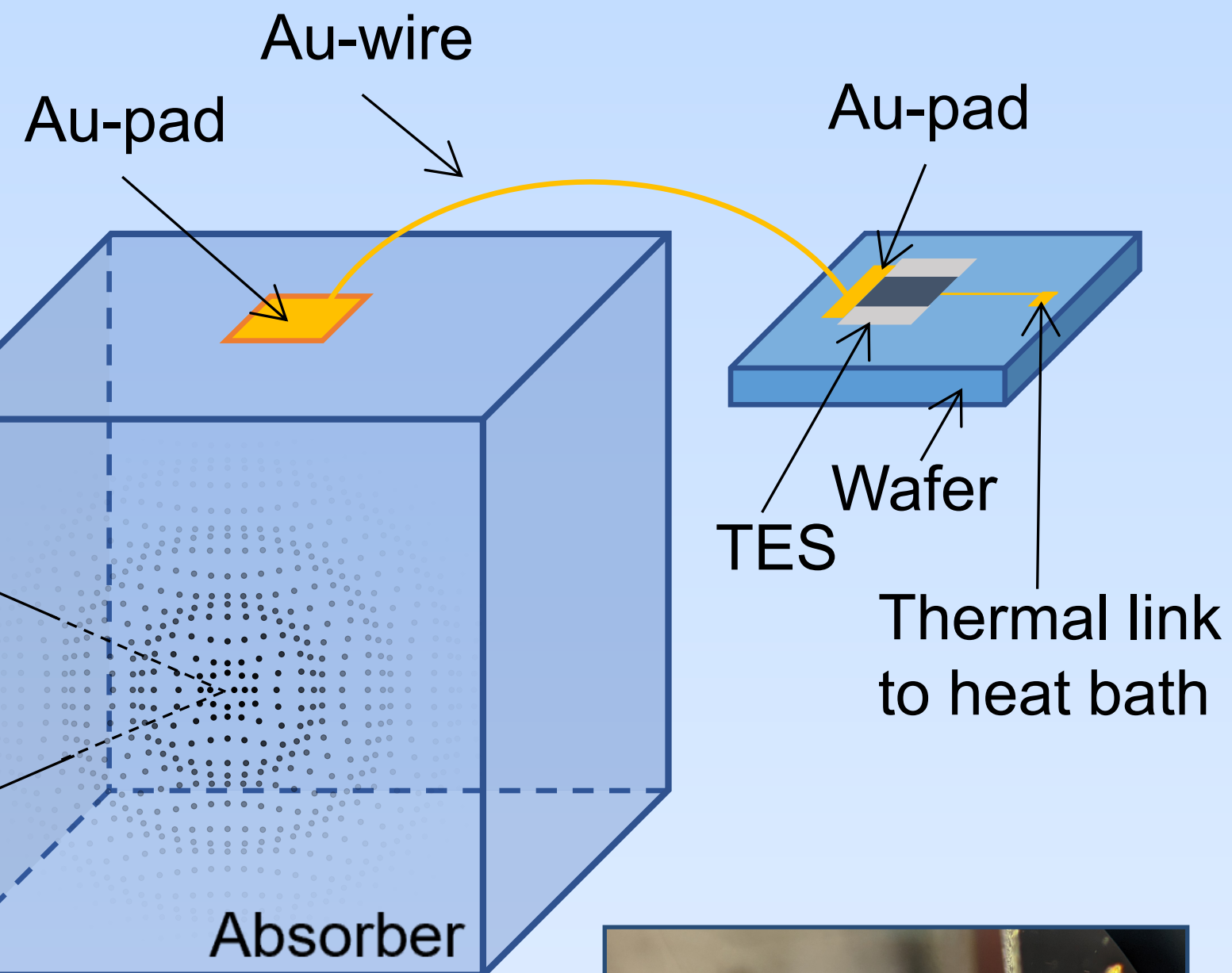
Detector design



Why *remoTES*?

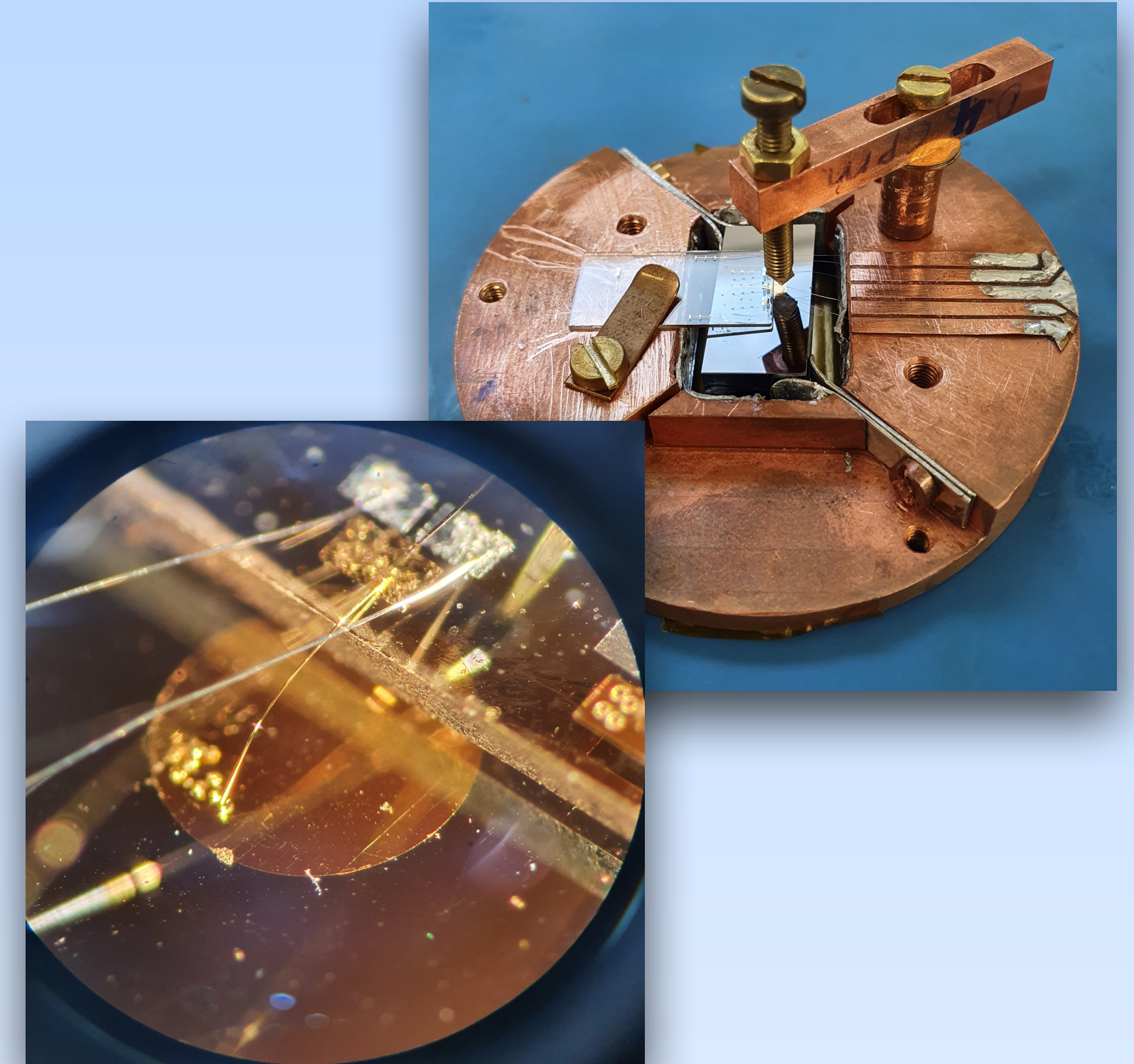
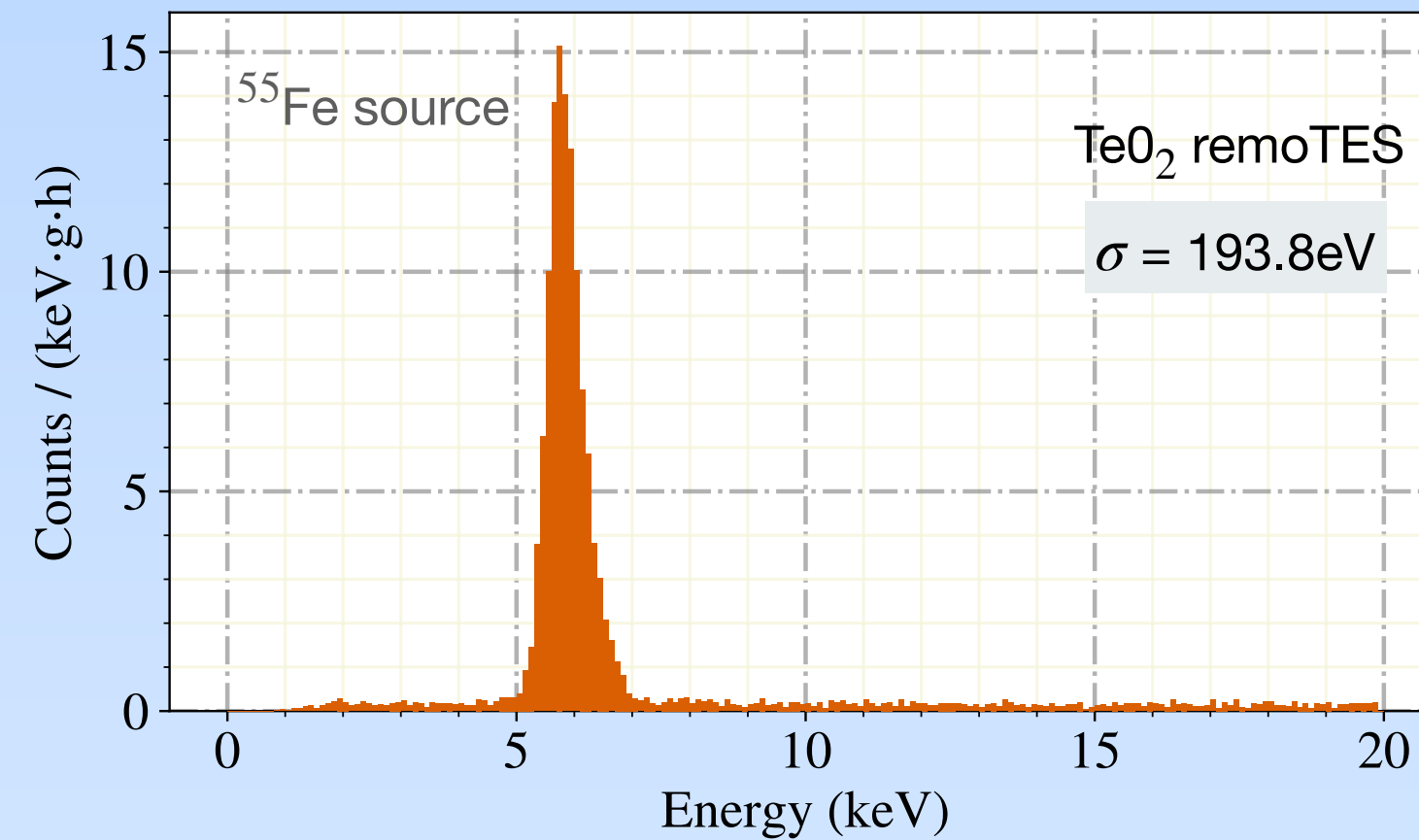
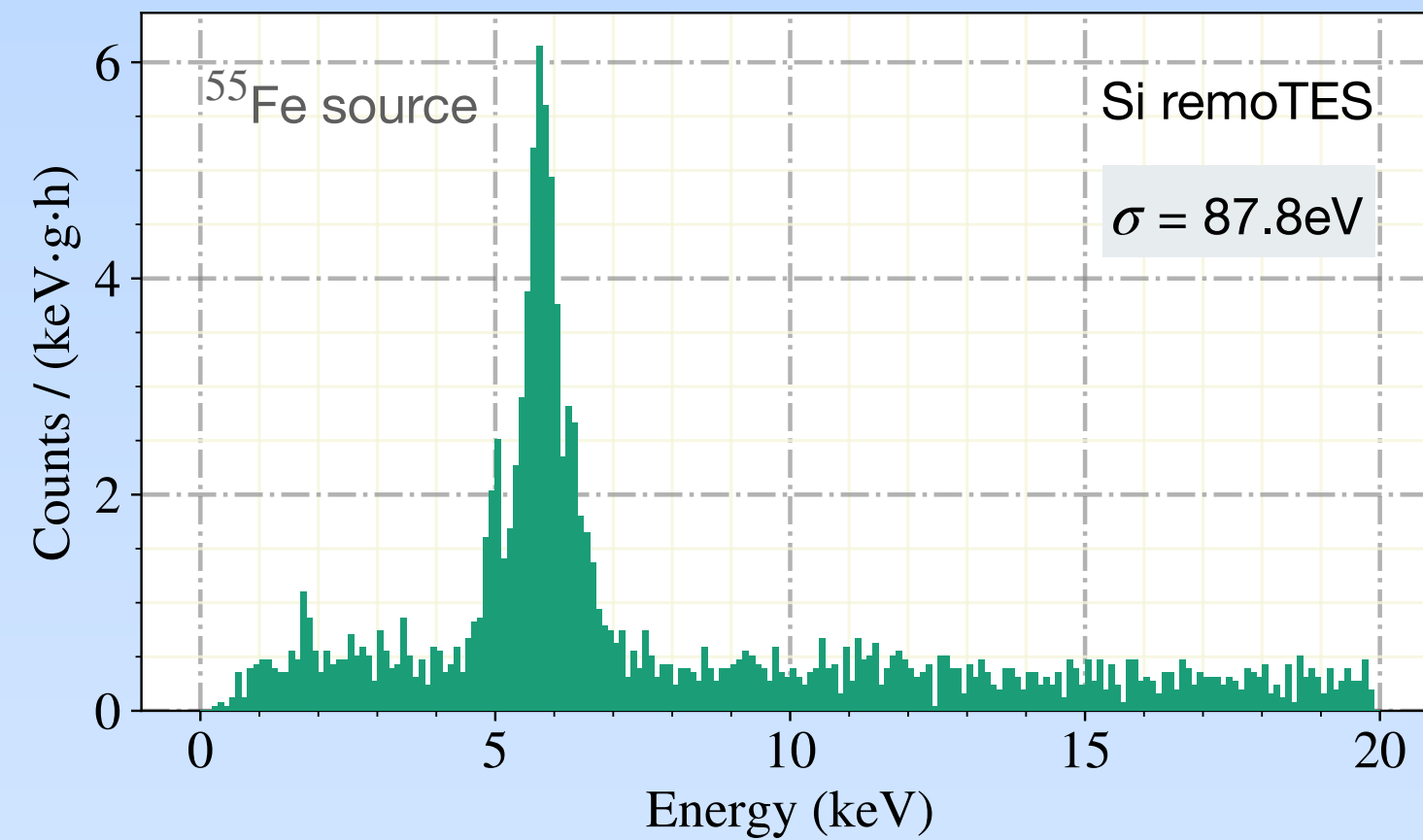
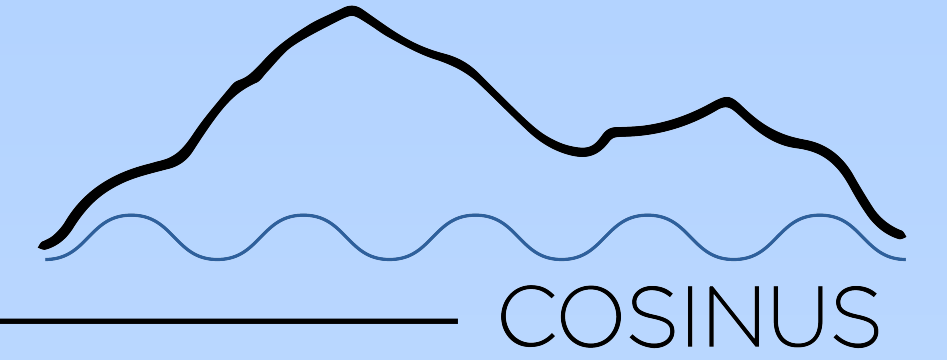
ADVANTAGES:

- Absorber is not subjected to manufacturing processing associated with TES fabrication.
- Opens possibility to test other non-standard absorbers as cryogenic calorimeters.
- Easier to fabricate large array of detectors with better reproducibility.



First prototypes

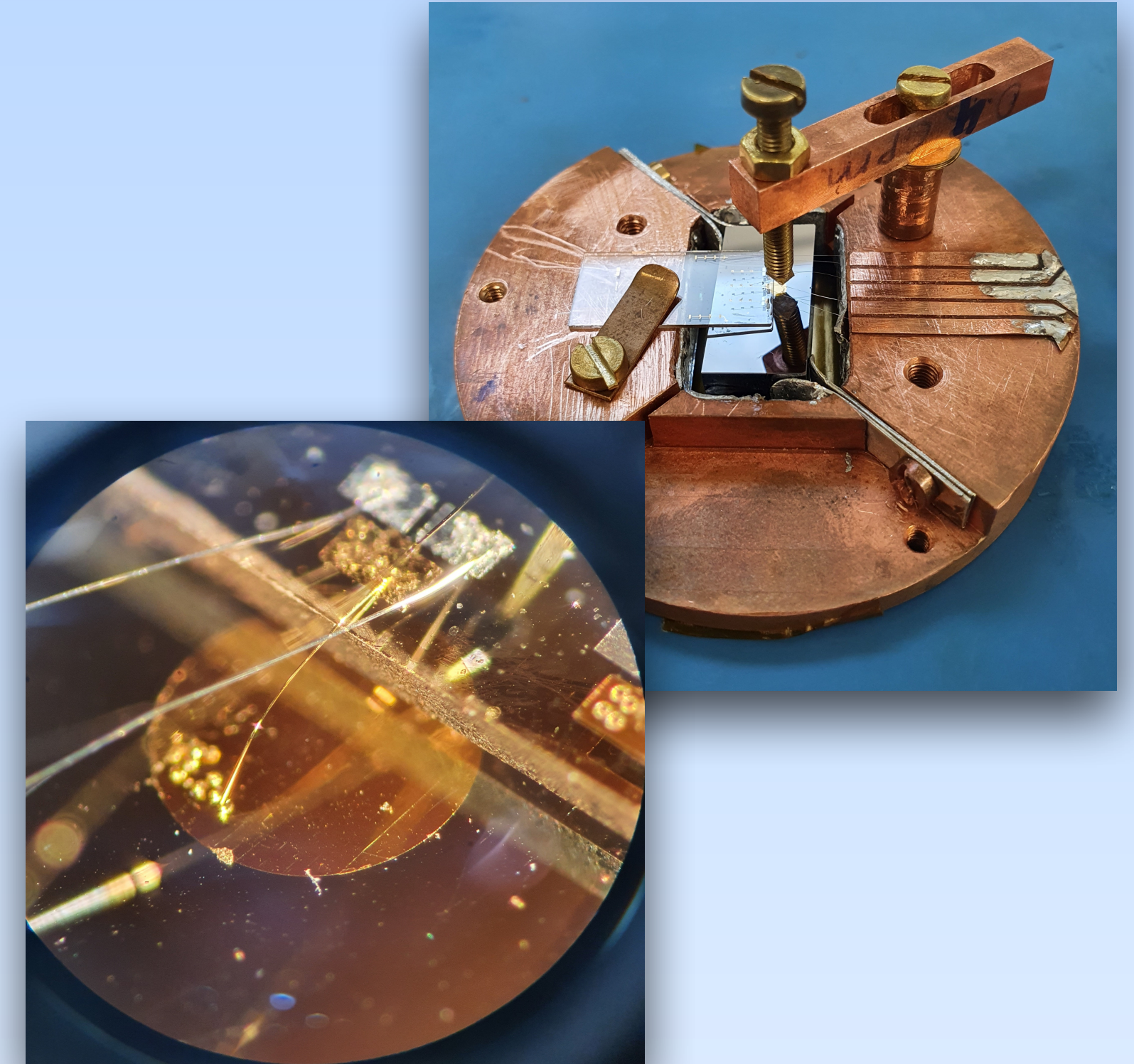
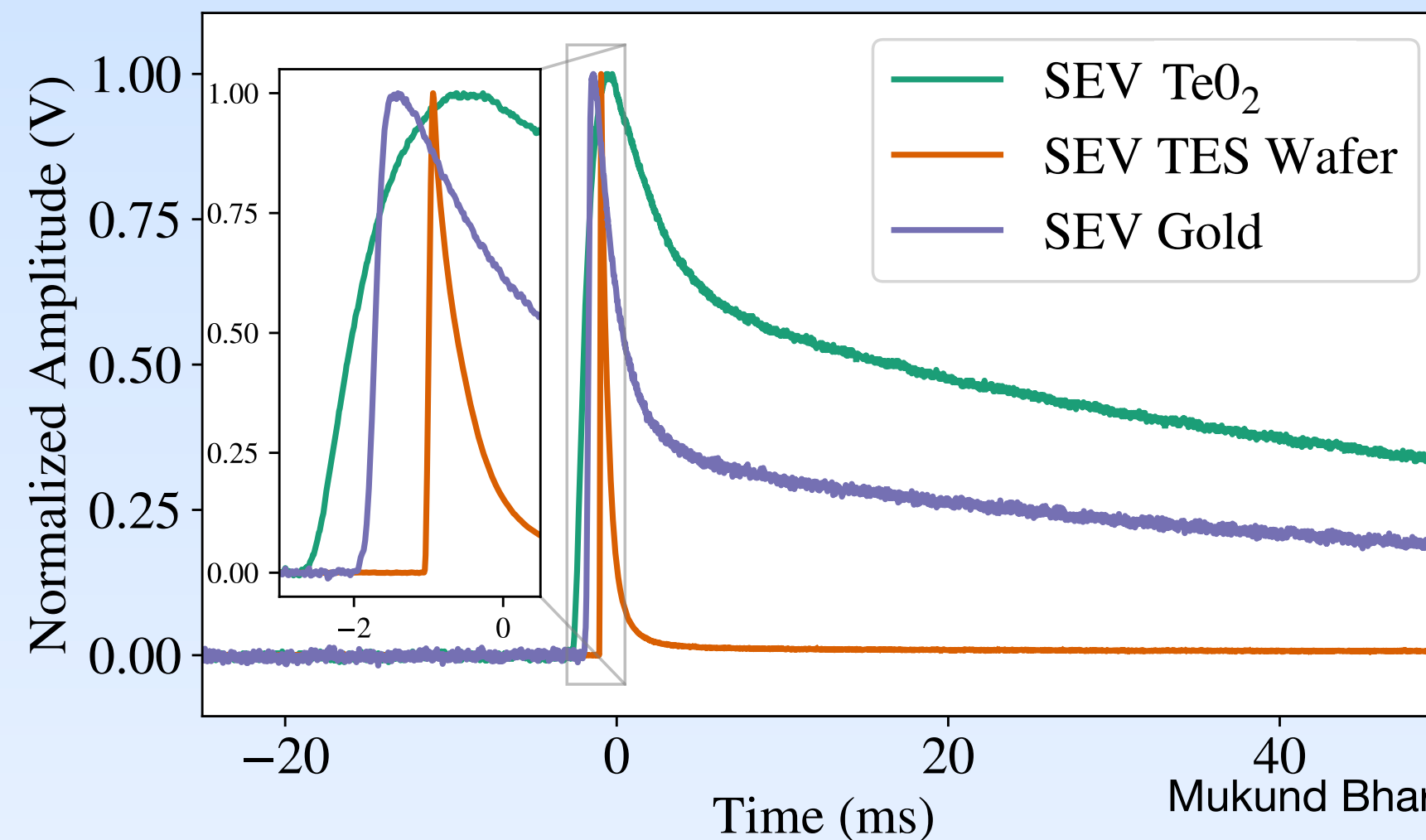
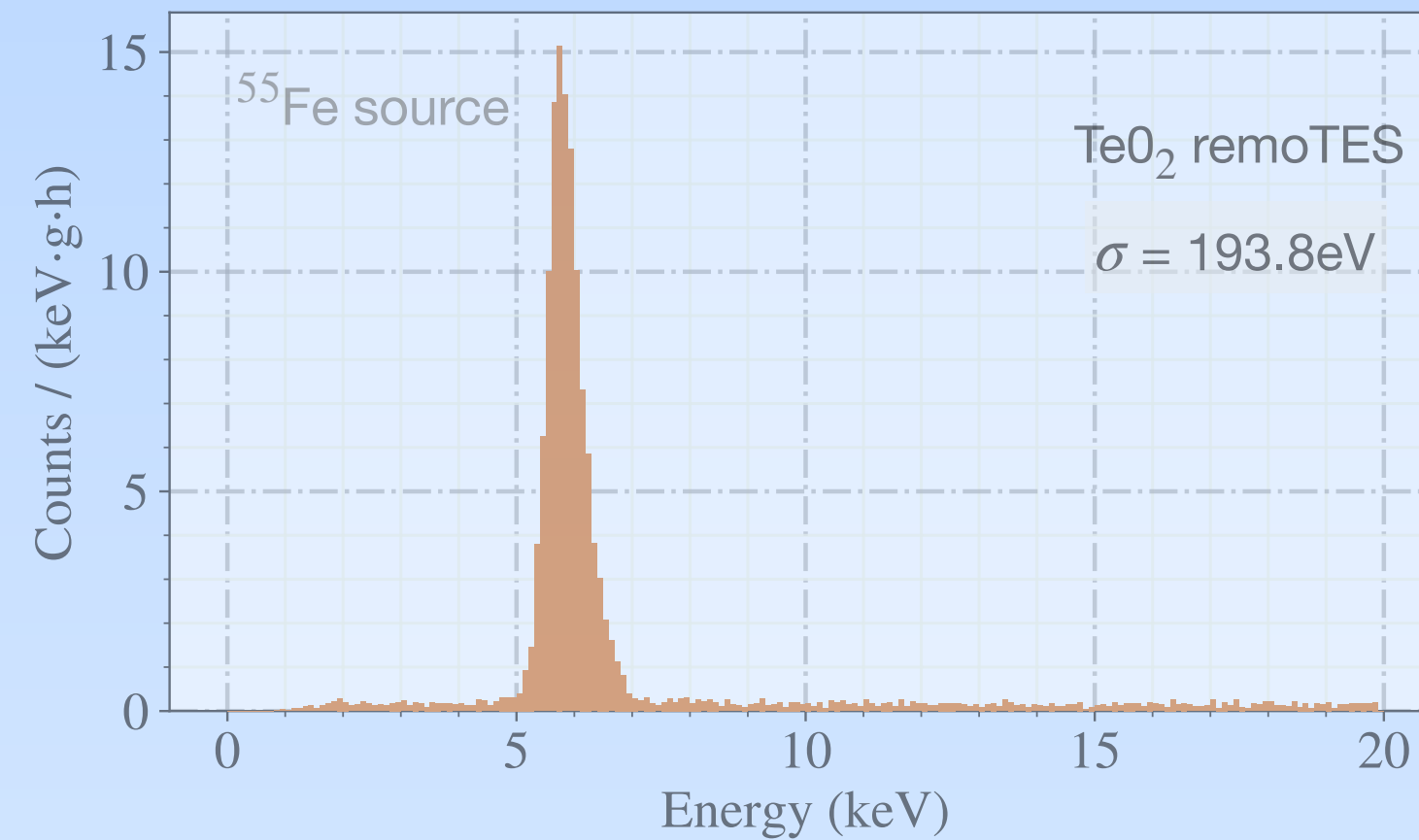
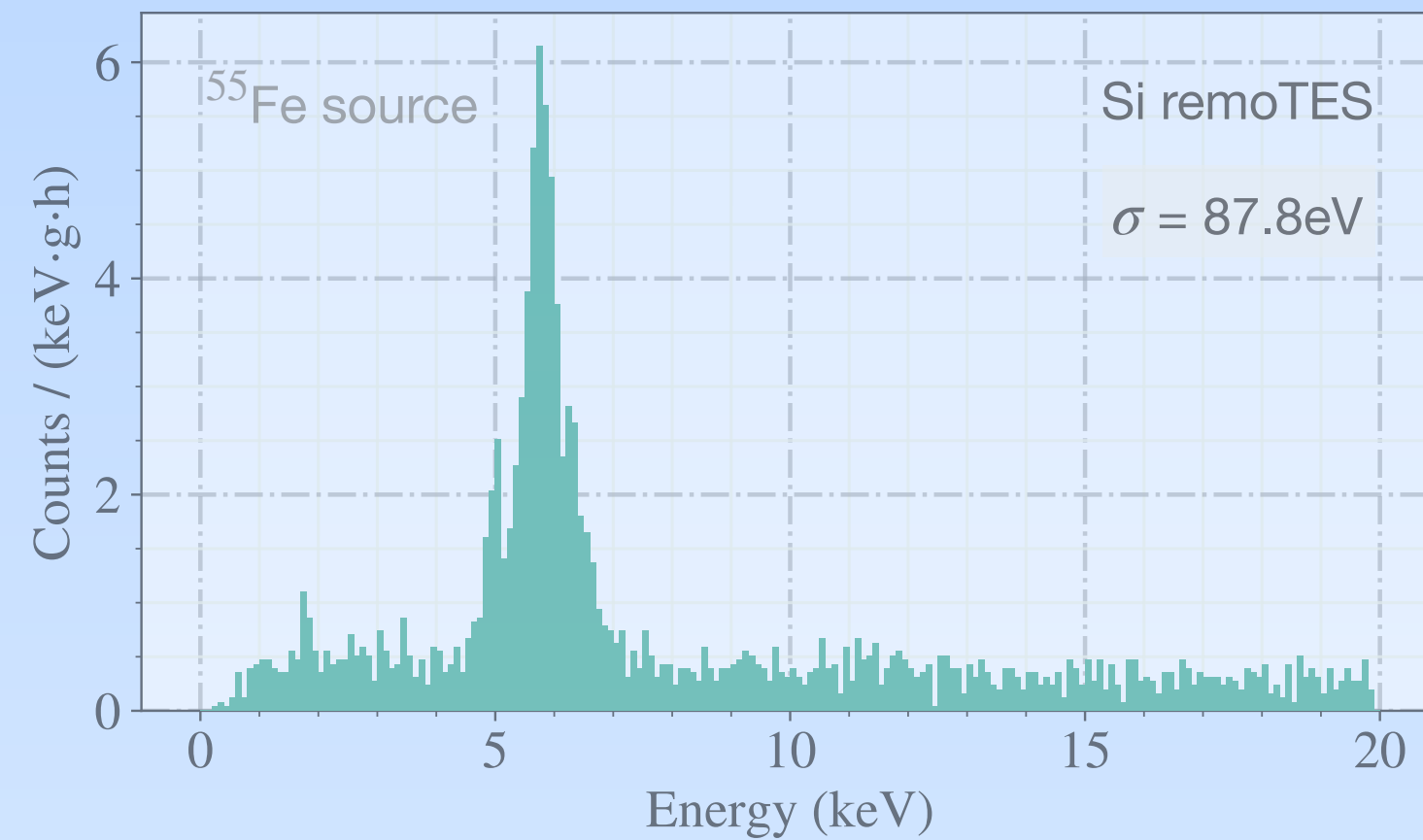
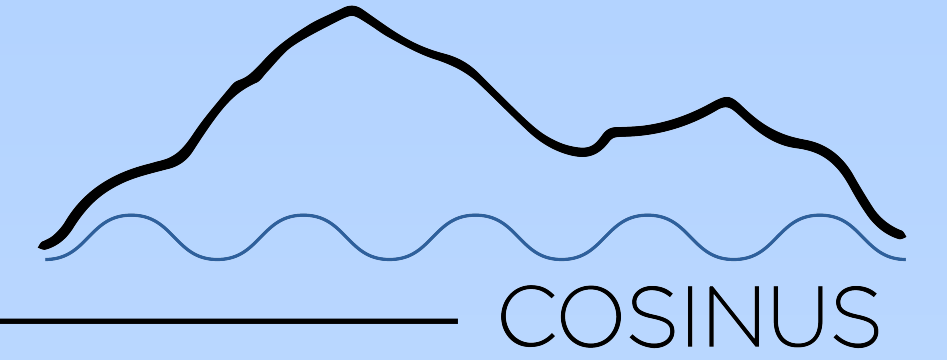
Proof-of-concept



[G. Angloher et al. \(COSINUS collaboration\), Nucl. Instrum. Methods:A, 1045, 167532 \(2023\).](#)

First prototypes

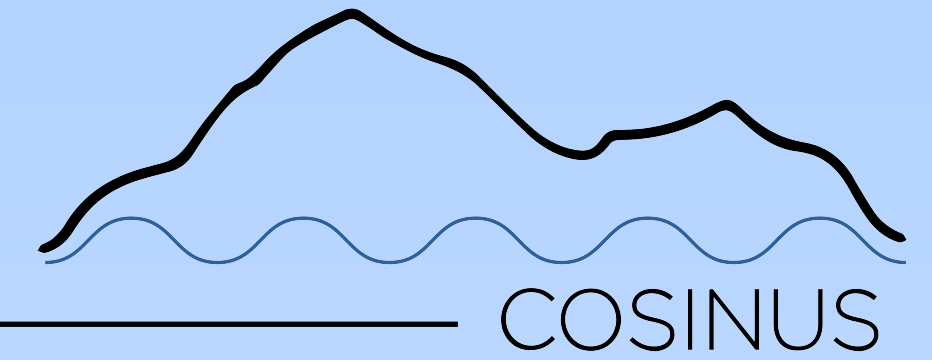
Proof-of-concept



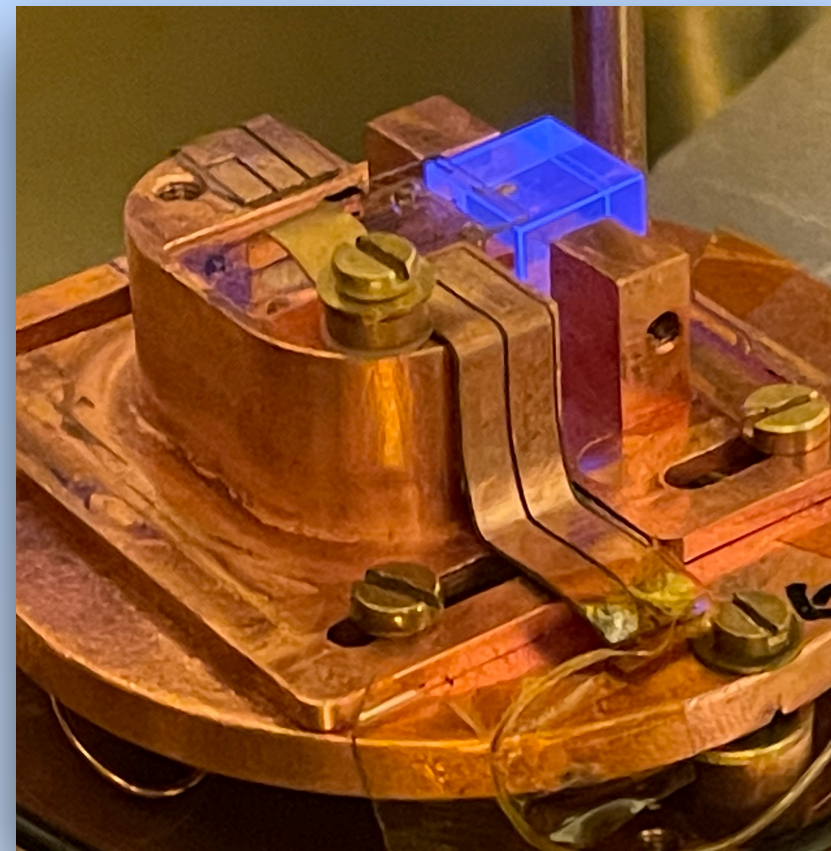
[G. Angloher et al. \(COSINUS collaboration\), Nucl. Instrum. Methods:A, 1045, 167532 \(2023\).](#)



Latest results

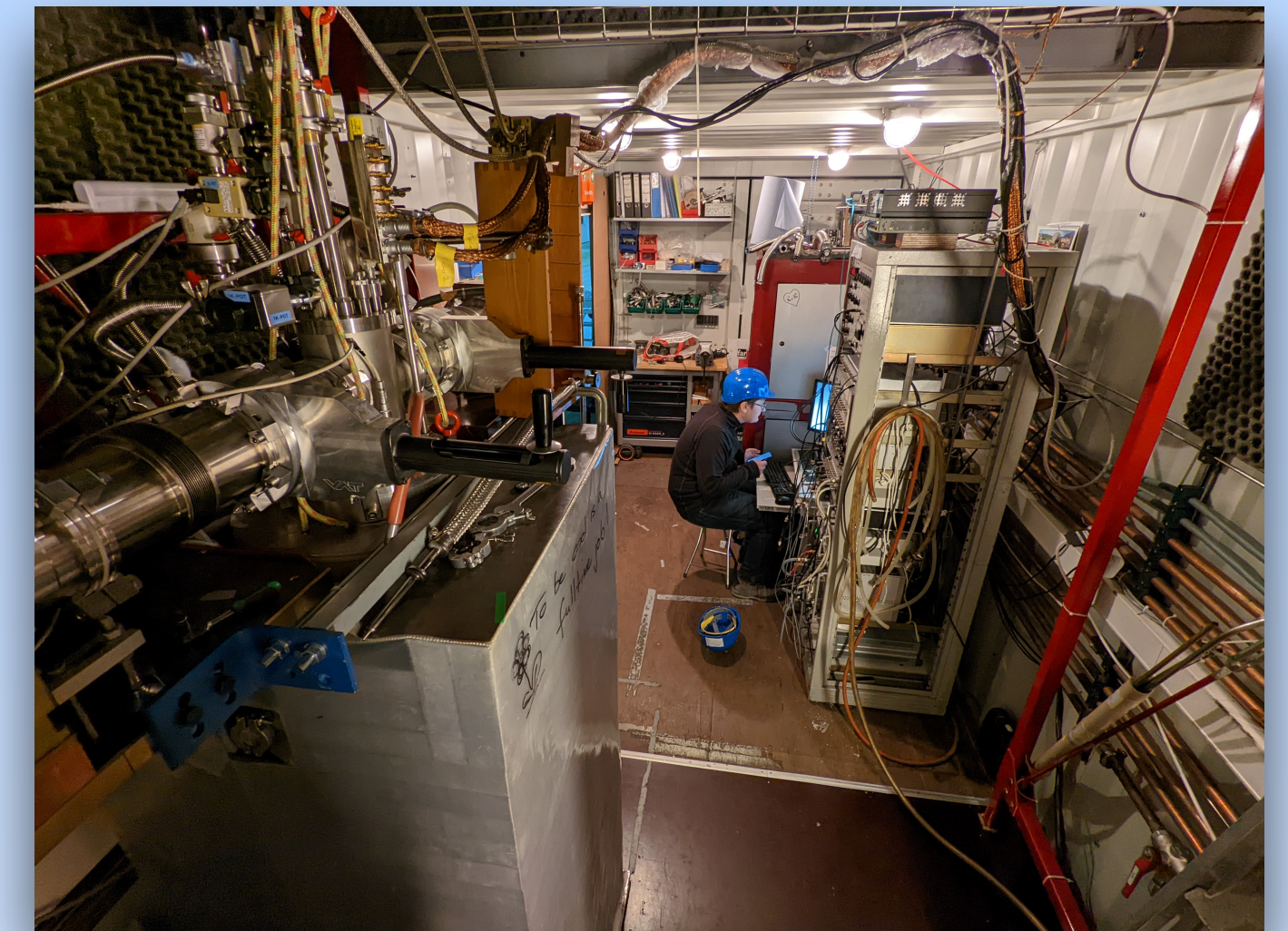


CHANNEL - 1: PHONON DETECTOR

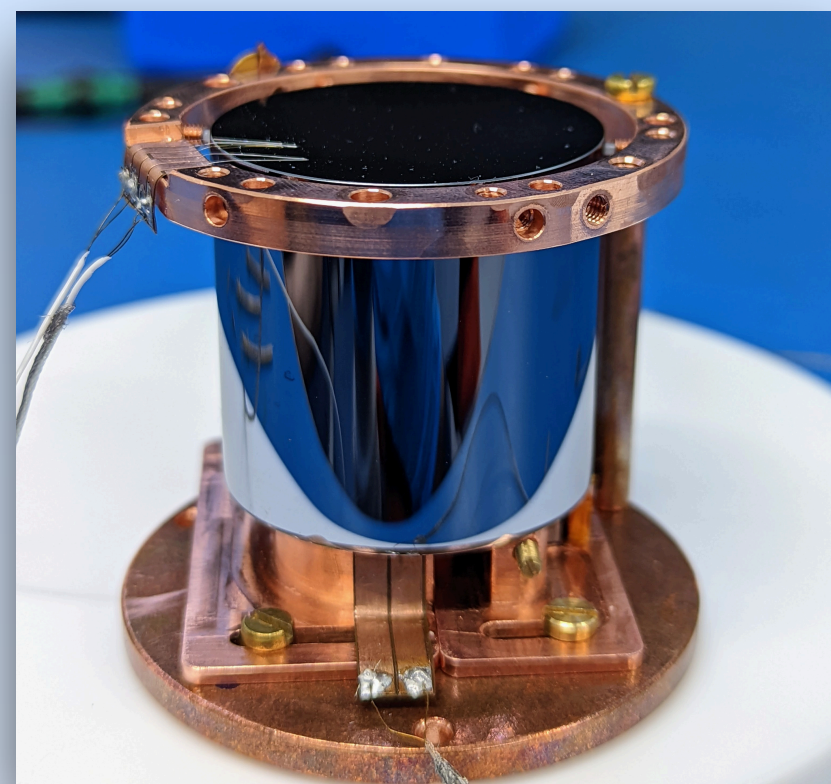


NaI-remoTES

- NaI grown by  Since 1928
- 6-22 ppb of ^{40}K
- 3.67 g, 1 cm³
- 730 ± 73 ppm thallium
- <1ppb of ^{208}Th and ^{238}U (ICP-MS)



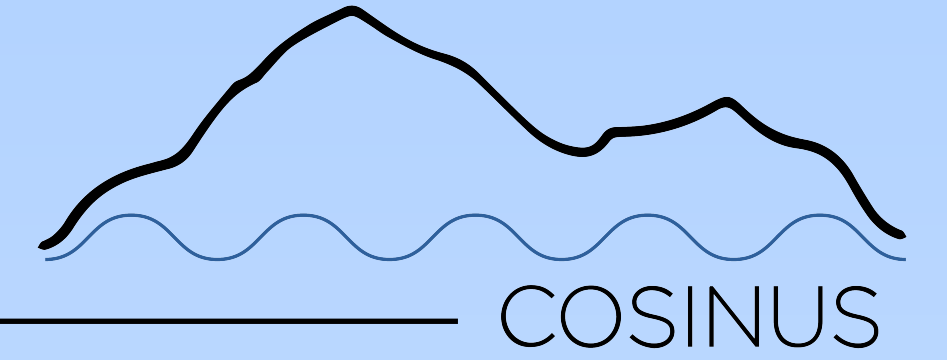
CHANNEL - 2: LIGHT DETECTOR



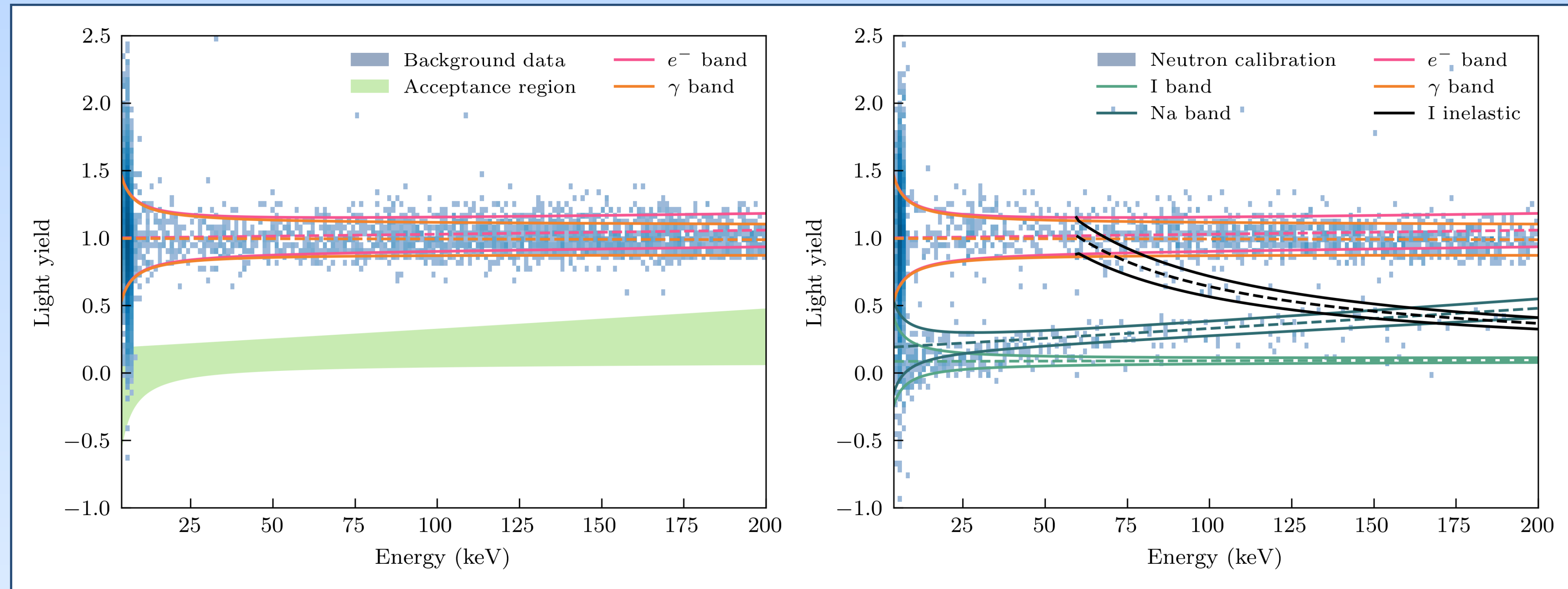
Silicon beaker

- 4 cm diameter and height
- 1 mm thickness
- 15.38 g
- Read out using W-TES evaporated on the surface

Latest results



Event-by-event particle discrimination demonstrated in NaI



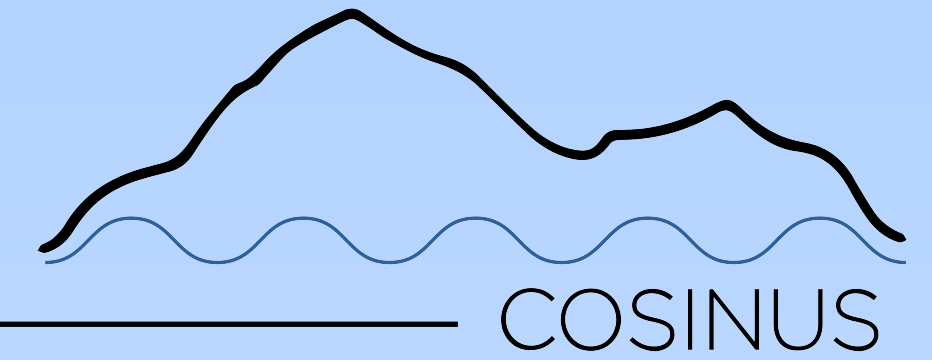
<https://arxiv.org/pdf/2307.11139.pdf>

$$QF_{Na}(10 \text{ keV}) = 0.2002 \pm 0.0093$$

$$QF_I(10 \text{ keV}) = 0.0825 \pm 0.0034$$

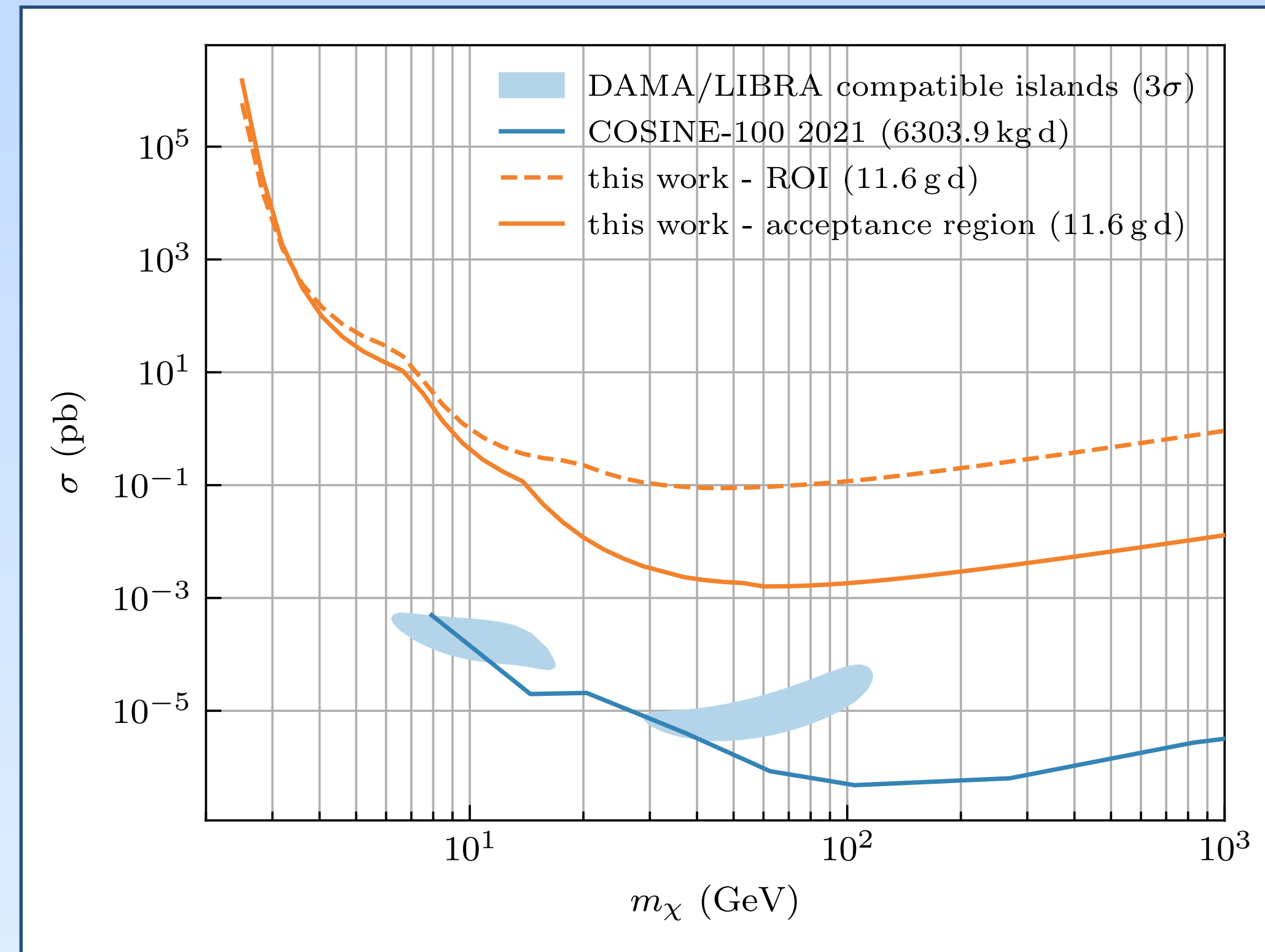


Latest results



PERFORMANCE COMPARISON

$$\sigma_{\text{NaI}} = (0.441 \pm 0.011 \text{ keV})$$



<https://arxiv.org/pdf/2307.11139.pdf>

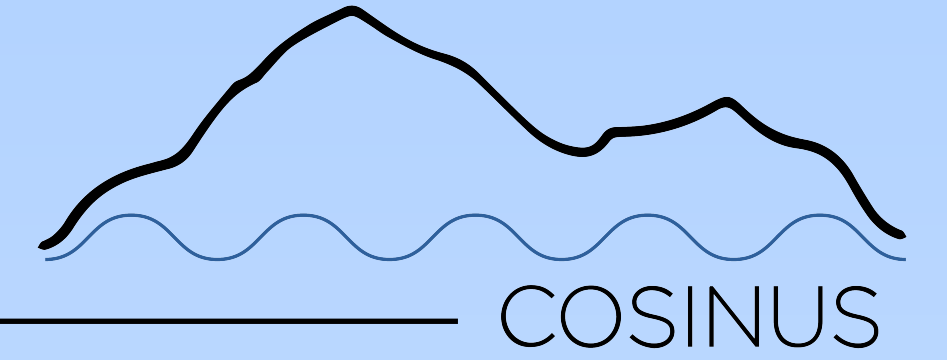
With 11.6 gd exposure



With 6303.9 kgd exposure

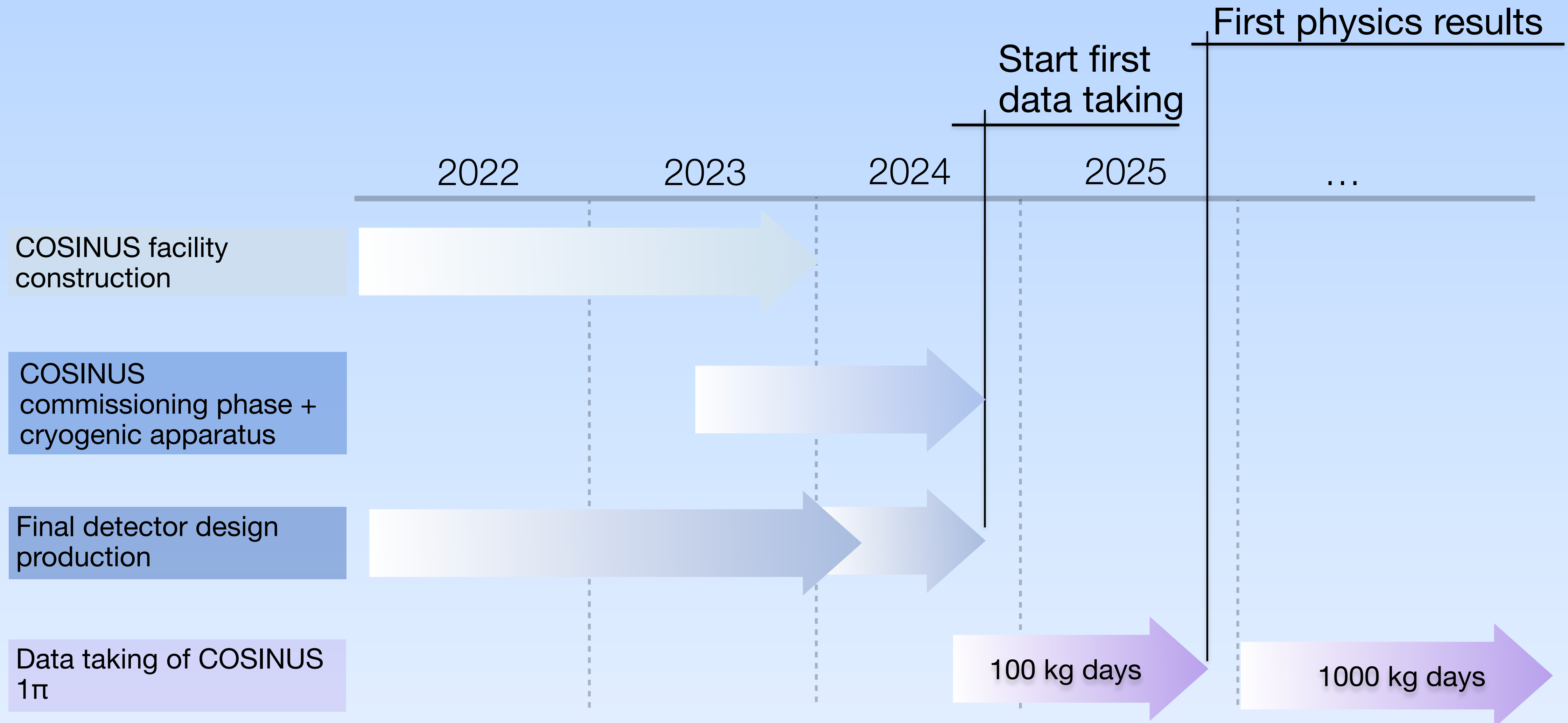
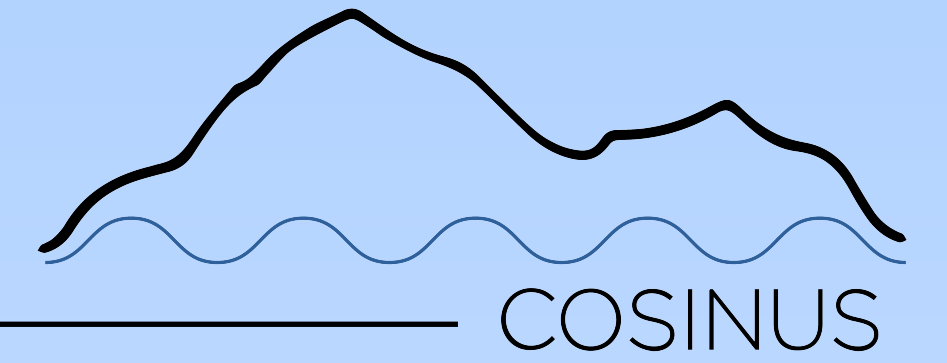


Conclusion

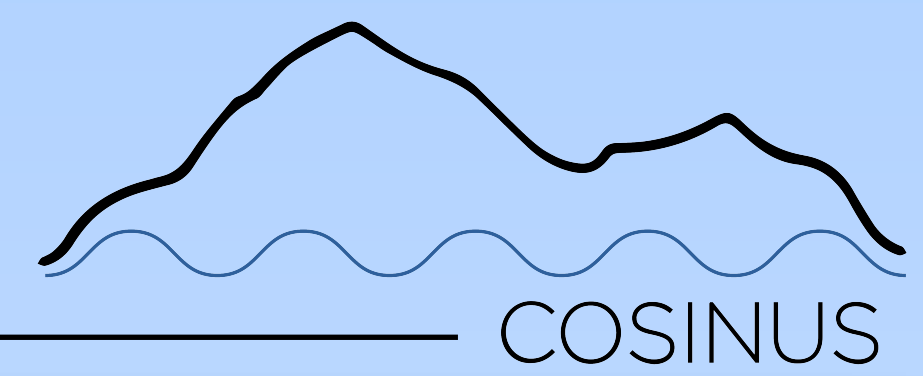


- COSINUS operates NaI detectors at mK temperatures.
- First proof-of-concept tests with standard absorbers successfully carried out.
- A 2-channel readout system allows for particle discrimination on an event-by-event basis and better sensitivity.
- NaI calorimeters operated using the remoTES readout design achieved a baseline resolution of $\sim 400\text{eV}$ for nuclear recoils.
- Updated NaI detector design with a 4π -veto currently under testing.

Outlook



Outlook

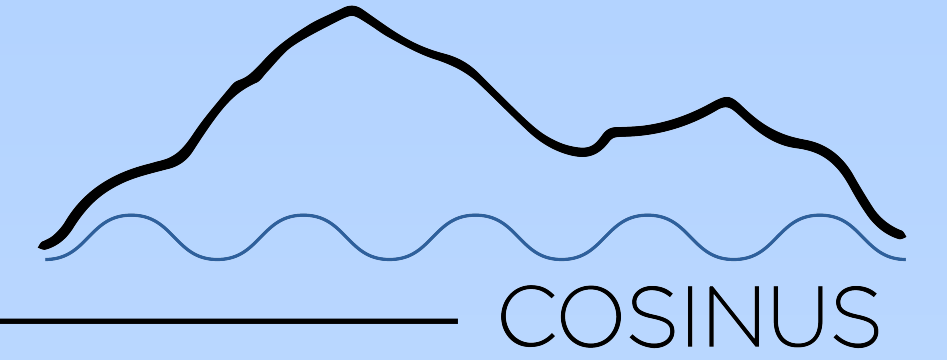


Mukund Bharadwaj | TeVPA 2023



Appendix

Decoupling



Three stages of decoupling

1. Global stage

Double frame

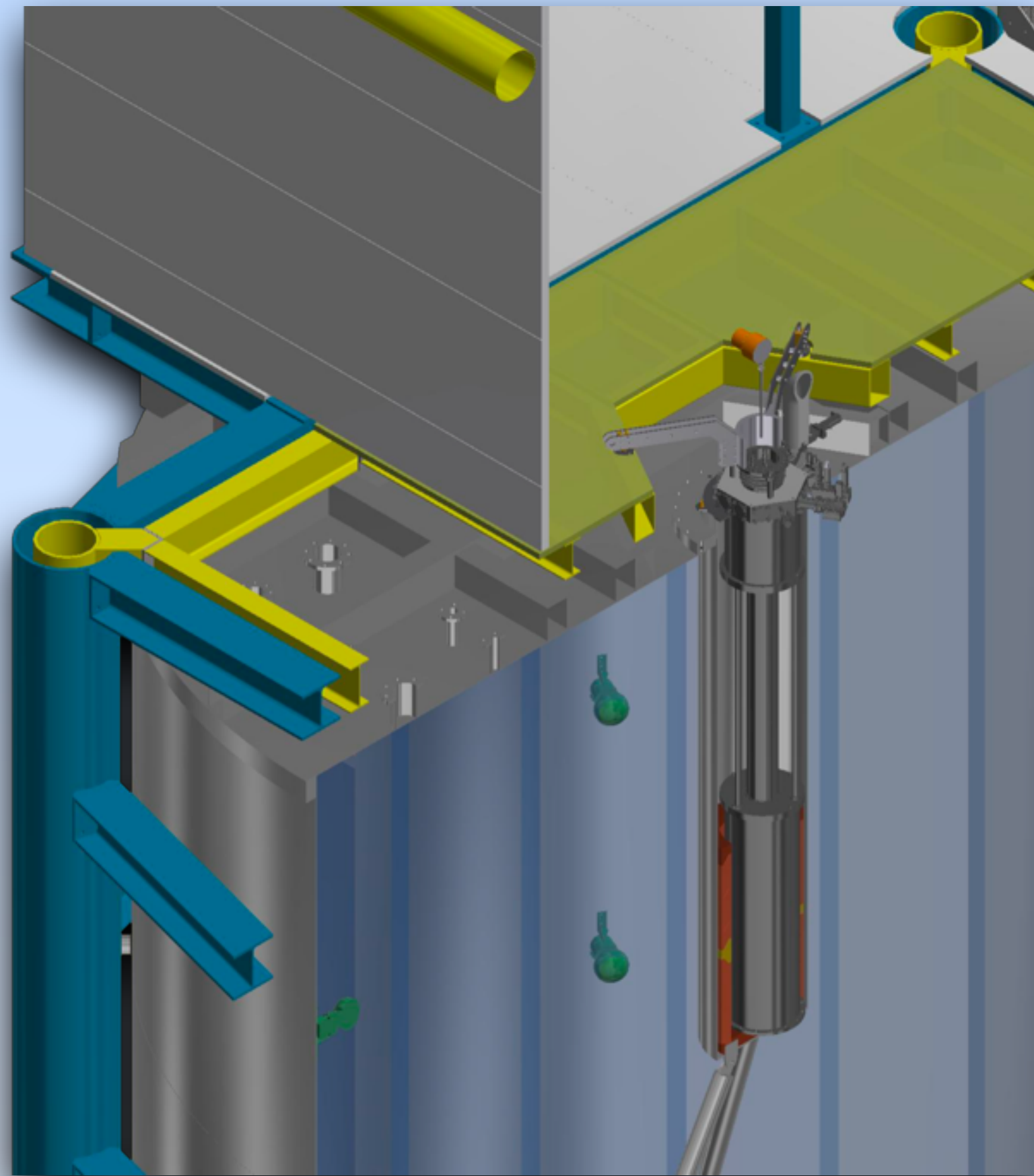
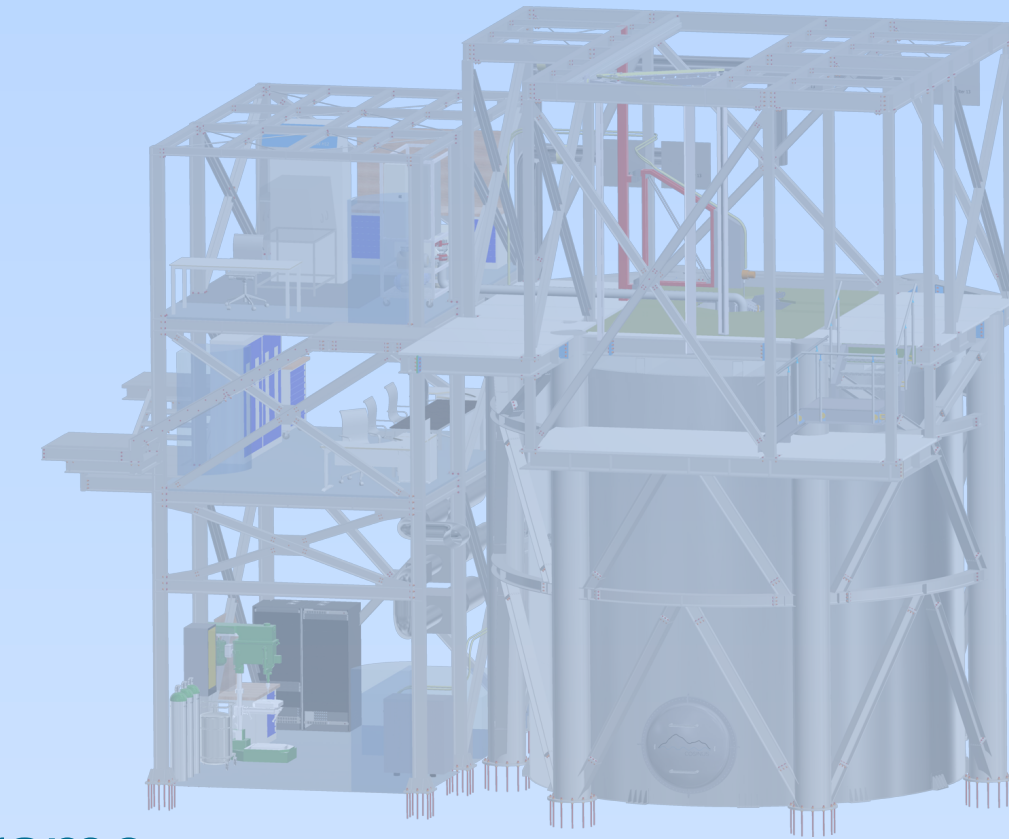
The infrastructure is built on the blue frame, subjected to most of the vibrations

The pulse tube on the yellow frame

The cryostat rests on the dry well, which is the most quiet part

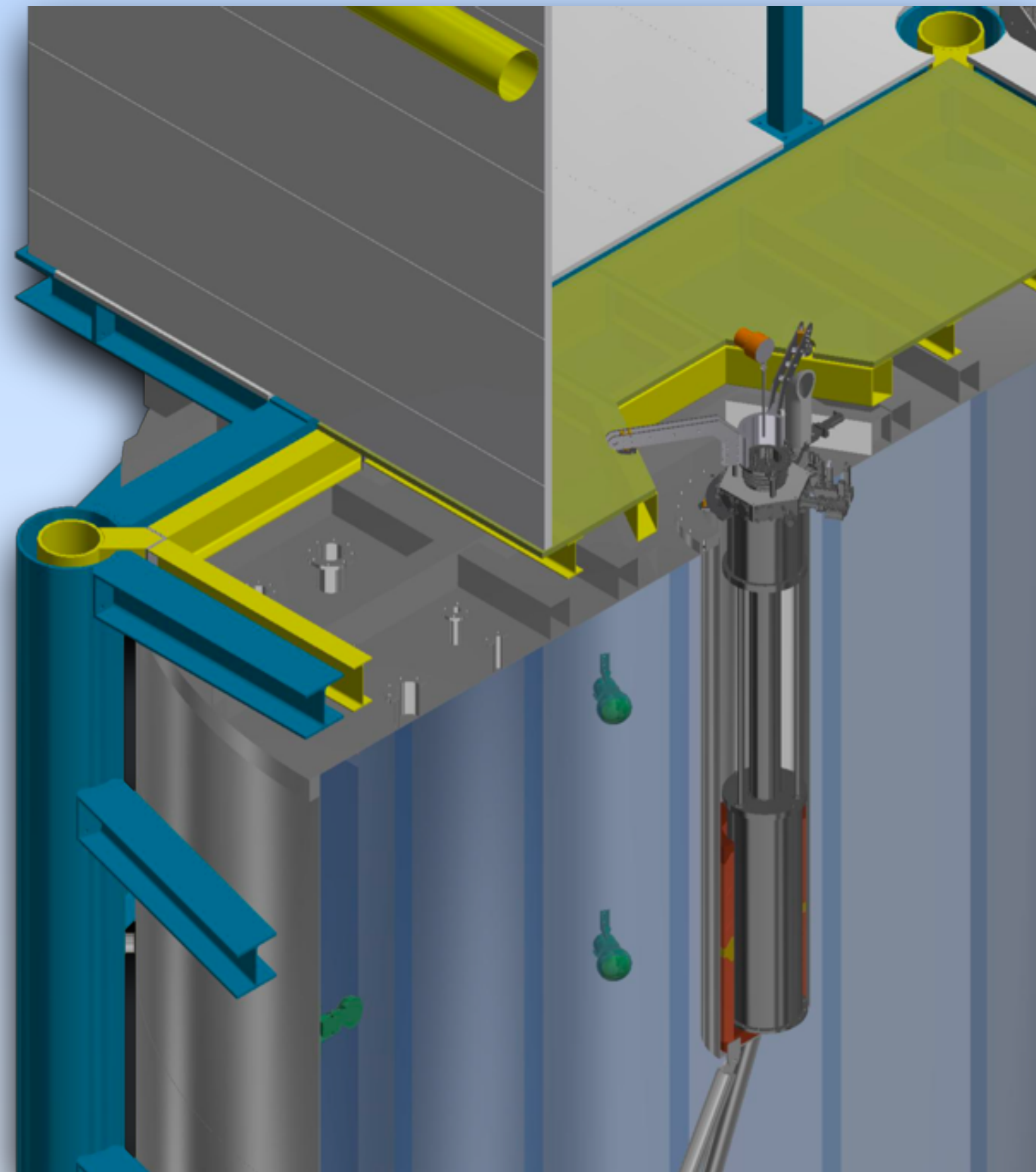
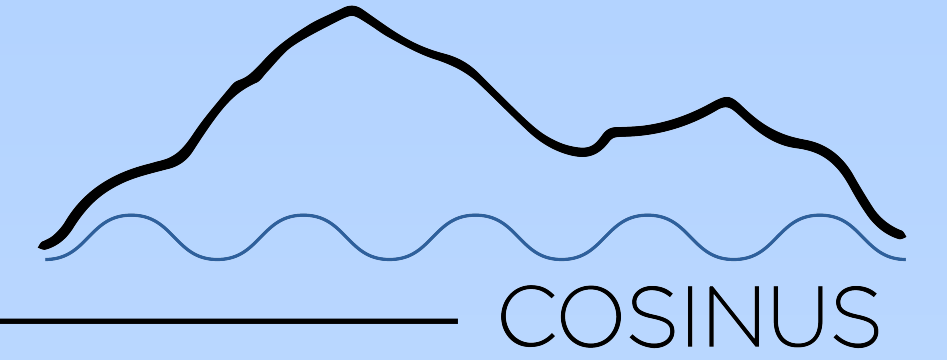
Bellow

The pulse tube is connected to a supply bellow which dumps the mechanical vibrations of the pulse tube



Appendix

Decoupling



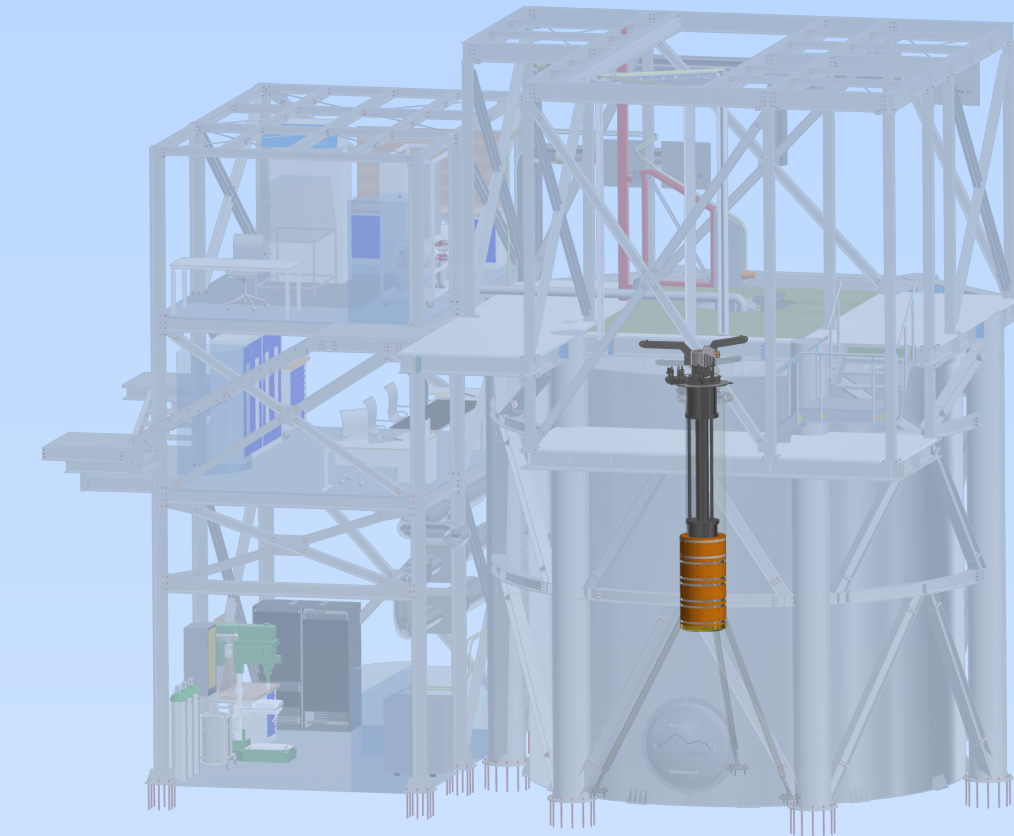
2. Cryostat stage

Pumping duct gas exchanger

The heat exchange between pulse tube and cryostat occurs via gas, no mechanical contact

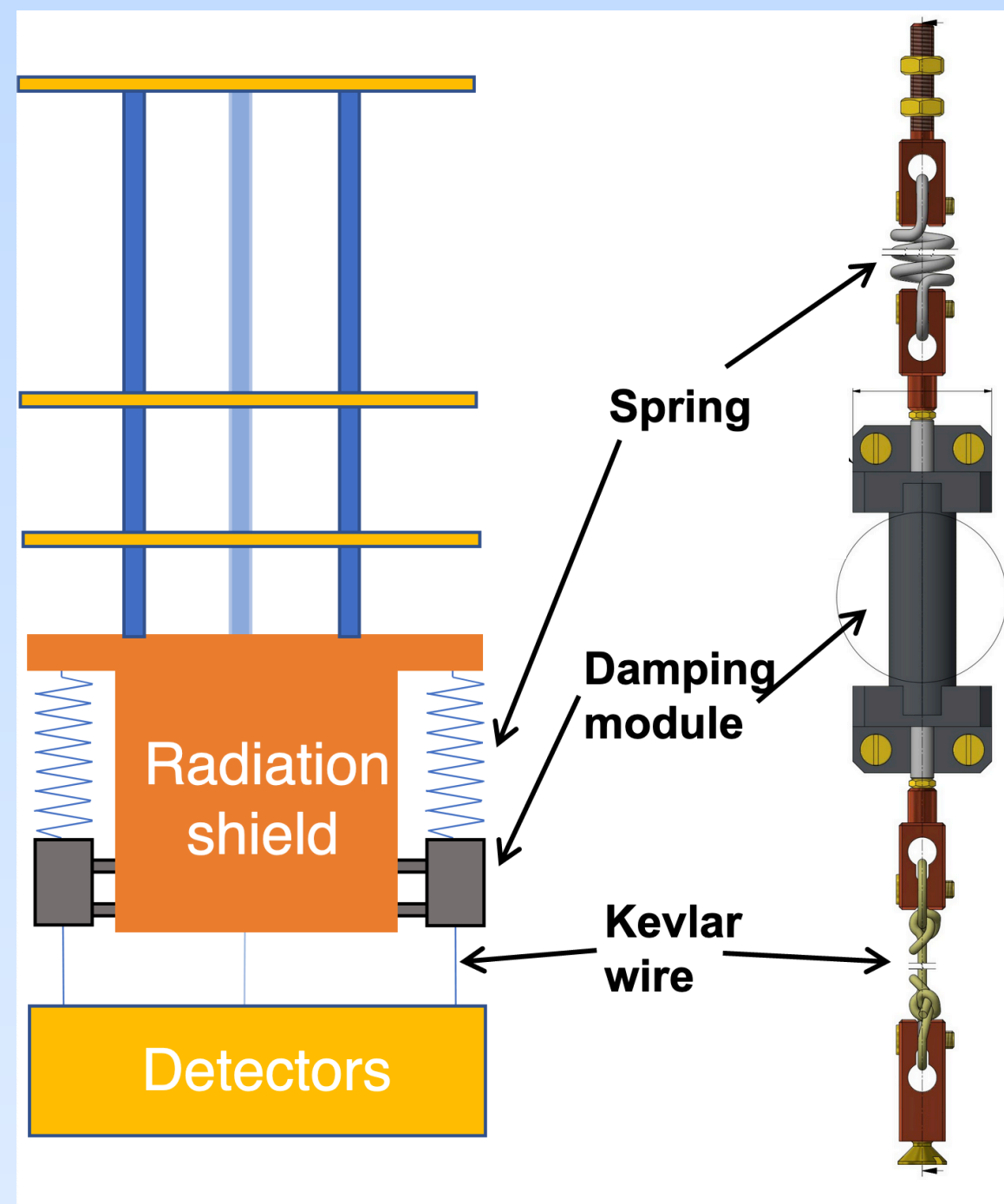
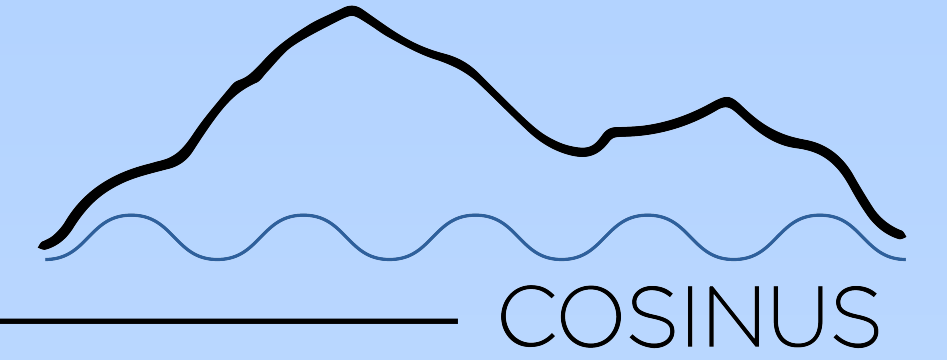
The Ultra-Quiet Technology™

<https://cryoconcept.com/product/the-ultra-quiet-technology/>



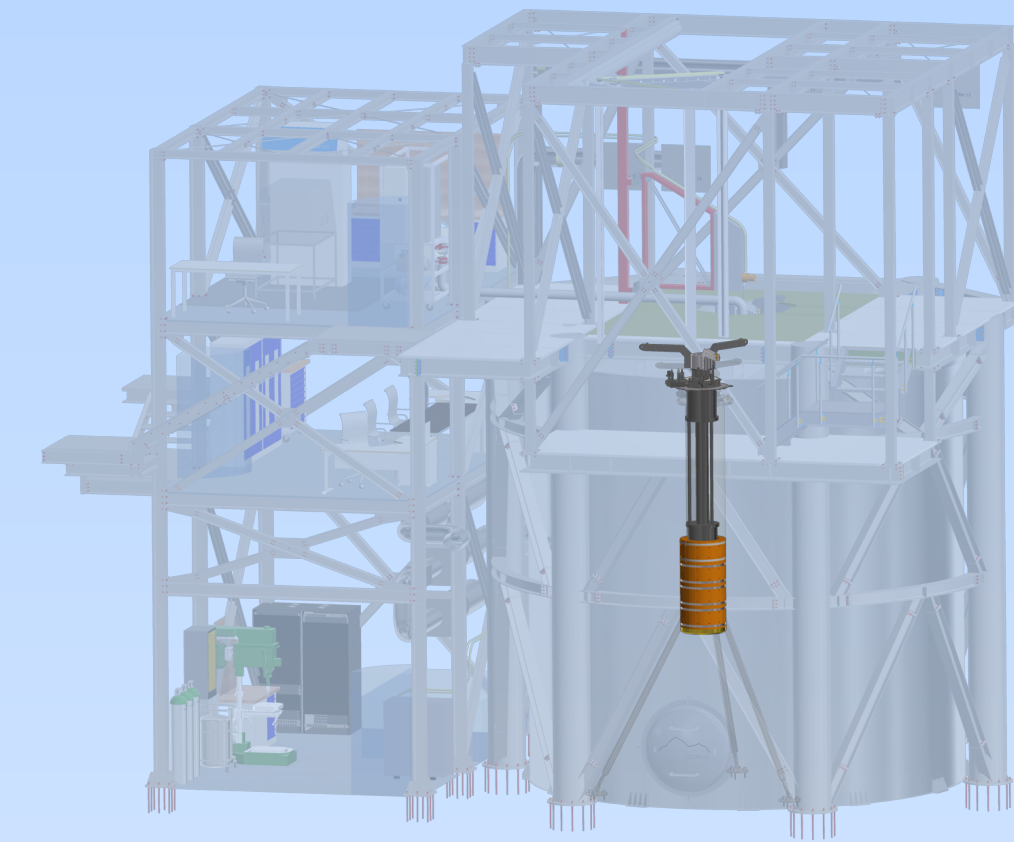
Appendix

Decoupling



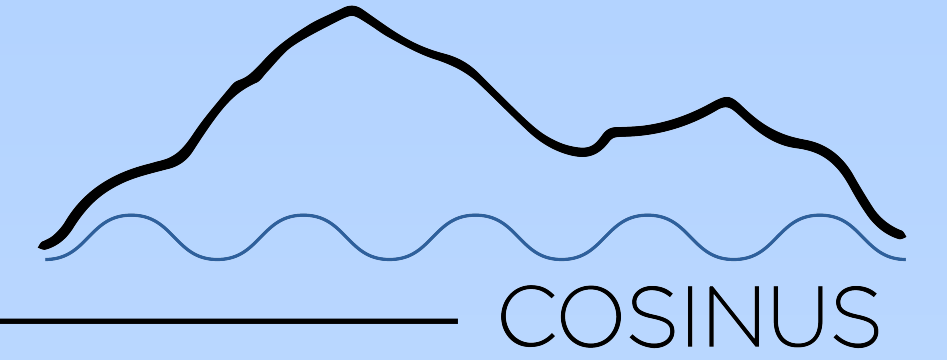
3. Detector stage

- Spring and damping modules to decouple the detector plate
- Magnetic eddy current damping
- Studies ongoing

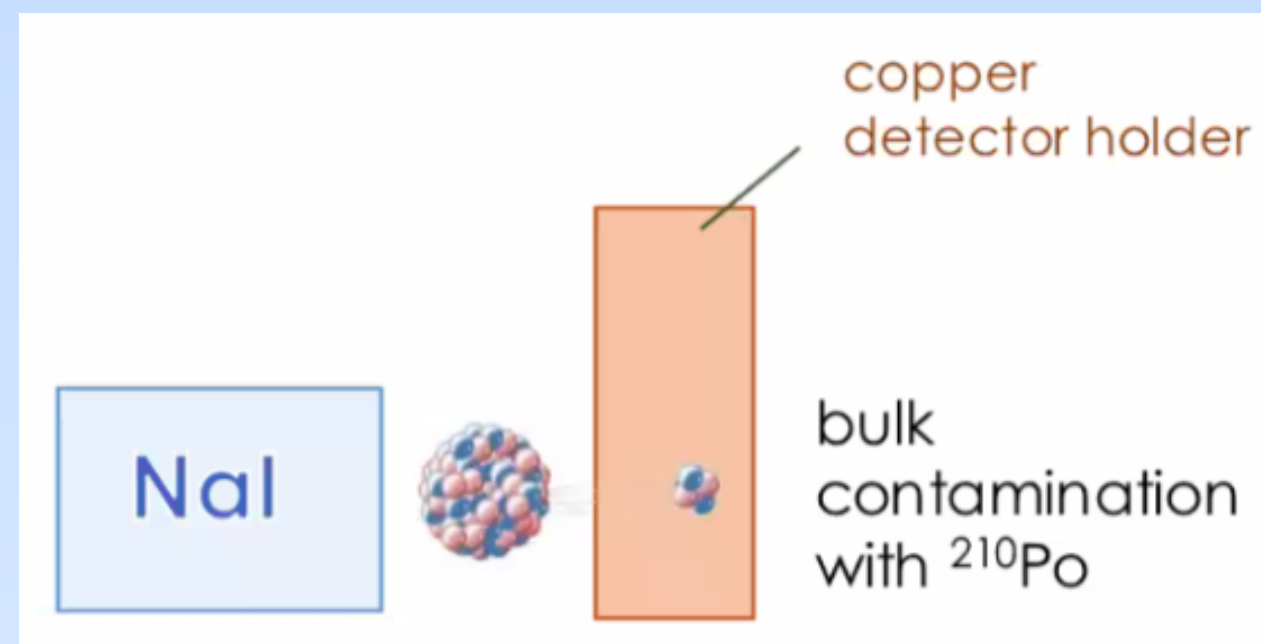


Appendix

The 4π design

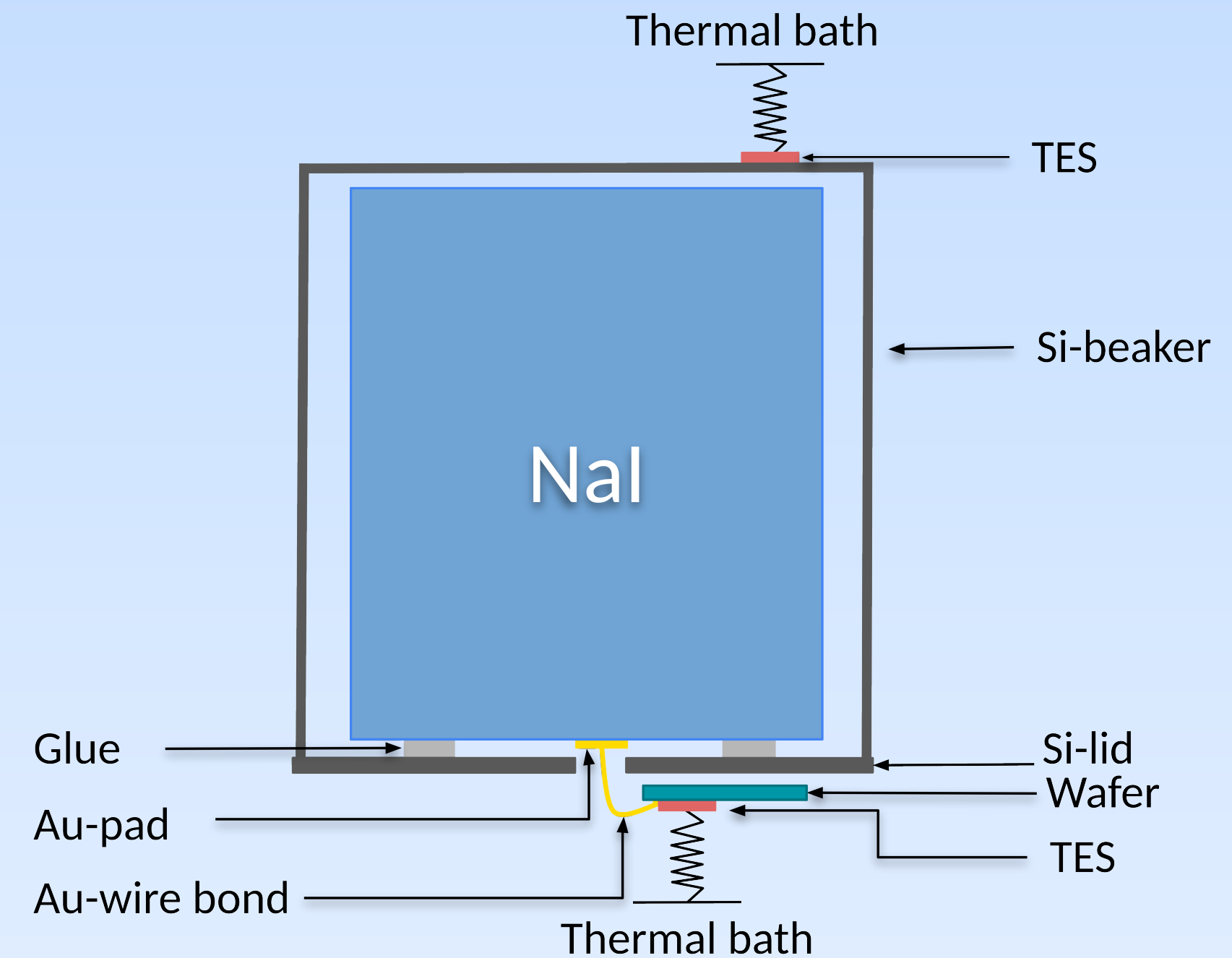


The problem



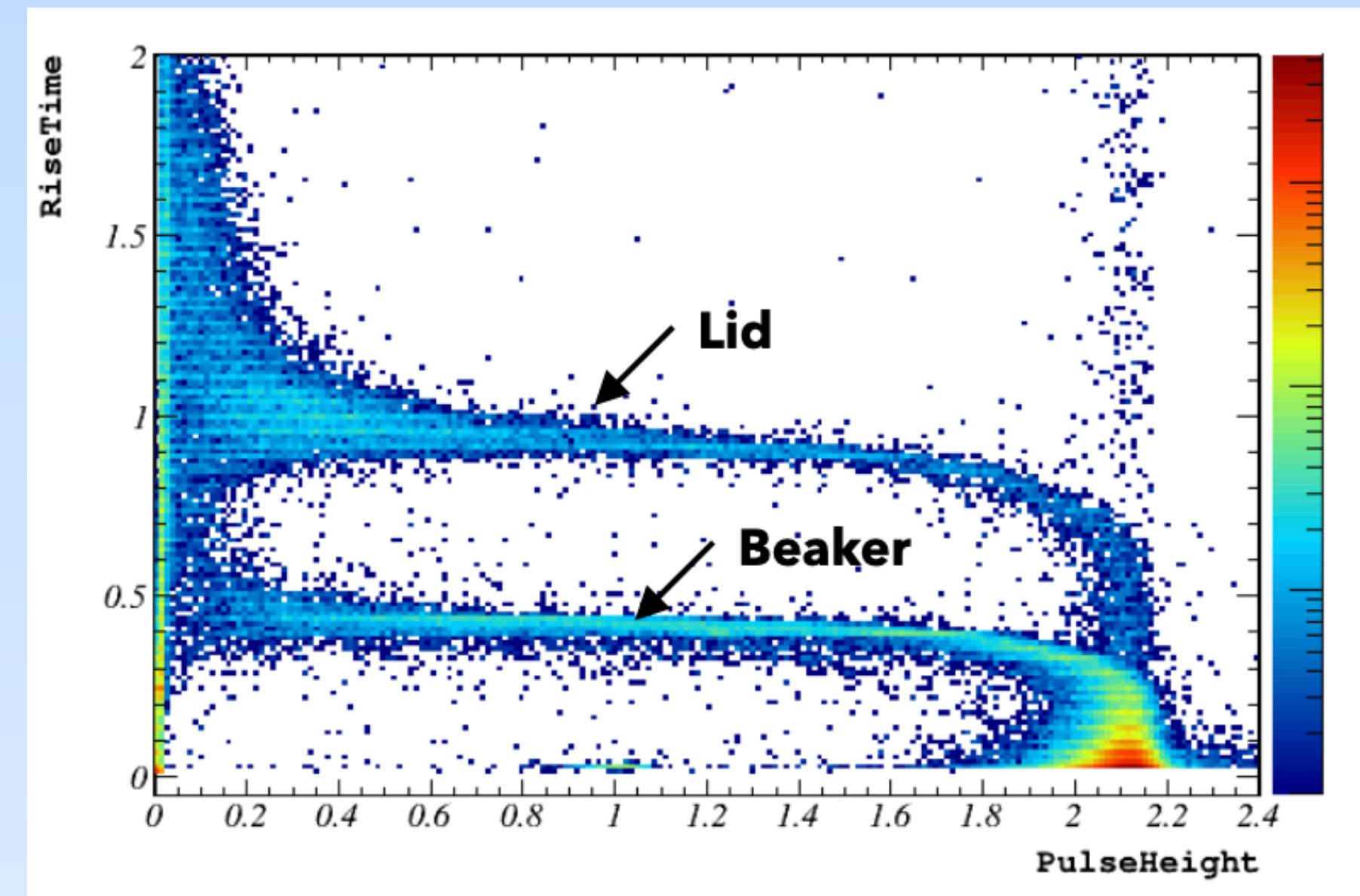
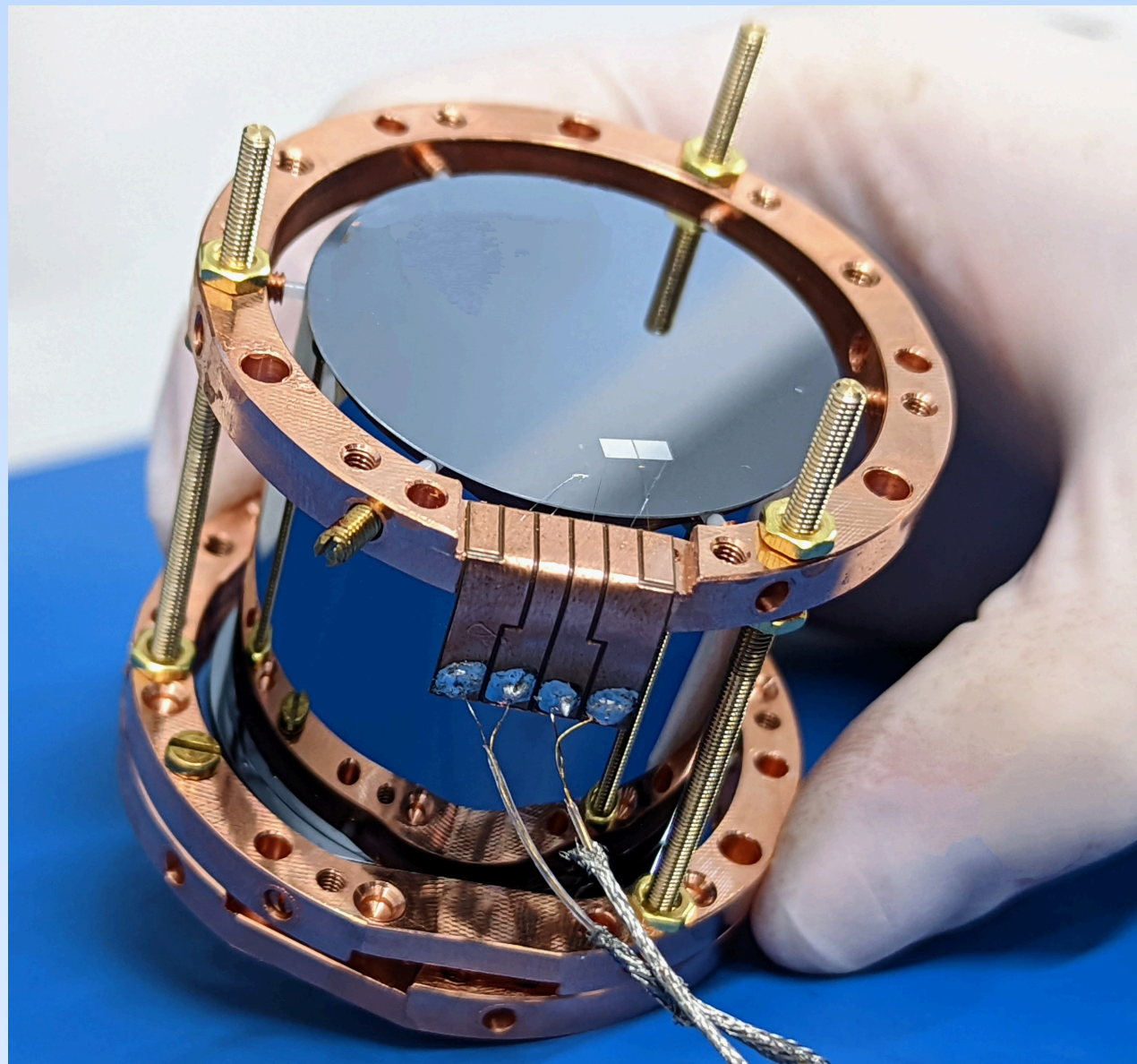
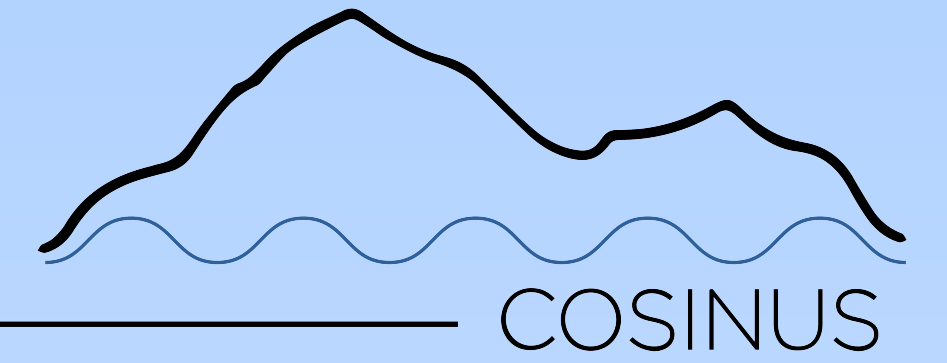
Inefficient collection of scintillation light emitted by crystal

Proposed solution



Appendix

The 4π design



Transmission factor: 54